UNIVERSITAT ROVIRA i VIRGILI

International Erasmus Mundus Master in

**QUATERNARY AND PREHISTORY**

Erasmus Mundus

# Relationship between age and sex: new Principal Components Analysis on pelvises and femurs of Anatomically Modern Human and Homo neanderthalensis


**Candidate**

**Mantoan Giorgia**

**Supervisor** **Prof. Carlos Lorenzo-Merino**


*Academic year 2022/2023*

# Index

# 1 Abstract

This paper considers a new Principal Components Analysis approach that can be applied to the femur and pelvis. The aim of this new approach is to understand how the morphology of the femur and pelvis are affected by the sex and age of an individual. To be able to do this we will apply this new methodology to a sample of Anatomocally Modern Humans equally divided by age and sex and see what their values are for the variable sex and age in the Principal Components Analysis, then we will use the values obtained to be able to apply them to a small sample of *Homo neanderthalensis* the same procedure and see if there are any differences or congruencies with the previously selected sample. Before applying Principal Components Analysis, however, we will explain how the 3Ds from which the data were obtained were obtained, then explain the results of Principal Components Analysis and finally attempt to give an explanation of the data obtained. All this is intended as a preliminary work in order to be able to investigate and study the Obstetrical Dilemma, an anthropological dilemma still unresolved in palaeoanthropology and anthropology, from a different point of view.

# 2 Introduction

One of the most important parts of the skeleton hand for its support and for the protection of internal organs is the pelvis, which through the hip joints articulates with the femurs, which are the proximal part of the lower limb and their function is to support and relieve the weight of the upper body on the ground in a bipedal position and allow walking, and movement in an upright position (White and Folkes, 2005; White, Black and Folkes, 2011).

This paper comes from wanting to extend and deepen the work done for my three-year thesis on the evolution of the pelvis from *Australopithecus* to *Homo sapiens* and the *Obstetrical dilemma*[1]. The evolution of the pelvis and the consequences this has on Anatomically Modern Human (henceforth AMH), how it has changed and the features that have been retained and lost throughout the history of human evolution, is a topic that has been little addressed. It is a topic that is little addressed because there is little material to study and many gaps in the fossil record. As will also be said several times later, the pelvis is unfortunately one of the most fragile bones in the human skeleton that is difficult to preserve in a complete and undistorted manner. This difficulty in finding material that is not distorted and/or highly fragmented means that there is little research on this subject, and sometimes much conflicting research.

The anatomical parts analysed in order to begin new studies of this anthropological dilemma are the pelvis and femurs. The pelvis and femurs are parts of the body that are subject to considerable change and stress during an individual's lifetime: for example, in women, the pelvis and femurs adapt as pregnancy progresses, so as to facilitate the pregnant woman's movements and delivery when the foetus is born; in men, for example, they may be greatly affected by the exertion during heavy, strenuous work. Moreover, in the case of both women and men, the femurs in particular are affected by lifestyle and also by advancing age, since throughout life they adapt to the changes in the various gaits that each individual assumes throughout his or her life (quadrupedal while an infant and then bipedal, then, perhaps, with advancing age one has to adapt to various diseases to which the bones are subject such as osteoporosis[2], arthritis[3] and rheumatism[4] that force the individual to use a walking aid and/or support that changes the postur and

[1] "The difficult birth process of humans, often described as the "obstetric dilemma, "is commonly assumed to reflect antagonistic selective pressures favouring neonatal encephalisation and maternal bipedal locomotion" (Wells, DeSilva and Stock, 2012).

[2] "In medicine, a process of bone rarefaction with a decrease in skeletal mass without a significant percentage change in the mineral component of residual bone tissue" (Vocabolario Treccani, 2023c).

[3] "Morbid process, acute or chronic, solely or predominantly inflammatory in nature, affecting various joint tissues" (Vocabolario Treccani, 2023b).

[4] 4 "Generic and not well-defined medical term designating a group of diseases or morbid manifestations, acute, subacute and chronic, primary or secondary, affecting the organs of the locomotor apparatus (joints, bones, muscles, etc.) and sometimes the nerves, resulting in pain, formerly known as rheumatism due to their wandering, changeable, discontinuous character' (Vocabolario Treccani, 2023d).

demabulation again for the third time in a man's life) (White and Folkes, 2005; White, Black and Folkes, 2011).

In this paper, we are going to do Principal Component Analysis (henceforth PCA) of precisely these two anatomical parts, to see how these parts may change over the course of an individual's lifetime; thus, relating different age groups (20 to 30 years, 31 to 40 years, 41 to 50 years), o not change (the possibility of non-change during an individual's lifetime is also taken into account). In addition, it will be seen how and if it also changes in relation to gender (males and females), this being useful to see if there are major differences in the two genders at a morphological level and which may perhaps affect the data obtained in some way.

But the analyses will not only stop at applying the parameters and considerations just made to AMH, but will also be applied to a restricted sample of *Homo neanderthalensis* finds, in order to see if it is possible to apply the same parameters and analyses to other *Homo* species. *Homo neanderthalensis* was chosen for the start of this new approach to these analyses, as it is the species of Homo closest to AMH and the one of which we have the most fossil finds, in some cases, better preserved.

However, the general problem with applying these analyses to a fossilised species of *Homo* (in general) is that the femur and, in particular, the pelvis are two anatomical parts of the human skeleton that are difficult to preserve optimally and without being too distorted by taphonomic processes or so damaged that their reconstruction may not be faithful to what they were in reality. For this very reason, the data o b t a i n e d f r om the application of landmarks and the data obtained from PCA may not reflect the reality of how they really were. An attempt will be made to apply the landmarks only to the unreconstructed and less distorted parts of the Neanderthal casts, in order to have the most truthful data possible. Furthermore, where it will not be possible to apply landmarks, data from other fossil finds will not be forced or used where they are present, so as not to distort and render the results of the analysis artefactual.

This paper will explain how the pelvis and femur are anatomically made. In the pelvis, each individual part that makes up the pelvis will be specifically explained, and the same will be done for the femur. In addition, what is already known about the morphology of the pelvis and femur of *Homo neanderthalensis* will be explained through articles and books by other authors (such as (Aiello and Dean, 1996)), so as to give a general explanation of the differences and similarities already known between AMH and Neanderthals.

Next, the material used will be explained (where the materials came from and the selection criteria applied to select them) and how the 3Ds of AMH and *H. neanderthalensis* were obtained, as two different techniques were used:

- CT scans from the NMDID database (Edgar *et al.*, 2020) were used for AMH using the 3dSlicer software (Martin *et al.*, no date; Fedorov *et al.*, 2012; Friess, 2012; Velazquez *et al.*, 2013; Ghesu *et al.*, 2017)(see section *3.2.2 3D obtained with 3DSlicer*);
- for *Homo neanderthalensis*, the technique of photogrammetry (Ficarra and Lauria, 2022) was used from the casts of some fossils from the Musée National de Histoire Naturelle (henceforth MNHN) in Paris (see section *3.2.3 3D obtained by photogrammetry*).

Finally, the graphs and analyses will be explained, trying to give a solution to the data obtained by answering the questions posed in a comprehensive manner. These questions concern the sex and age of the individuals: what can be deduced from the data collected? Is the age or sex of the individual more influential for the morphology of the femur and/or pelvis? Can the same methodology and parameters be applied to other *Homo species*? And if so, to what extent can the data be taken as reliable? These are some of the questions that have been asked in order to produce this paper, but surely there are many others that will be attempted to be answered.

The main objective and guideline that one tries to maintain throughout the analysis and in the interpretation of the results is objectivity, to interpret the results obtained as analytically a possible, trying not to be too subjective when coming to conclusions.

# 3 Anatomy of the pelvis and femur

The anatomical parts under consideration are the pelvis (or pelvic girdle) and the femur (**Fig.1**). These two parts of the human skeleton are fundamental for supporting body weight and enabling walking (White and Folkes, 2005; White, Black and Folkes, 2011).

We will now go on to explain in detail the two individual parts separately.

## 3.1 Pelvis or pelvic girdle

The pelvis or pelvic girdle (**Fig.2**) is a bony complex that connects the lower limbs (including the femur, which will be discussed in a moment) to the trunk. Its main purpose is to support and protect the abdominal and pelvic organs (White and Folkes, 2005; White, Black and Folkes, 2011).

The pelvis is formed by a bony complex firmly attached to the axial skeleton by the sacrum (it is part of the vertebral column and consists of the sacral vertebrae). In addition to the sacrum, there are also four other parts that make up the pelvis and that fuse together at the end of bone development: the ilium, ischium, pubis, and acetabulum. These four parts should always be studied as a whole, because their function would not be clear (White and Folkes, 2005; White, Black and Folkes, 2011).

It should be borne in mind that today's conformation of the human pelvis is the result of a long evolutionary process, during which some features have been retained, others have been lost and still others have been modified. The main factors that led to the conformation of the AMH pelvis are (White and Folkes, 2005; White, Black and Folkes, 2011):

- obstetrical: it must be able to allow delivery and, therefore, be large and/or flexible enough to widen and to be able to pass the head of the foetus (White and Folkes, 2005; White, Black and Folkes, 2011);
- locomotion: the muscles must be able to anchor themselves firmly so that bipedal walking is stable (White and Folkes, 2005; White, Black and Folkes, 2011).

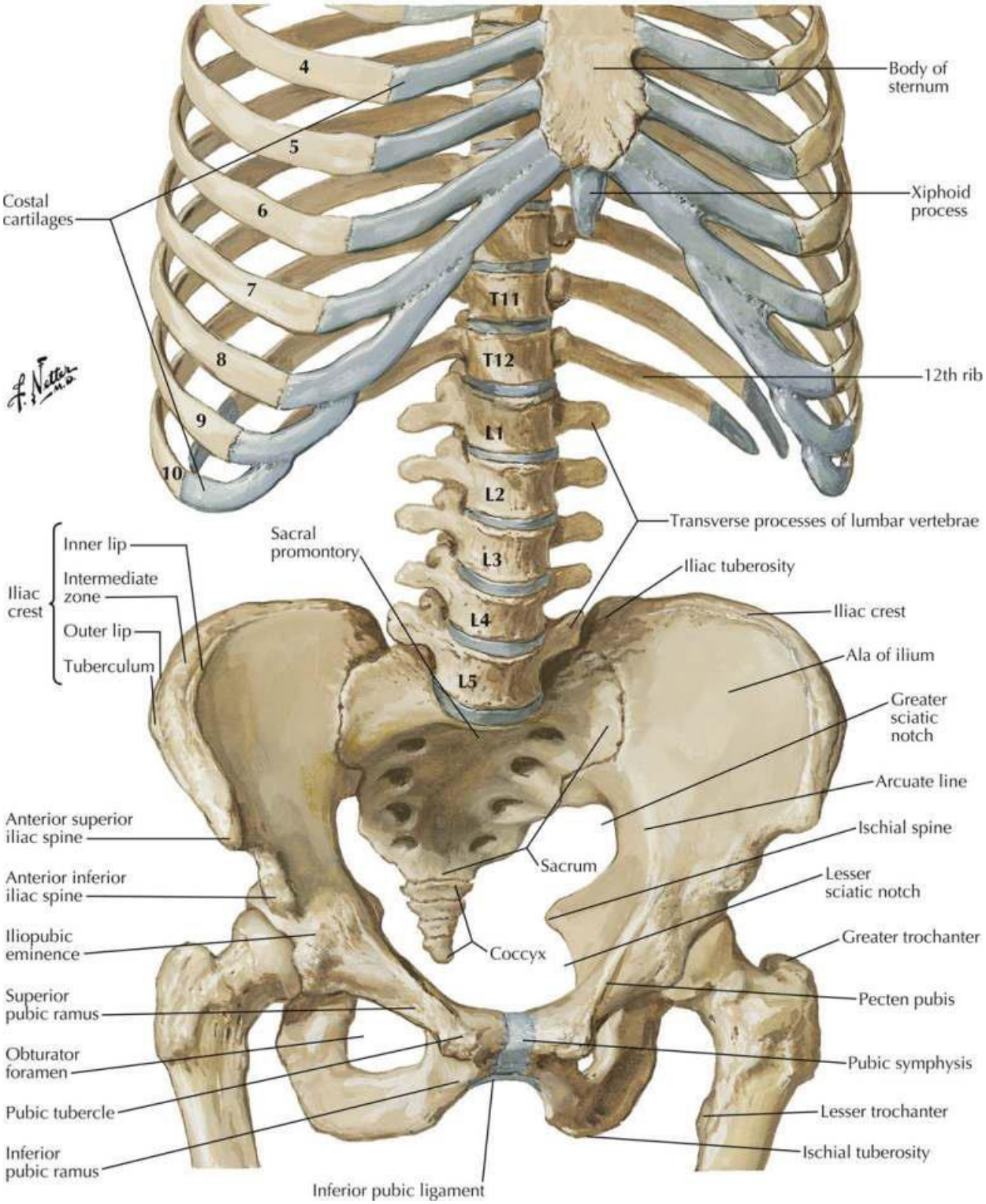


**Fig. 1** *Skeletal system with associated cartilage showing part of the thorax, part of the spine, pelvis and femurs* (Netter, 2022).

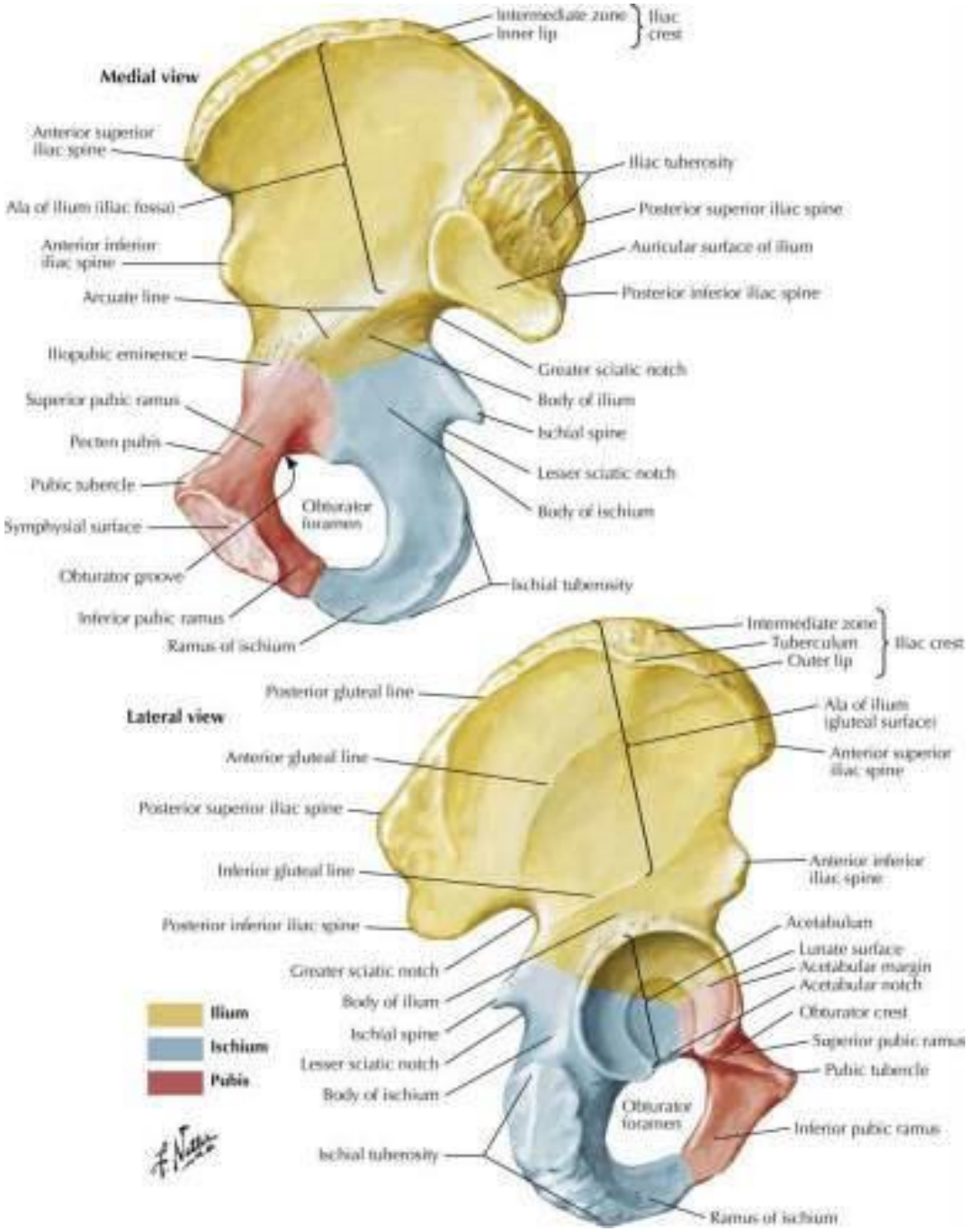


**Fig.2** *Complete image of the pelvic bones. In yellow the ilium, in blue the ischium and in red the pubis. In the intersection of the three colours and parts that make up the pelvis is the acetabulum (image modified from* Netter Atlas of Human Anatomy by Frank H. Netter) (Netter, 2022)

### 3.1.1 Ilium

The ilium (**Fig.3**) is the proximal part of the pelvis, whose shape resembles that of a blade and is triangular; its surface is wider than high. Its shape helps relieve stress on the sacroiliac joint, i.e. it helps relieve stress on that part of the ilium that transmits the entire weight of the upper body from the spine to the hip joint in bipedal posture (Aiello and Dean, 1996).

The orientation of the blade forms the walls of the typical funnel shape of the pelvis and is articulated into a convex surface, a concave iliac fossa and an S-shaped iliac crest. These peculiar features create a complex that reflects the demands placed on the pelvis for bipedal locomotion (Aiello and Dean, 1996).

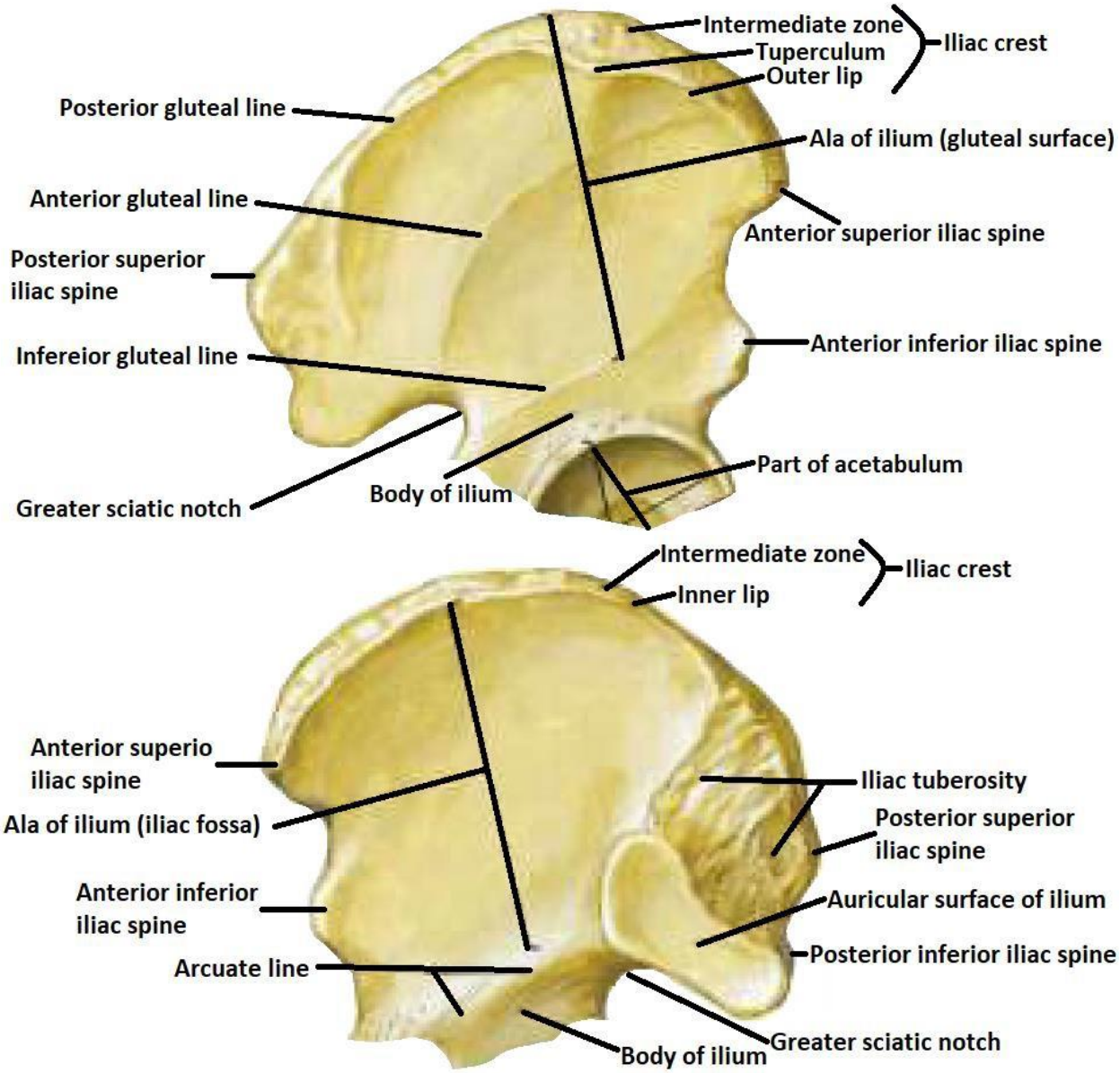


**Fig.3** *Lateral view (above) and medial view (below) of the ilium with its parts. (image modified from* Netter Atlas of Human Anatomy *by Frank H. Netter)* (Netter, 2022)

### 3.1.2 The ischium

The ischium (**Fig.4**) is located in the postero-lower part of the pelvic bone. Its distinguishing feature is the large bony protuberance known as the ischial tuberosity, which provides the attachment area for the posterior thigh muscles that also extend to the hip joint. The ischiatic tuberosity is connected to the ischiatic body, which in turn is joined to the ileum just above the ischial spine and the pubis via the ischio-pubic branch or inferior pubic branch (Aiello and Dean, 1996).

The ischial spines are an adaptation to bipedal locomotion. The prominent ischial spines are the direct result of stress caused on the ischium by the horizontally oriented pelvic floor or diaphragm, a muscle that must support the weight of the abdominal-pelvic organs in the bipedal posture. The pelvic floor inserts into the two ischiums via the ischial spines through the sacrospinal ligament and the tendon arch that surrounds the pelvic floor muscles (Fig. (N)) (Aiello and Dean, 1996).

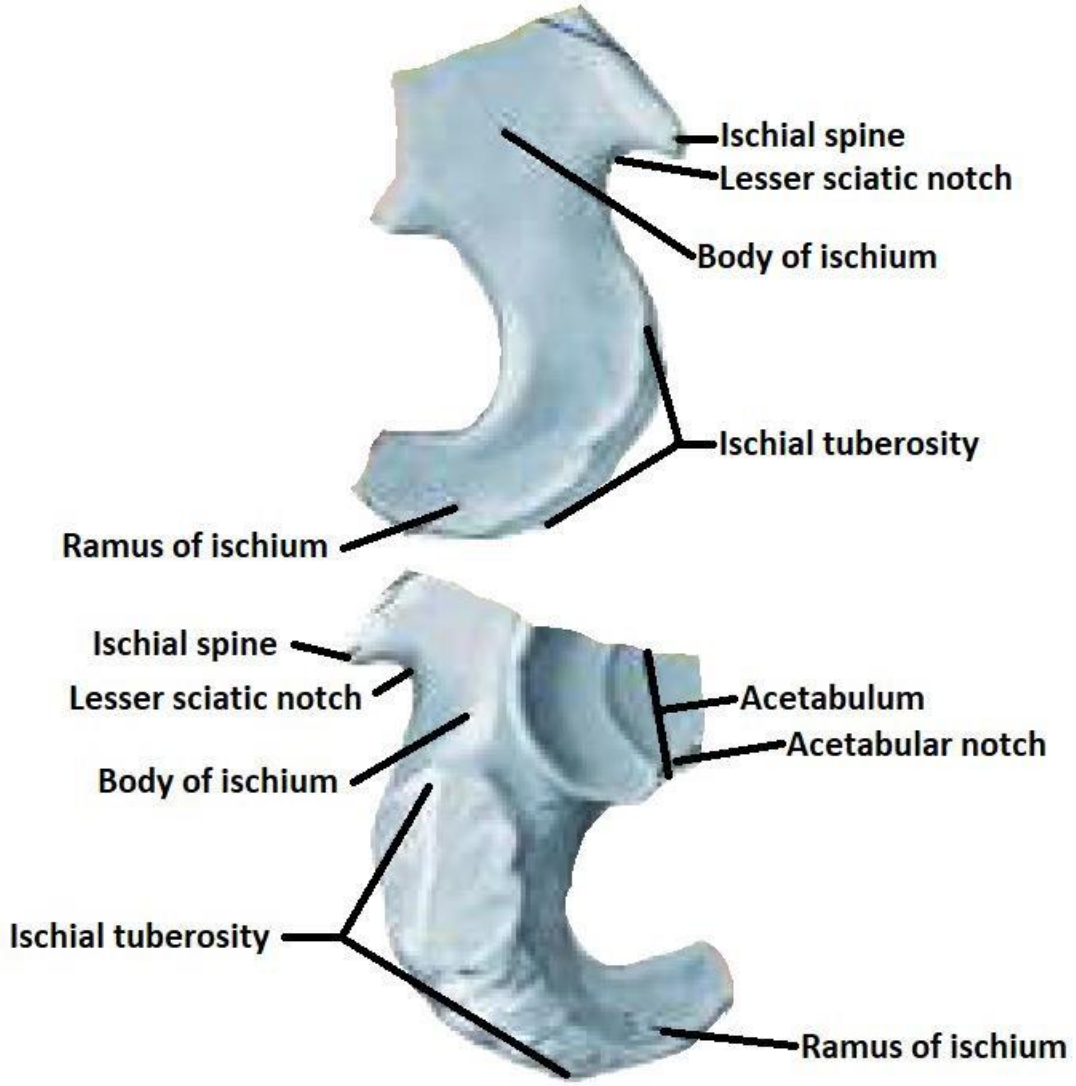


**Fig.4** *Lateral view (above) and medial view (below) of the ischium and its parts. (image modified from* Netter Atlas of Human *Anatomy by Frank H. Netter)* (Netter, 2022).

### 3.1.3 The pubis

The pubis (**Fig.5**) is the antero-inferior bone of the pelvic bone and is articulated in a surface divided into two parts joined together. The pubic symphysis is a joint formed by fibrocartilage and the two bones, which are separated by a disc of fibrous tissue. Superiorly, the body of the pubis is connected to the rest of the pelvic bone by the superior pubic branch, and inferiorly to the ischium by the inferior pubic branch (Aiello and Dean, 1996).

The pubic crest is the attachment site for one of the main muscles supporting the intestine, the rectus abdominis, and the pubic tubercle is associated with the strongly developed inguinal ligament (Aiello and Dean, 1996).

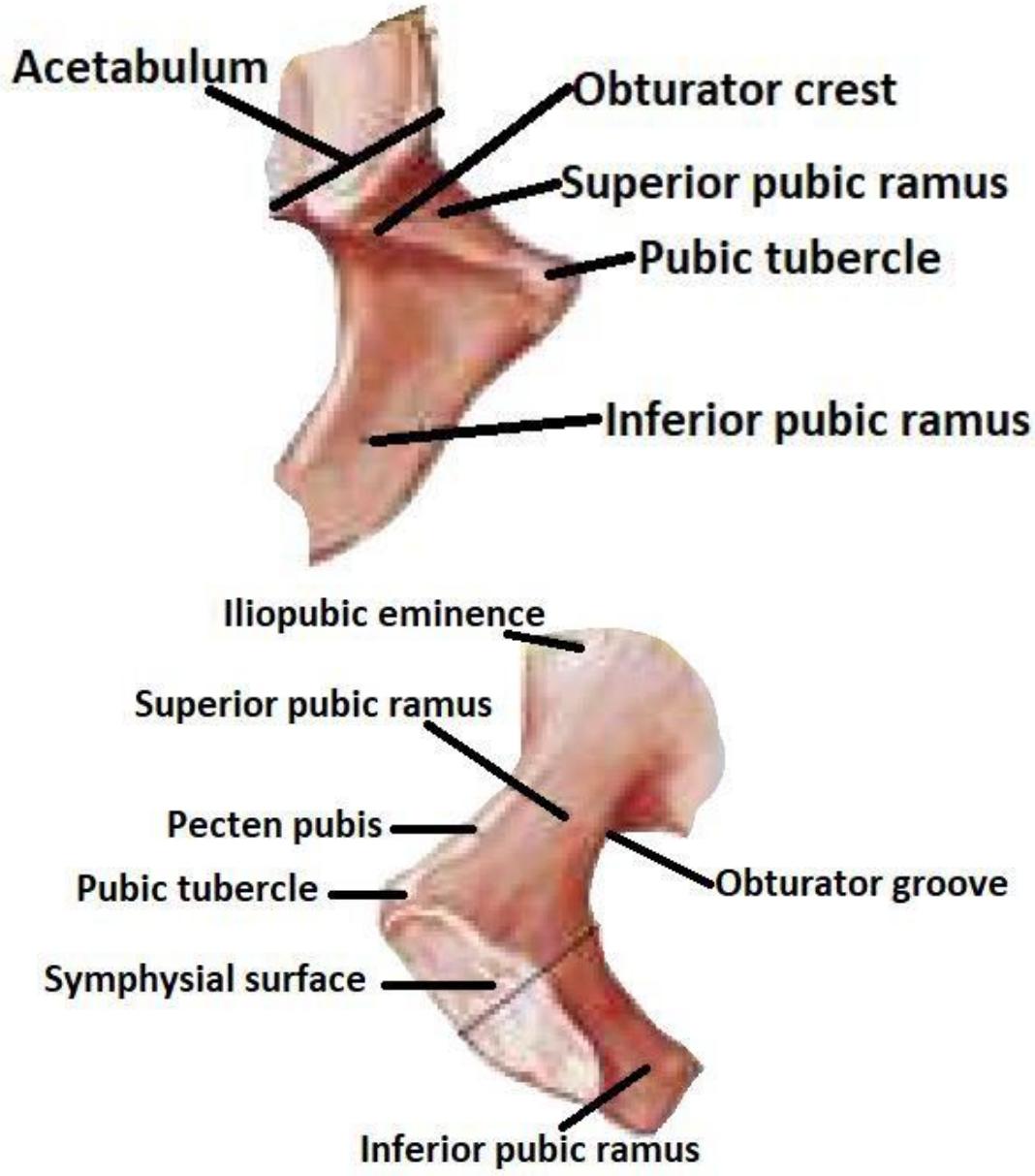


**Fig.6** *Lateral view (above) and medial view (below) of the pubis with its parts. (image modified from* Netter Atlas of Human Anatomy *by Frank H. Netter)* (Netter, 2022).

### 3.1.4 The sacrum and coccyx

The sacrum (**Fig.6**) is a wedge-shaped bone that is part of both the spine and the pelvis. The body of the sacrum consists of five serrated vertebrae that not only form the dorsal aspect of the pelvis, but also provide a solid base to support the weight of the upper body. At the bottom of the sacrum is the coccyx, which comprises the last four rudimentary signs of the vertebral column (Aiello and Dean, 1996).

The sacrum is wide and positioned at a more acute angle than the lumbar spine, which is supported. Both of these characteristics are related to bipedal locomotion. The width of the sacrum increases the distance between the sacroiliac joints and positions them more vertically on the hip joints. This reduces stress on the pubic symphysis and limits the rotation of the pelvic bones around the sacroiliac joint. The large dorsal surface of the sacrum together with the large iliac tuberosities also provide more leverage for the pelvis (Aiello and Dean, 1996).

The horizontal orientation of the sacrum in AMH has been attributed to the needs of the fetal head at birth, as it is larger than that of other hominins. However, the orientation of the sacrum together with its position distal to the acetabulum may also be eclipsed by the needs of bipedal locomotion (Aiello and Dean, 1996).

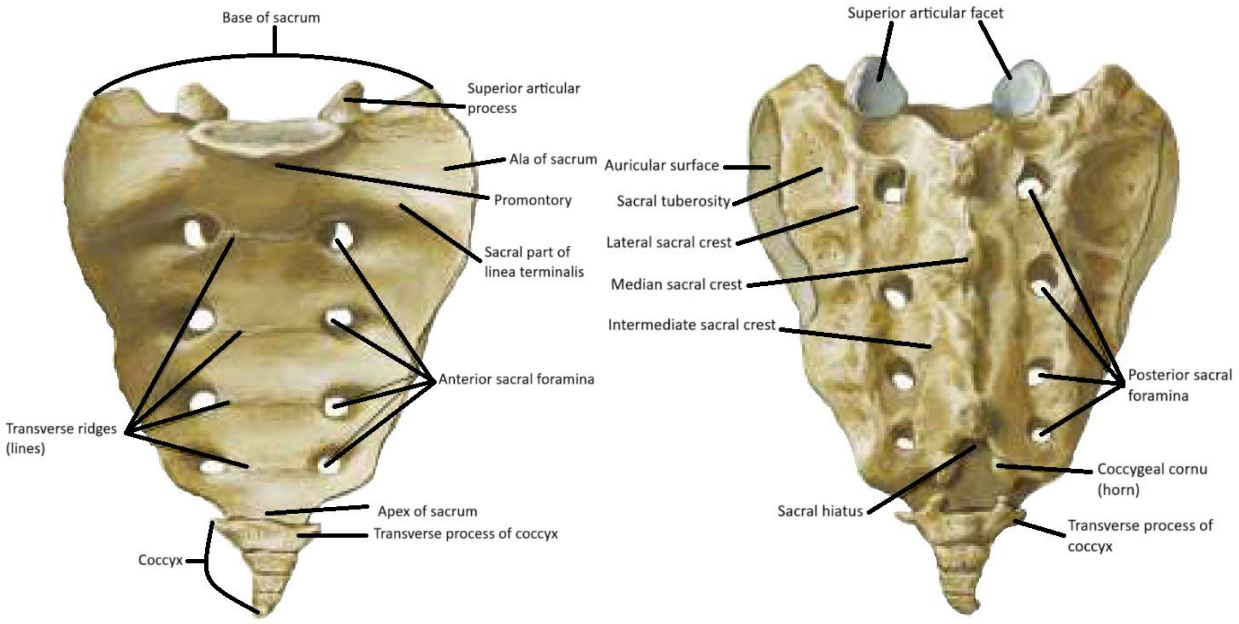


**Fig.6** *Anterior view (right) and posterior view (left) of the sacrom and coccyx with their parts. (image modified from* Netter Atlas of Human Anatomy *by Frank H. Netter)* (Netter, 2022).

### 3.1.5 The acetabulum and the hip joint

The ilium, ischium and pubis meet in the acetabulum, the cavity of the hip joint. However, these bones do not meet in the centre of the acetabulum. The largest part of the acetabulum is the ischium (Aiello and Dean, 1996).

The acetabulum faces in three directions: inferior, lateral and anterior. The upper edge of the acetabulum protrudes from the centre of the femoral head by approximately 30° and bears more pressure during bipedal locomotion. In the horizontal cross-section, the acetabulum faces anteriorly at 30-40° from the coronal plane. Because of this orientation, when the femoral head is articulated with the acetabulum in an upright posture, the anterior part of the joint is open. This arrangement of the acetabulum results simultaneously in joint stability during standing and maximum freedom of movement of the leg anterior to the body in flexion, adduction and medial rotation (Aiello and Dean, 1996).

### 3.1.6 *Homo neanderthalensis* pelvis

The morphology of the pelvis of *Homo neanderthalensis* (**Fig.7-8**), the best descriptions, are based on the pelvis of Kebara 2, as it is the best preserved pelvis. The pelvis bone and sacrum are in a different relationship to the hip bones (acetabula) unlike AMH. The iliac blades are rotated outwards, which also affects the orientation of the acetabula, causing them to be positioned more laterally than in AMH (Aiello and Dean, 1996; Adegboyega *et al.*, 2021).

This position of the iliac blades causes Neanderthals to have a more elongated pubis. In addition, the pubic symphysis is more anterior than in AMH because the promontory of the sacrum is placed closer to the line connecting the anterior acetabular margins. The iliac blade also widens equally anteriorly and posteriorly, causing the greater sciatic notch to be less pronounced than in AMH (Aiello and Dean, 1996; Adegboyega *et al.*, 2021).

In its frontal view, the pubic body appears to be more elongated anteromedially, resulting in an elongated upper pubic ramus and a more amber subpubic angle than in AMH (Aiello and Dean, 1996; Adegboyega *et al.*, 2021).

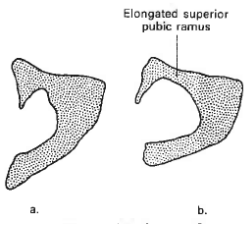


**Fig.7** *(a.) AMH pubic bone; (b)* Homo neanderthalensis *pubic bone (image modified from* An Introduction to Human Anatomy *by L. Aiello & C. Dean)* (Aiello and Dean, 1996)

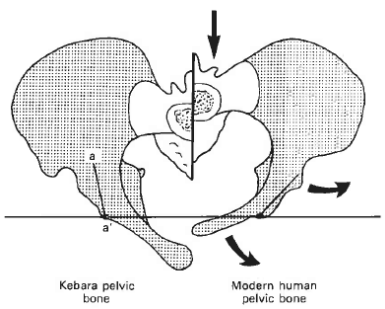


**Fig.8** *Comparison between* Homo neanderthalensis *(left) and AMH (right) pelvis bones* (Aiello and Dean, 1996).

## 3.2 Femur

The largest and longest bone in the whole body of AMH is the femur (**Fig.9**), which can be divided into three parts: proximal end (head-neck), shaft and distal end (condyle). In this paper we will only consider the upper end of the femur (Aiello and Dean, 1996).

The femoral head consists of three main parts: head, neck and the two trochanters (major and minor) (Aiello and Dean, 1996).

### 3.2.1 Femoral head

The head (**Fig.10**) is about two-thirds the shape of a sphere, which articulates with the pelvis via the acetabulum and forms the hip joint. In the medial part of the head is the fovea capitatis, which is a depression on the head that serves to attach the head ligament, inside of which are the blood vessels that supply this part of the femur (Aiello and Dean, 1996).

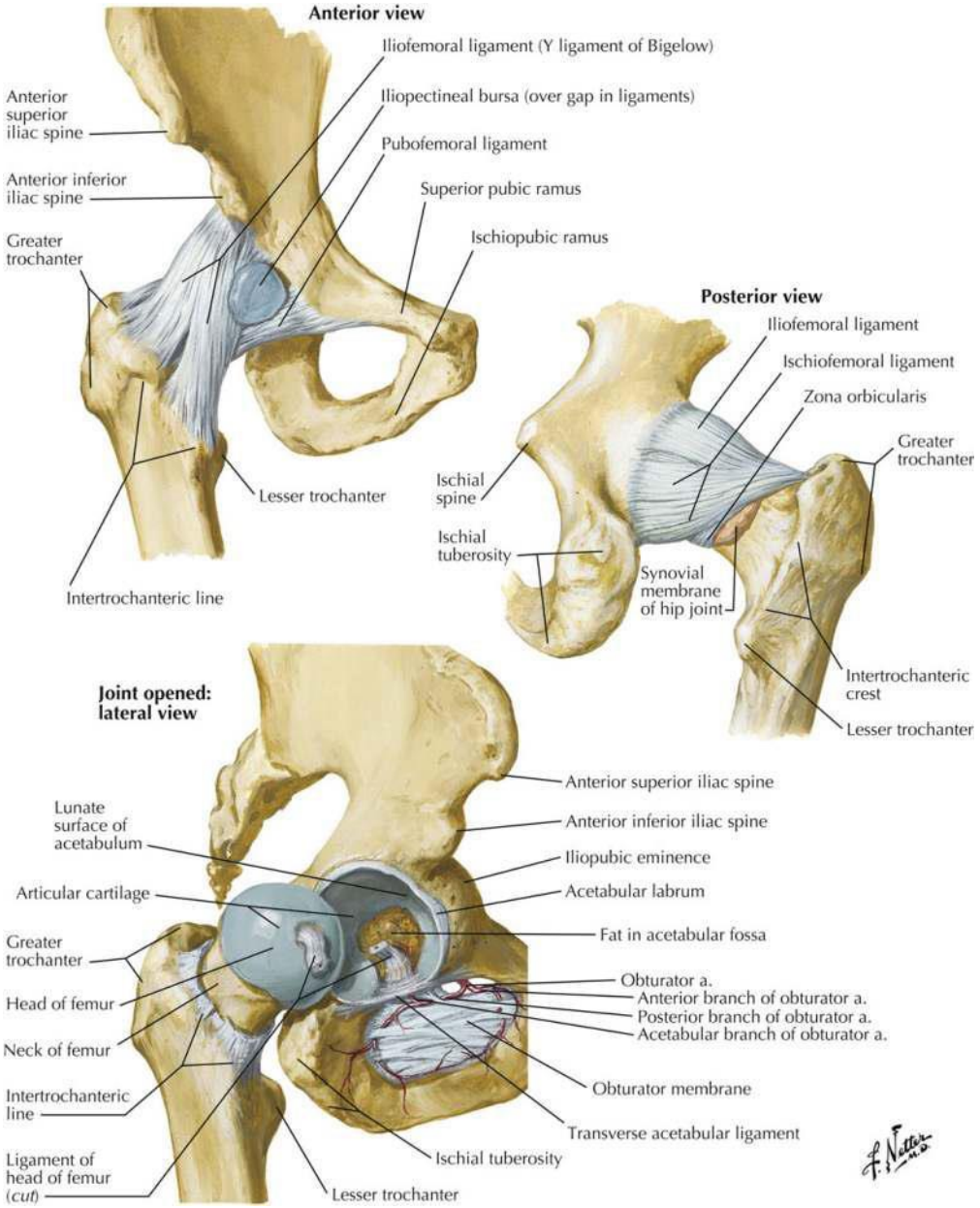


**Fig.9** *Hip joint, junction between femur and pelvis (Netter, 2022).*

### 3.2.2 Femoral neck

The femoral head (**Fig.10**) is connected to the rest of the femoral body via the neck. At the front of the proximal femur, the boundary between the neck and the femoral body is marked by the intertrochanteric line and is also the line of attachment of the most important ligament of the hip joint, the iliofemoral ligament. The neck of the femur has an hourglass shape and extends from the lateral part of the femoral head to the greater trochanter (always located laterally) (Aiello and Dean, 1996).

Many ligaments of the femoral muscles anchor to it and it is covered by other ligaments thatanchor to the pelvis and also serve to form the hip joint (Netter, 2022).

### 3.2.3 Major trochanter

The greater trochanter (**Fig.10**), as mentioned earlier, is located lateral to the head and neck of the femur. On the lateral surface of the greater trochanter is the insertion area of the gluteus medius, which is an important adductor of the pelvis in the AMH. What resembles a fossa and is located medial to the greater trochanter is called the trochanteric or digital fossa and is the insertion area of one of the rotator ligaments of the thigh (Aiello and Dean, 1996).

### 3.2.4 Lesser trochanter

At the back of the proximal femur is the lesser trochanter (**Fig.10**), a protuberance in the shape of an inverted triangle and the insertion area of the main hip flexors, the iliopsoas. The two trochanters are connected by the intertrochanteric crest. In the proximal portion of the intertrochanteric crest is a protuberance, called the square tubercle, which is the insertion area of a lateral thigh rotator, the quatratus femoris (Aiello and Dean, 1996).

### 3.2.5 *Homo neanderthalensis* femur

The main characteristic of the femurs of *Homo neanderthalensis* is that they exhibit remarkable robustness. This robustness is also from the well-developed gluteal ridges, which suggest a very large and very powerful gluteus maximus, especially compared to that of AMH. The trochanteric fossae have a different shape and position than those of AMH, in fact they are located in distinct depressions within the gluteal crests, as opposed to being located laterally (Aiello and Dean, 1996).

Perhaps associated with a well-developed gluteal crest is the general rounded contour of the proximal trunk. Instead of being flattened anteroposteriorly, the metric index indicates that in Neanderthals this region is more rounded, as in modern humans (Aiello and Dean, 1996).

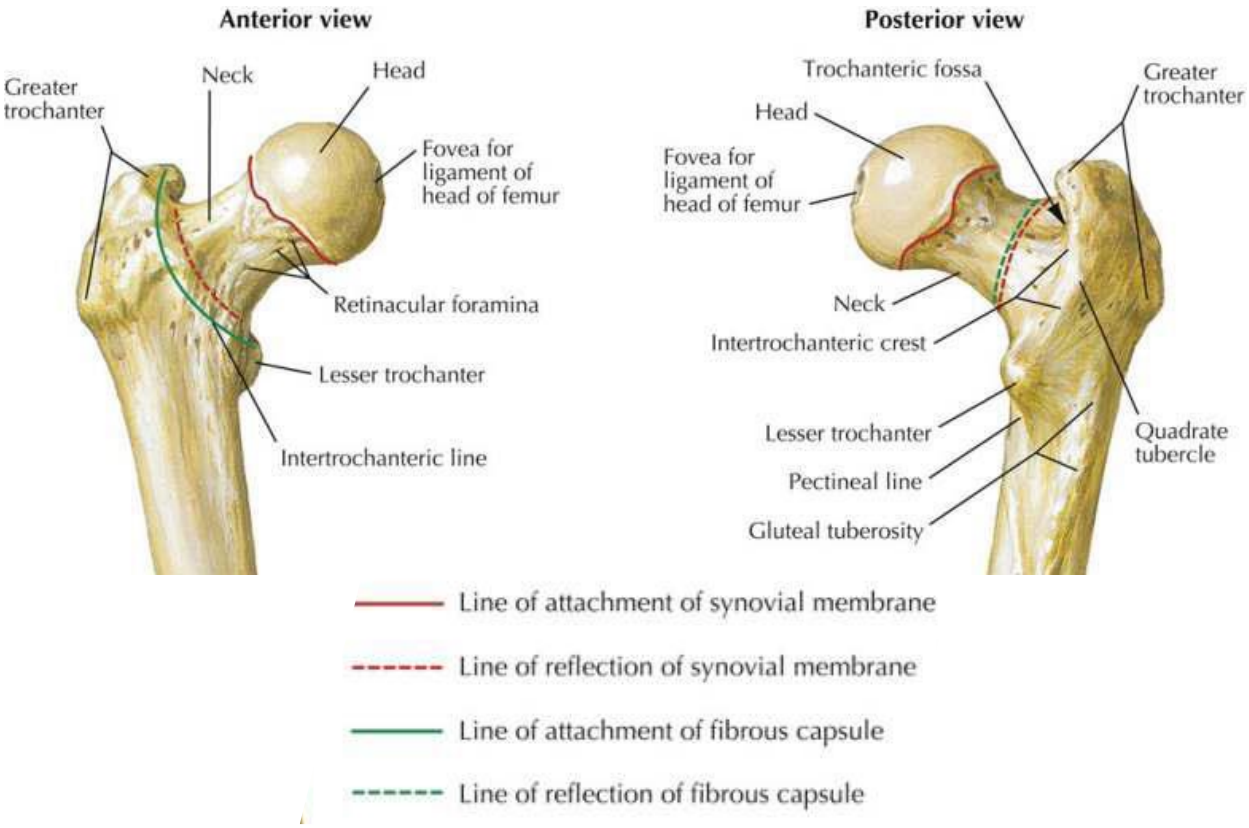


**Fig.10** *Anterior and posterior view of the proximal part of the femur (head, neck and two trochanters)* (Netter, 2022).

# 4 Materials and methods

## 4.1 Materials

### 4.1.1 Anatomically Modern Human (AMH)

The preliminary analyses for this paper were conducted on Anatomically Modern Human, i.e. Homo sapiens living today. In order to gain access to the material to be studied, the New Mexico Decedent Image Database (NMDID) was used. NMDID is a database that provides free access to CT scans of deceased persons (Edgar *et al.*, 2020).

Within NMDID it is possible to make a request to acquire CT scans - after subscribing to the site - by being able to choose which CT scans one wants. The search you can do within them can be general (age, gender, cause of death) or even very specialised, if you are looking for certain parameters in your analysis (Edgar *et al.*, 2020).

In the case of this paper, the following parameters were used:

- sex: male or female, individuals who had completed or were in the process of transitioning sex change were not considered;
- age: all selected individuals are between 20 and 50 years old
    - an age of less than 20 years was not chosen because only individuals who had completed physical development and whose bones were fully fused were chosen (it was taken into account that the age of bone fusion and physical development may differ from individual to individual);
- Causes of death: individuals who died in traffic accidents, bone tumours or from violent trauma to the lower part of the body and who may have damaged the part being analysed (pelvis and femur) were not taken into account; therefore, individuals who died mainly from natural causes (such as heart attacks), drug or alcohol overdoses, and/or trauma to the upper body were chosen;
    - medical history: all individuals with a medical history:
    - severe obesity;
    - bone tumours or tumours of the reproductive system;
    - previous pelvic and/or lower limb trauma;
    - possibility of bone or reproductive system tumours;

  they were discarded and not considered.

There are a total of 23 individuals taken into consideration (12 female individuals between the ages of 20 and 50; 11 male individuals between the ages of 20 and 50), and **Table 1** shows the two macro-divisions (male-female; age), the relative codes with which they are coded in NMDID, the relative codes assigned for the search of the elaborate and the specific age of each individual.

| Gender | Age Groups | NMDID ID Code | MT ID Code | Individual Age |
|---|---|---|---|---|
| Female | 20-30 | 102480 | AMH_F_01 | 24 |
| Female | 20-30 | 106665 | AMH_F_02 | 25 |
| Female | 20-30 | 108185 | AMH_F_03 | 30 |
| Female | 20-30 | 112802 | AMH_F_04 | 24 |
| Female | 31-40 | 102924 | AMH_F_05 | 37 |
| Female | 31-40 | 104735 | AMH_F_06 | 34 |
| Female | 31-40 | 107024 | AMH_F_07 | 34 |
| Female | 31-40 | 108398 | AMH_F_08 | 37 |
| Female | 41-50 | 101982 | AMH_F_09 | 48 |
| Female | 41-50 | 107090 | AMH_F_10 | 46 |
| Female | 41-50 | 109733 | AMH_F_11 | 43 |
| Female | 41-50 | 110062 | AMH_F_12 | 44 |
| Male | 20-30 | 100749 | AMH_M_01 | 23 |
| Male | 20-30 | 101358 | AMH_M_02 | 21 |
| Male | 20-30 | 103497 | AMH_M_03 | 27 |
| Male | 20-30 | 103559 | AMH_M_04 | 29 |
| Male | 31-40 | 100221 | AMH_M_05 | 34 |
| Male | 31-40 | 101427 | AMH_M_06 | 33 |
| Male | 31-40 | 111218 | AMH_M_07 | 32 |
| Male | 41-50 | 102253 | AMH_M_08 | 46 |
| Male | 41-50 | 103634 | AMH_M_09 | 43 |
| Male | 41-50 | 103772 | AMH_M_10 | 49 |
| Male | 41-50 | 104337 | AMH_M_11 | 42 |

**Tab.1** *All complete individuals with their subdivisions, codes (NMDID and Master Thesis (MT)) and the ages of each individual.*

### 4.1.2 *Homo neanderthalensis*

For the fossil record, it was not very easy to find and select the material. As is well known, one of the parts that is difficult to find in the fossil record and/or is in good condition is the pelvis. The femur, on the other hand, is better preserved than the pelvis because it is a much stronger bone. In order to be able to examine *Homo neanderthalensis*, permission was sought from the Muséum National d'Histoire Naturelle (MNHN) in Paris to do photogrammetry of some casts of fossils belonging to this species (how the photogrammetry was done will be explained later in Method) (MNHN citation).

The selected femurs and pelvises (**Tab.2**) come from different archaeological sites and many of them are not from the same individual. This non-connection between pelvis and femur may not

| MNHN NUMBER | NUMBER | INDIVIDUL | DESCRIPTION | TYPE |
|---|---|---|---|---|
| 17648 | 17648 | Krapina | Cast of the upper end of a femur from Krapina, Croatia | Femur Left |
| 213-2 | 213-2 | Krapina | Casting of a femur fragment from Krapina | Femur Left |
| 27806 | 27806-CL | Tabun | Cast of left coxal fron Tabun, Isreale | Coxal Left |
| 27825 | 27825-FR | Neanderthal | Cast of the femurs of Homo neanderthalensis, from the Neander Thal valley, Germany | Femur Right |
| 28120 | 28120-CL | La Ferrassie I | Moulding of the Neanderthal post-cranial skeleton of La Ferrassie I, from La Ferrassie, Dordogne (including 2 iliacs and 2 femurs) | Coxal Left |
| 28120 | 28120-CR | La Ferrassie I | Moulding of the Neanderthal post-cranial skeleton of La Ferrassie I, from La Ferrassie, Dordogne (including 2 iliacs and 2 femurs) | Coxal Right |
| 28120 | 28120-FR | La Ferrassie I | Moulding of the Neanderthal post-cranial skeleton of La Ferrassie I, from La Ferrassie, Dordogne (including 2 iliacs and 2 femurs) | Femur Right |
| 28123 | 28123-CR | Tabun | Cast of right coxal from Tabun, Isreal | Coxal Right |

**Tab.2** *Fossils from MNHN in Paris: (starting from the left) the first column is the museum's identification number, the second column is the identification number used for the analysis of the work, the third is the provenance, the fourth the description provided by the museum, the fifth the anatomical part to which it corresponds.*

bring truthful data regarding the analyses that were carried out on the fossil record, but we still want to see if this type of methodology is also applicable on them.

When choosing the fossil record, it was also taken into account that the casts had some nonoriginal parts, i.e. areas where the missing part was filled in with other material in order to give the fossil as true a shape as possible. In addition, it was not possible to analyse all the casts provided by the MNHN because many of them were only small fragments or only parts of the pelvis, as almost complete pelvises were needed for the analysis of this paper. Precisely for this reason, the sample to be used was reduced even further and considerably.

### 4.1.3 Software

The following software was used to analyse the data collected from AMH and *Homo neanderthalensis:*

- *3DSlicer*: is an open access programme that allows a 3D to be obtained from CT scans requested from NMDID. With this programme it was possible to select the body parts that were of interest for research and make a 3D (Fedorov *et al.*, 2012);
- *AgisoftMetashape*: is a paid programme, but offers a free trial of 30 of a calendar month, during which I was able to make 3Ds of casts from MNHN. This programme orients all the high quality photos of the casts from MNHN in order to be able to make 3Ds of them (the process will be explained later in the methods in the 3D section) (ask how to quote AgisoftMetashape);
- *Landmark*: is a free programme that allows you to apply landmarks on 3Ds obtained with AgisoftMetashape and saved in .ply format, after applying the landmarks you can obtain information about each of them (ask how to quote Landmark).
- *PAST*: is a statistics programme that is always free of charge. The acronym PAST stands for Paleontological Statistics. This programme is used to perform all the statistical analyses to derive the necessary data and conclusions for this programme (ask how to quote PAST).

## 4.2 Methods

### 4.2.1 Landmarks

The first thing that was done was to identify the landmarks that were then used for all the 3Ds obtained by both CTscans and photogrammetry.

In order to be able to select which landmarks were the most suitable, the anatomy of the pelvis and femur was studied in great detail and in every part, mainly using anatomical atlases, such as (Netter, 2022), and osteology books, such as (Aiello and Dean, 1996; Rohlf, 2000; White and Folkes, 2005; White, Black and Folkes, 2011; Richtsmeier, Lele and Cole, 2018).

For the pelvis, it was decided to analyse its entire surface, both the lateral and the medial side (**Fig.11**). It will be noted that many of the landmarks are located mainly on the lateral side of the pelvis, as this is the side where the hip joint is located (insertion of the femur into the pelvis), and therefore of fundamental importance for this research.

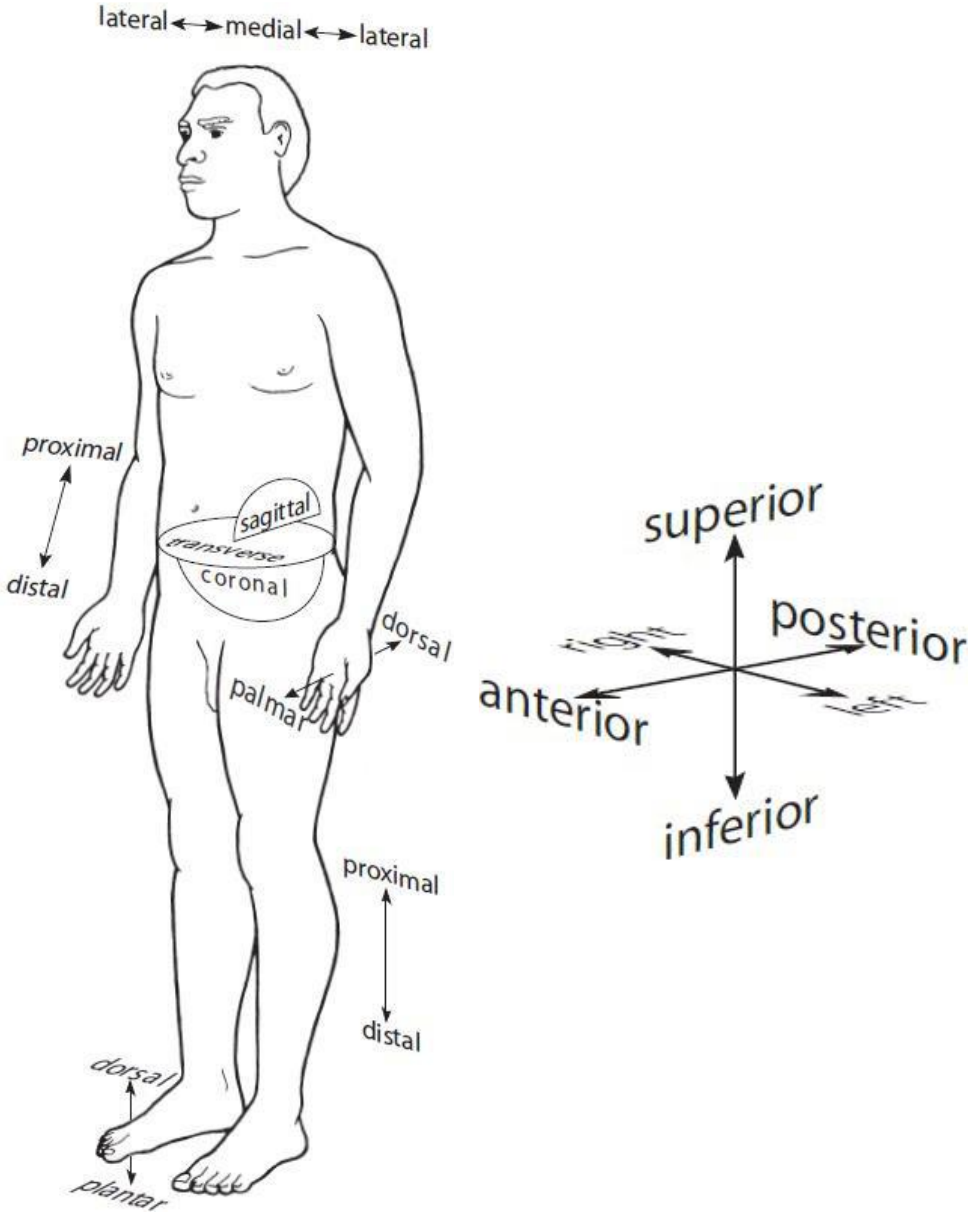


**Fig.11** *Terms and directional plans used in the osteological study of an AMH and for a hominin (modified from The Human Bone Manual by T. D. White and P. A. Folkens* (White and Folkes, 2005).

In order to select the various landmarks applied to the pelvis - shown below in **Tab.3** and visible in **Fig.12** - articles on other studies applied to the pelvis were read (Lycett and von Cramon-Taubadel, 2013; Candelas González *et al.*, 2017; Ward, Maddux and Middleton, 2018; Audenaert *et al.*, 2021).

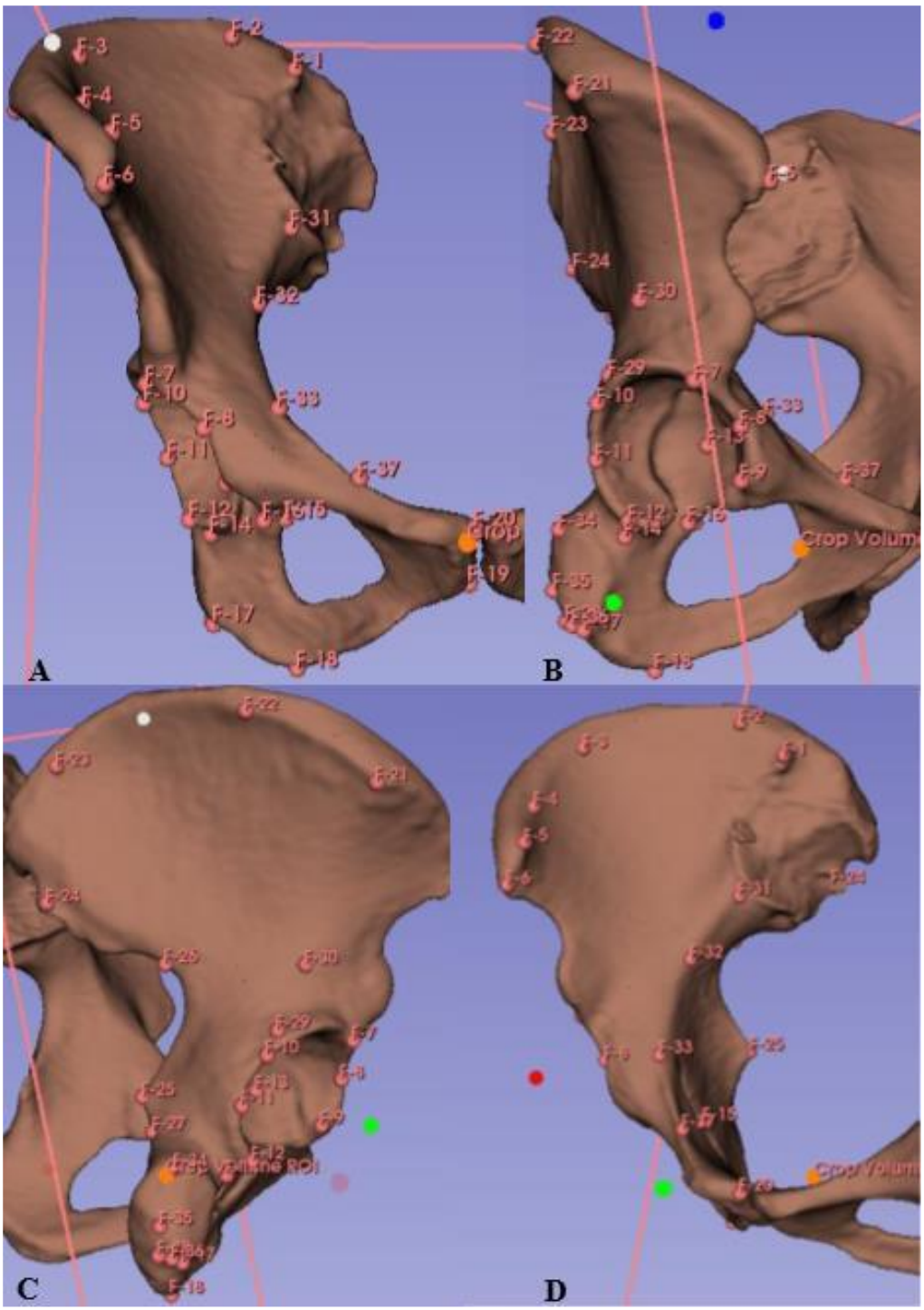


**Fig.11** *Landmarks applied to all individuals examined, both AMH and H. neanderthalensis; (A) Front view; (B) Front-lateral view; (C) Rear-lateral view; (D) Front-superior view.*

| n. landmark | Landmark Code | Name Landmark |
|---|---|---|
| 1 | PLMR_ILCR | Posterior lateral margin of the iliac crest |
| 2 | PSMR_ILCR | Posterior superior margin of the iliac crest |
| 3 | PMR_ILCR_B2-4 | Posterior margin of the iliac crest between 2 and 4 points |
| 4 | PIMR_ILCR | Posterior inferior margin of the iliac crest |
| 5 | MPR_PS_ILSP | Most prominent point of the posterior superior iliac spine |
| 6 | MPR_PI_ILSP | Most prominent point of the posterior inferior iliac spine |
| 7 | ASMR_ACMR | Anterior superior margin of the acetabular margin |
| 8 | MAMR_ACMR | Most anterior point of margin the acetabular margin |
| 9 | AIMR_ACMR | Anterior inferior margin of the acetabular margin |
| 10 | PSMR_ACMR | Posterior superior margin of the acetabular margin |
| 11 | MPMR_ACMR | Most posterior point of margin the acetabular margin |
| 12 | PIMR_ACMR | Posterior inferior margin of the acetabular margin |
| 13 | C_AC_INAR | Centre of the acetabulum, obtained from the midpoint of the connection of points 7, 8, 9, 10, 11, 12, inside the articulation |
| 14 | INS_BAC-IS | Insertion between acetabulum and ischium |
| 15 | PS_OBFO | Posterior superior point of obturator foramen |
| 16 | PRJLM_OBFO | Projection of landmarks 15 over the anterior rim of the obturator formen |
| 17 | V-L_LCRIS | Ventrolateral of the lateral crest of the ischium |
| 18 | V-L_TBIS | Ventrolateral of the tuberosity of the ischium |
| 19 | CIMR_PBSY | Caudal inferior margin of pubic symphysis |
| 20 | CSMR_PBSY | Caudal superior margin of pubic symphysis |
| 21 | MPRMR_ILCR | Most prominent point of margin of iliac crest |
| 22 | DMR_ILCR | Deepest point of margin of iliac crest |
| 23 | MPMR_ILCR | Most posterior point of margin of iliac crest |
| 24 | ASMR_ILSP | Anterior superior margin of the iliac spine |
| 25 | ILSP | Ischial spine |
| 26 | LSCNT | Lesser sciatic notch |
| 27 | GRSCNT | Greater sciatic norch |
| 28 | PBTBC | Pubic tubercle |
| 29 | S_ACGR | Superior acetabular groove |
| 30 | ILFS | Iliac fossa |
| 31 | S_ARLN | Superior arcuate line |
| 32 | P_B31-33 | Point between 31 and 33 points |
| 33 | I_ARLN | Inferior arcuate line |
| 34 | MPR_TBIS | Most prominent point of ischial tuberosity |
| 35 | D_TBIS | Deepest point of ischial tuberosity |
| 36 | MI_TBIS | Most inferior point of ischial tuberosity |
| 37 | MPR_IS-PBEM | Most prominent point of ischio-pubic eminenscence |

**Tab.3** *Landmarks used (all and/or in part) for the 3Ds of the pelvis of both AMH and Homo neanderthalensis*.

For the landmarks of the femur, the same procedure was followed as for the pelvis. Note well that the landmarks of the femur are concentrated only on the proximal part of the femur, i.e. on the head, the neck and the two trochanters (Witham, 1987; Harmon, 2007, 2009; Holliday *et al.*, 2010; Bonneau *et al.*, 2012; Pujol *et al.*, 2014).

The landmarks selected for the femur are as follows **Fig.12** and **Tab.4**:

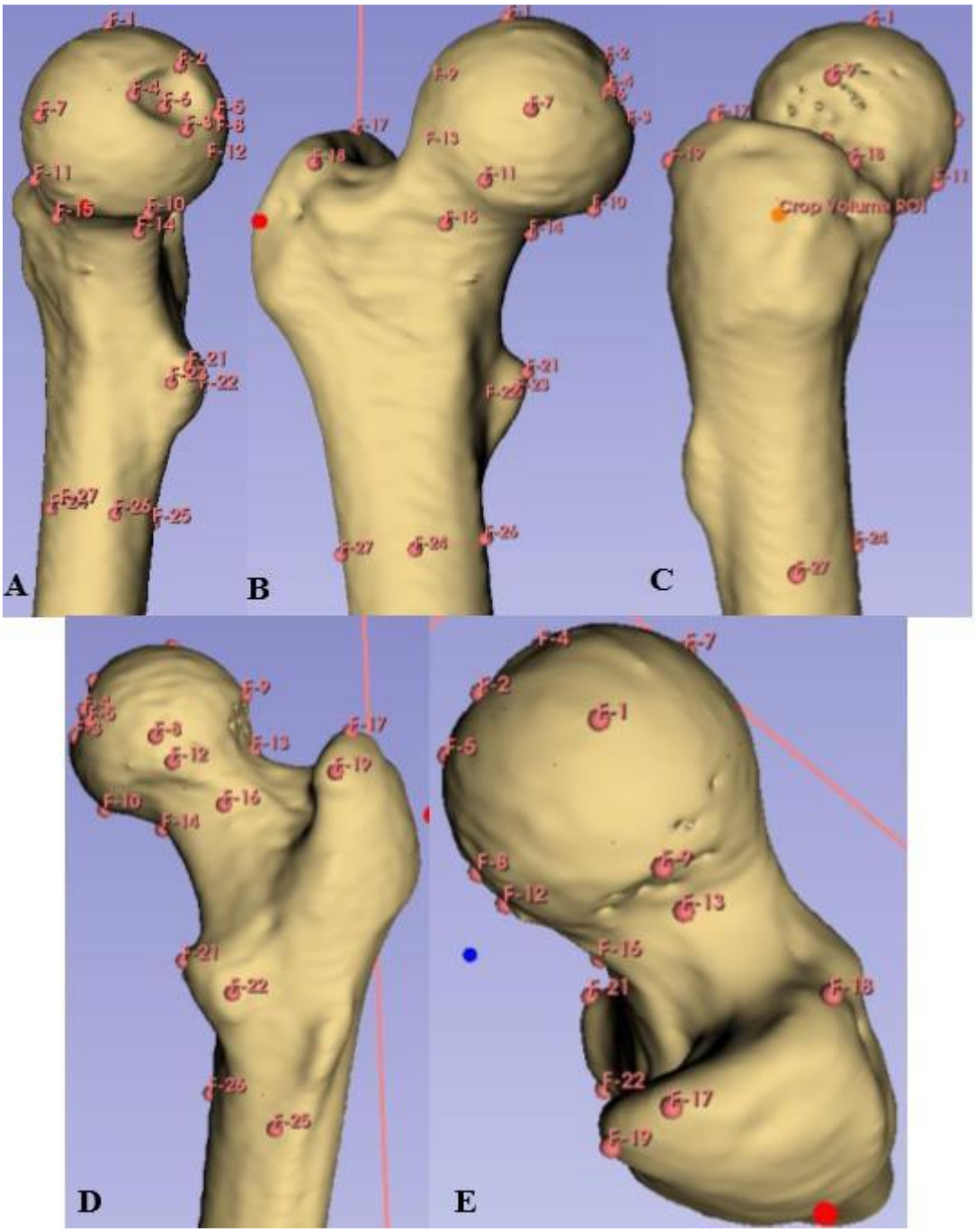


**Fig.12** *Landmarks applied to all individuals examined, both AMH and H. neanderthalensis; (A) Medial view; (B) Anterior view; (C) Lateral view; (D) Posterior view; (E) Superior/ view.*

| n. landmark | Landmark Code | Name Landmark |
|---|---|---|
| 1 | MS_FH | Most superior point (tangential) of femoral head |
| 2 | MS_FC | Most superior point of superior of fovea capitis of femoral head |
| 3 | MI_FC | Most inferior point of inferior of fovea capitis of femoral head |
| 4 | MA_FC | Most anterior point of fovea capitis of femoral head |
| 5 | MP_FC | Most posterior point of fovea capitis of femoral head |
| 6 | C_FC | Center of fovea capitis of femoral head (obtained by joining points 2, 3, 4, 5) |
| 7 | MA_FH | Most anterior point of femoral head |
| 8 | MP_FH | Most posterior point of femoral head |
| 9 | MS_HNI | Most superior point of head-neck intersection |
| 10 | MI_HNI | Most inferior point of head-neck intersection |
| 11 | MA_B5-6P_HNI | Most anterior point between 5and 6 points (above) of head-neck intersection |
| 12 | MP_B5-6P_HNI | Most posterior point between 5and 6 points (above) of head-neck intersection |
| 13 | MS_FN/M | Most superior point of femoral neck/midsharft (along axis of neck) |
| 14 | MI_FN/M | Most inferior point of femoral neck/midsharft (along axis of neck) |
| 15 | MA_FN/M | Most anterior point of femoral neck/midsharft (along axis of neck) |
| 16 | MP_FN/M | Most posterior point of femoral neck/midsharft (along axis of neck) |
| 17 | MPR_GT | Most prominent point of greater trochanter |
| 18 | MA_GT | Most anterior point of greater trochanter |
| 19 | MP_GT | Most posterior point of greater trochanter |
| 20 | D_TF | Deepest point of trochanteric fossa |
| 21 | MPR_LT | Most prominent point of lesser trochanter |
| 22 | MP_LT | Most posterior point of lesser trochanter |
| 23 | MA_LT | Most anterior point of lesser trochanter |
| 24 | MA_PRX1/3S | Most anterior point of proximal one-third of shaft (just inferior to lesser trochanter) |
| 25 | MP_PRX1/3S | Most posterior point of proximal one-third of shaft (just inferior to lesser trochanter) |
| 26 | MM_PRX1/3S | Most medial point of proximal one-third of shaft (just inferior to lesser trochanter) |
| 27 | ML_PRX1/3S | Most lateral point of proximal one-third of shaft (just inferior to lesser trochanter) |

**Tab.4** *Landmarks used (all and/or in part) for the 3Ds of the femur of both AMH and Homo neanderthalensis.*

Landamrks were not applied with the same programme for AHM and *H. neanderthalensis*. In fact, for AHM, *3DSlicer* was used (will be explained in section 3.2.2), as it offers an extension that allows them to be applied; for *H. neanderthalensis*, the special *Landmarks* programme was used (will be explained in section 3.2.4).

**4.2.2 3D obtained with 3DSlicer**

In order to be able to have useful data for research purposes for this paper, permission was sought (as explained in the previous subsection Materials) from NMDID to have the CT scans in their database. As explained above, some basic requirements were chosen in order to be able to select the best individuals for this research (to see which ones see the previous subsection Materials).

Once permission had been obtained to download the CT scans from their site, the CTscans containing images of the thorax, pelvis and femurs were extracted from the compressed folder. These files in DICOM format[5] were uploaded to the 3DSlicer programme. As explained above in the Materials subsection, this is a free programme that allows you to create a 3D model from CTscans.

In this case, only the parts that were needed for this elaboration, pelvis and femurs (including the sacrum), were culled; in some cases, the torsos had to be removed. In order to do this, you have to choose the search button (it is shaped like a magnifying glass) from the menu bar and look for "*Crop Volume*" and after selecting it, click on "*Switch to module*". On the facade that appears, in order to click "*Create a new ROI*", you have to select the "*Input ROI*" drop-down list. With "*Create a new ROI*" it is possible to reduce the portion of the CTscan, so that only the part affected by the search is shown in 3D.

Once this was done, you went to select "*Segmentation editor*" and then clicked on "*Threshold*". On "*Threshold*" you have to choose parameters to be able to have a 3D with less aberrations due to the muscles attached to the bones, you don't have fixed parameters, as they depend on the quality with which the CT scan was done. Once the parameters have been chosen, one clicks on "*Apply*", then on "*Show 3D*" and on the red view quadrant or marked with the number 1, one clicks on "*Central view*", so that one can see the result of all the operations performed previously. In some cases, the 3D also included the pipes of the IV or cadaver bag hinges and then proceeded to remove them using the "*Scissors*" setting, which allows the affected portion to be selected and removed.

After all these operations have been done, we proceed to the selection of the various parts that make up the pelvis and femur. On click on "*Paint*" and a panel will appear allowing you to select the various settings for the cursor. In order to speed up the work, a cursor of between 3 and 5 per

[5] Digital Imaging and Communications in Medicine (DICOM) is the standard format used for the communication and management of medical imaging information and related data (DICOM, 2019).

cent is chosen, then in "*Sphere brush*" mode so that the parts you are going to select also appear on the next slice. Careful attention is paid to the edges of each anatomical part when it is close to another, so as not to select, even minimally, a section of the adjoining part.

Once the femur, pelvis and sacrum had been selected and coloured in different colours, they were darkened by clicking on "*Segment visibilty*" so that on the various portions showing the three different views and the 3D only the part one wanted to see remained. By doing this, it was possible to clean up and arrange each part of the 3D as best as possible, so that the data would also be as true as possible.

Landmarks, as mentioned earlier in section 3.2.1, were entered with this programme via the "*Landmarks registration*" extension. This extension can be found in the drop-down menu under "*Registration*". In the window that appears where it asks "*Pick the volumes to use for landmarks based linear registration*" you have selected, for both "*Fixed volume*" and "*Moving volume*", "*THIN ST TORSO cropped*", then click on "*Apply*". To add a new landmark each time, clicked on "*Add*". Once positioned, everything was saved. Among the saved files was a file called "*F.mrk*", in which all the coordinates of each landmark for the X, Y and Z axes were saved. This data was subsequently entered into the *PAST* programme, which will be explained in section 3.2.5.

### 4.2.3 3D obtained by photogrammetry

The technique of photogrammetry[6] was used to obtain 3D casts of fossils from MNHN. After requesting the consent of certain pre-selected casts (selection parameters explained in section 3.1.2), the collection contained within the structure of the *Musée de l'Homme* was accessed.

In order to do the photogrammetry, the protocol developed by Ficarra *et al.* (2022) (Ficarra and Lauria, 2022) was followed and adapted. The first thing that was done was to create a background that was as neutral as possible; since there was not a background neutral enough to allow photos with excellent quality, several white sheets were joined together so as to have a background and a base that were the same colour. The artefact was placed in the centre of this sort of camera obscura that was constructed so that by rotating it, it was always in the centre of the camera lens.

The Xiaomi Redmi Note 10 5G smartphone, which has three Leica cameras, was used to take the photos:

- the main camera is a 48 MP camera that allows HD photos to be taken;
- two 2 MP cameras:
    - one F/2.4 - Depth;
    - one F/2.4 - Macro.

[6] "Photogrammetry is a technique that allows high-resolution 3D models to be reconstructed from one or more sets of 2D digital images" (Ficarra and Lauria, 2022).

Photos were taken first of one side and then the other of the artefact. At each side of the find, a series of photos was taken from two different angles: the first angle was at 0° to the tabletop on which the cast being photographed was resting; the second angle was at 30° to the tabletop on which the cast being photographed was resting.

Once the photos had been obtained and uploaded to the computer, we switched to the *AgisoftMetashape* software[7]. In the article by Ficarra et al. (2022) (Ficarra and Lauria, 2022) they recommend dividing the photos into two groups, in each of which photos for each side of the find are contained. In the case of this research this was not possible, because the scales provided by the *AgisoftMetashape* programme were not used, but had to be added manually. Therefore, the photos were grouped into a single set of photos (**Fig.14-15**).

After uploading the photos, the "*Workflow*" drop-down menu was chosen from the menu bar, in which "*Align Photos*" was selected. In the window that appeared, the parameters were chosen (**Fig.16-17**):

- Accuracy: High;
- Key point limit 40,000;
- Limit constraint points: 4,000.

The other settings were not selected, so the blue tick did not appear.

Once the programme had finished aligning the photos (it took a few minutes).

The measurement scale was applied at this stage, so that landmarks that were later applied with the *Landmark* programme would have true measurements.

One selected the first images to be uploaded and by right-clicking on them selected "*Add Marker*" and repeated the operation two to four times, depending on how many stable and measurable visible points were present in the photos. Then for each photo they were placed in the exact spot where they were located.

In the menu on the side under "*Workflow*", two markers were selected at a time and in the "*Georeferences*" menu the correct measurements were entered by clicking on the pair of markers. The measurements that the programme requires are in metres, so the conversion from centimetres or millimetres to metres was made (**Fig.18-**).

Having done this, we proceeded to select, again from the "*Workflow*" menu, "*Build Dense Cloud*". The following parameters were selected in the settings (**Fig.18-19**):

- Quality: High;
- Depth filter: Aggressive.

[7] Agisoft Metashape is a stand-alone software product that performs photogrammetric processing of digital images and generates 3D spatial data to be used in GIS applications, cultural heritage documentation, and visual effects production as well as for indirect measurements of objects of various scales' (Agisfot LLC, 2006).

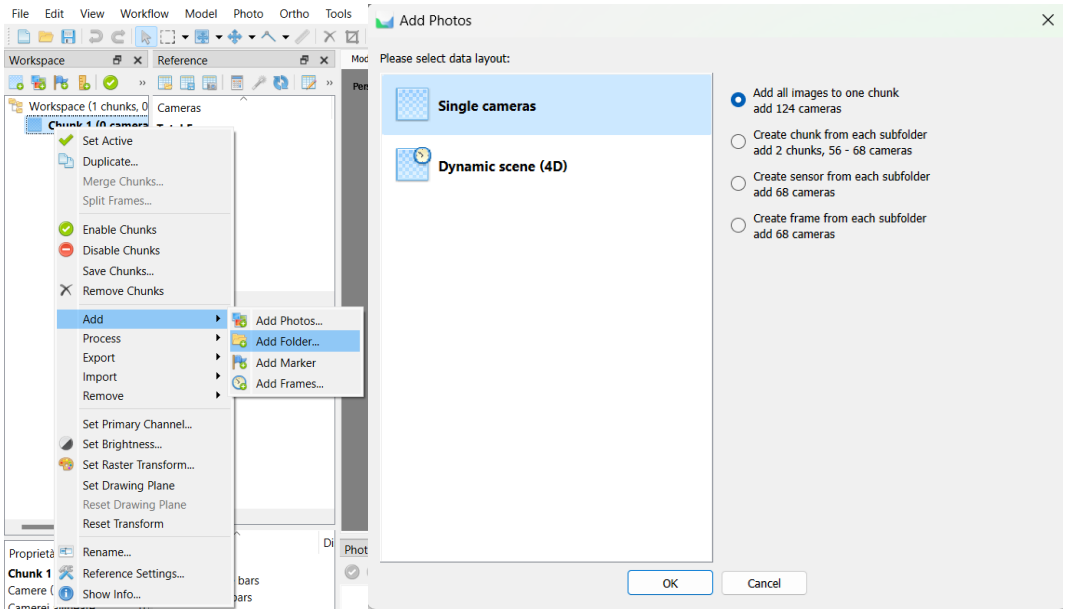


**Fig.14 (left) - 15 (right)** *How to upload photos into* AgisoftoMetashape Professional software (64 bit)

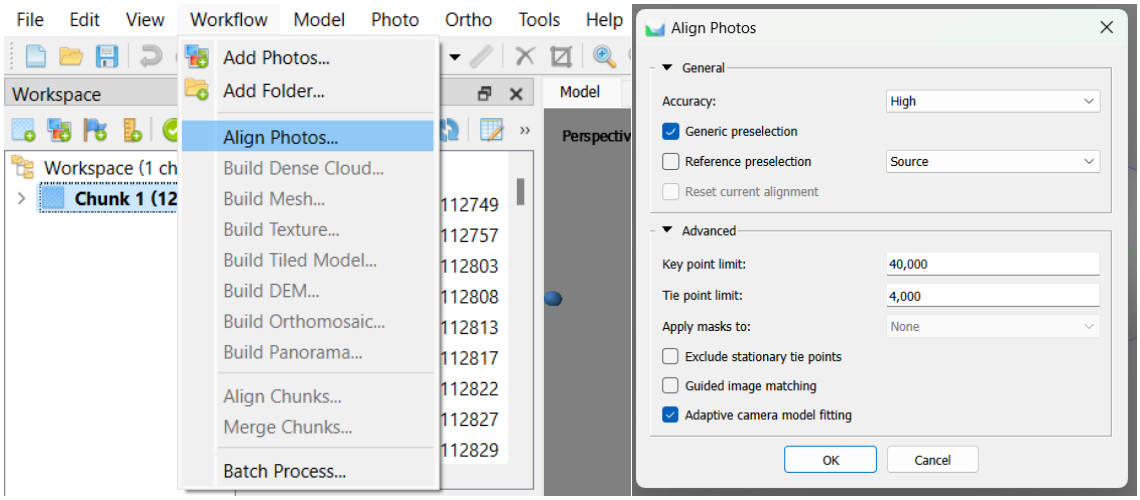


**Fig.16 (left) - 17 (right)** *How to align photos and what parameters to use into* AgisoftoMetashape Professional software (64 bit)

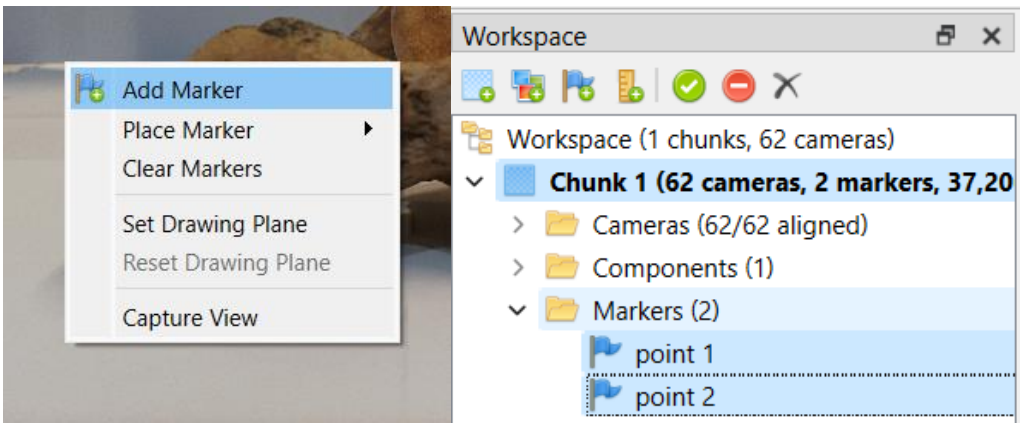


**Fig.18 (left) - 19 (right)** *How to Add and Select Markers into* AgisoftoMetashape Professional software (64 bit)

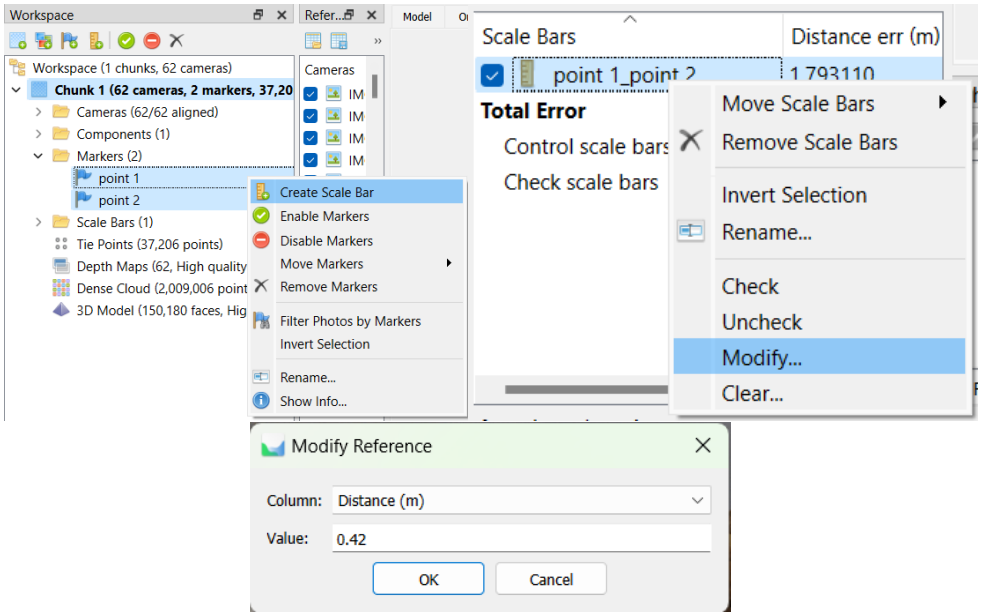


**Fig.20 (up-left) – 21 (up-right) – 22 (down)** *How to create a Scale Bar and how to add/correct Scale Bar values into* AgisoftoMetashape Professional software (64 bit)

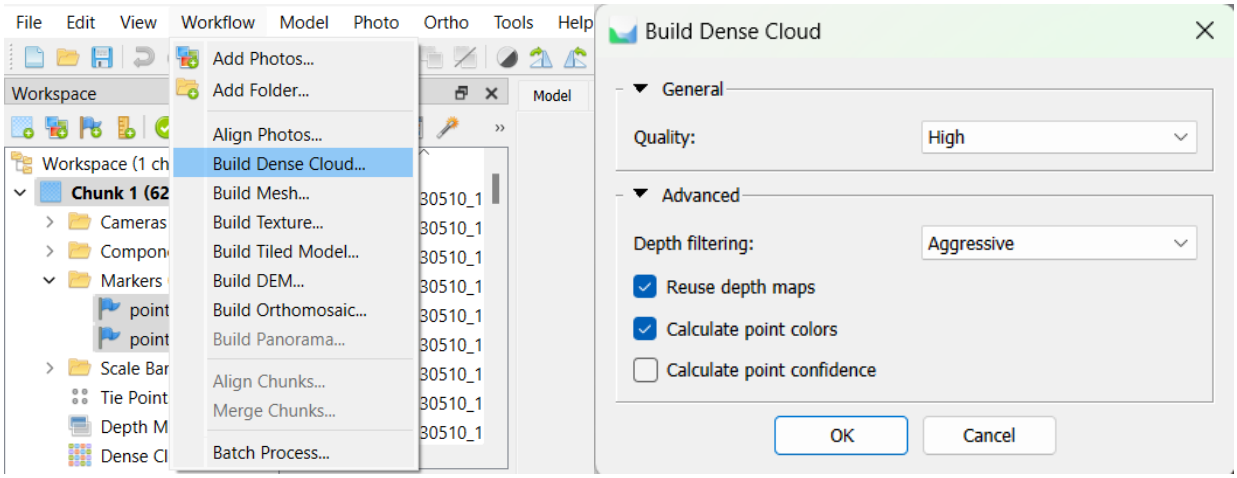


**Fig.23 (left) – 24 (right)** *How to apply Build Dense Cloud and what parameters to use into* AgisoftoMetashape Professional software (64 bit) *into* AgisoftoMetashape Professional software (64 bit)

- Reuse depth maps: Selected;
- Calculate colour points: Selected.

This process took from a few minutes to a couple of hours. Once finished you will get a very clear picture of what the final result will look like. If you do not select "*Calculate colour points*", what you will get is a blue 3D.

The next step is "*Build 3D mesh (triangulation)*" (**Fig.25-26**), which is always located under the "*Workflow*" menu. This again opens a menu for selecting the settings for the process that generates the 3D mesh. The parameters selected are as follows:

- Source data: Depth maps;
- Surface type: Arbitrary (3D);
- Quality: High;
- Face count: High;
- Interpolation: Enabled (default);
- Calculates vertex colours: Selected;
- Reuse depth maps: Selected.

This part of the process can take a few minutes if the previous steps have been done correctly, while if there was any problem it will take several minutes. At this point you will have the 3D done, the colour of which is blue. In order to have a 3D reflecting the colours of the cast, we proceeded to do "*Build Texture*" again from the " *Workflow* " menu. The following parameters were selected (**Fig.27-28**):

- Texture type: Diffuse map;
- Source data: Images;
- Mapping mode: Maintain UV;
- Blending mode: Mosaic (default);
- Texture size/count: 8192 x 1;
- Enable hole-filling: Selected;
- Enable ghosting filter: Selected.

Once the procedure was finished, three-dimensional images of the exhibits were obtained that are very much the same as the real ones in the MNHN.

Once this was done, the project was saved both in a format that could only be opened with *AgisoftMetashape Professional (64 bit)* and in the PLY format[8], so that it could be opened with the *Landmark* programme (**Fig.29-30**).

[8] PLY (Polygon File Format) is a file format, textual or binary, for defining 3D objects (Bourke, 2020).

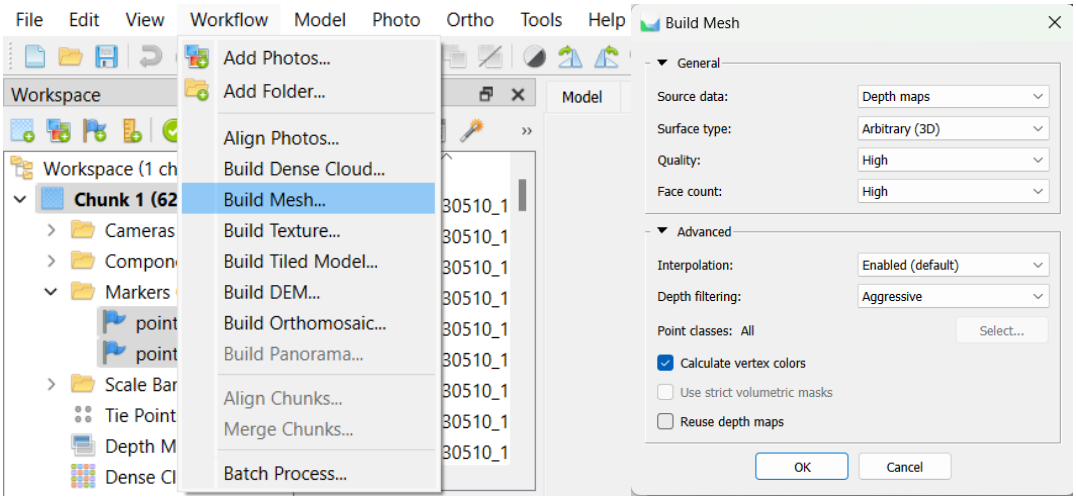


**Fig.25 (left) - 26 (right)** *How to apply Build 3D mesh (triangulation) and which parameters to use in* AgisoftoMetashape Professional software (64 bit)

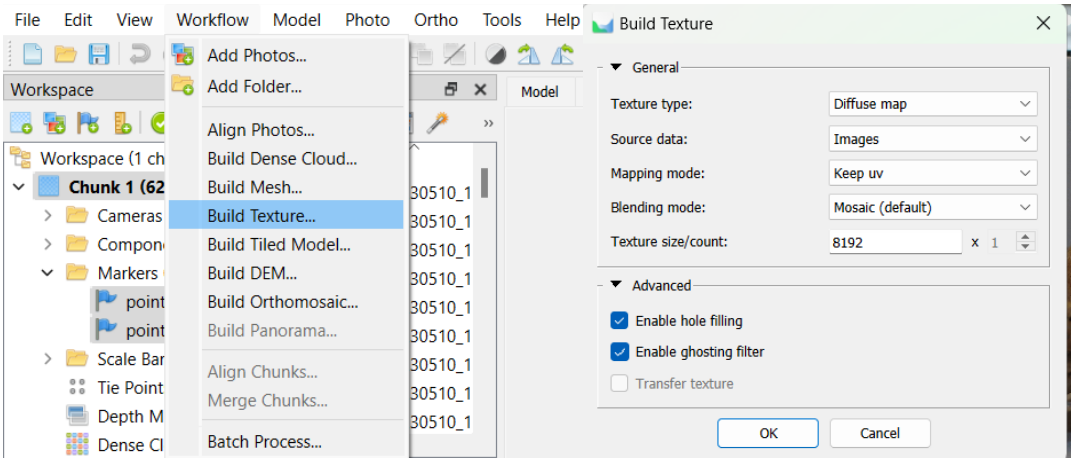


**Fig.27 (left) - 28 (right)** *How to apply textures and which parameters to use in* AgisoftoMetashape Professional software (64 bit)

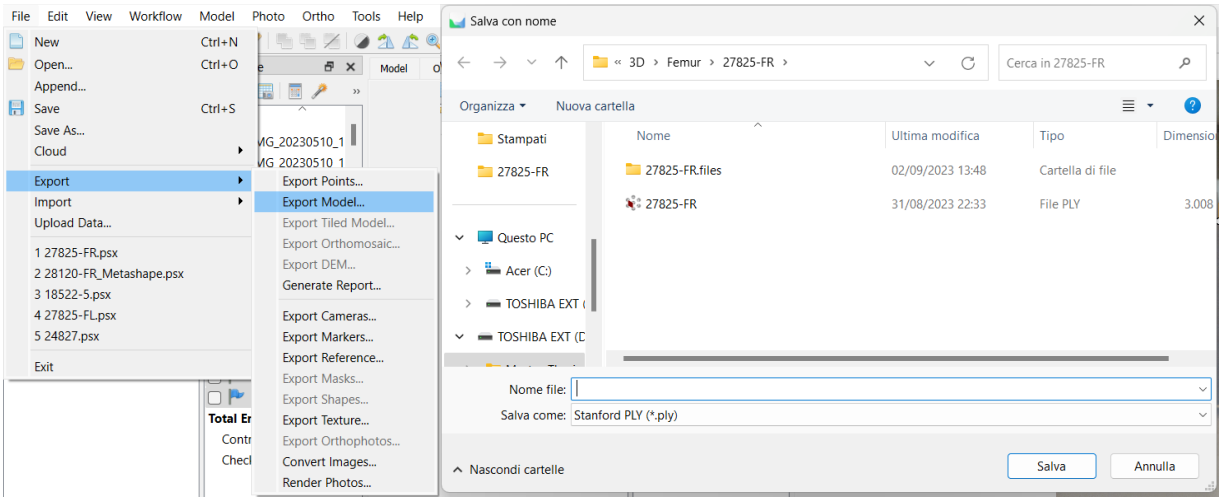


**Fig.29 (left) - 30 (right)** *How to save the 3D model in PLY format in* AgisoftoMetashape Professional software (64 bit)

### 4.2.4 *Landmark* software

The *AgisoftMetashape Professional (64 bit* programme does not allow landmarks to be applied and therefore does not allow coordinates to be obtained directly from it, as could be done with the *3DSlicer 5.3.0* programme. For this reason, another programme had to be used to obtain the data needed and provided by the landmarks; for this reason, the Landmark software was used. This software allows landmarks to be applied to files saved in PLY format (as explained in section 3.2.3).

In order to be able to apply landmarks, you need to upload PLY files into the programme. The only limitation of Landmark is that the working screens that can be used to apply landmarks, i.e. A and B do not both work, but only screen B can be used.

Before you can apply the landmarks, you must click on "*File*" and then on "*New*". In the window that appears, you will be asked for the name you want to give the project in the "*Project name*" box and where you want to save it in the "*Folder*" box. Once you have given the name and selected where to save it, click on "*Ok*".

Right-click after placing the cursor over the project, and from the drop-down menu that appears, select "*Import...*". A window will appear where you can choose the PLY file you wish to upload. Once selected, click on "*Open*" to open it. The name of the file will appear below the project you have created, and you will be able to see it in the B, you must right-click on the file name and select "Load to B" from the drop-down menu and wait for it to load (it may take a few minutes before you see it appear on the B screen).

Once the 3D is visible, in order to apply the landmarks you must simultaneously click the SHIFT key on the keyboard and the left mouse button. If you then want to move a landmark because you have realised that it is not in the correct position, simply place the cursor over the landmark and press the SHIFT key and the left mouse button simultaneously to move it.

Once you have finished applying all the landmarks, save the project. During saving, a file in PTS format will be created in which all information on the applied landmarks will be found, which will then be entered into the PAST programme (explained in section 3.2.5).

### 4.2.5 PAST or Paleontological Statistics

In order to do all the statistical analyses required for this paper, the programme *PAST 4.13* or *Paleontological Statistics 4.13* was used. This programme is a free programme that allows you to do all the analyses that can be done in palaeontology[9] and/or palaeoanthropology[10].

[9] A discipline that studies animals and plants that lived on Earth in past eras, revealed through their fossil remains (Enciclopedia Treccani, 2023c).

[10] A discipline that emerged in the second half of the 19th century [...], to study the origin and evolution of humans from the skeletal remains of fossilised hominins, in order to reconstruct their modification process after diverging

In order to be able to do the analyses, all the data must be brought back into the programme. Both the data obtained via 3DSlicer and those obtained via Landmark were directly copied and pasted as they were saved within the text files. Each column has the X, Y and/or Z co-ordinate of a specific landmark and each line is a specific individual.

After you have copied and pasted all the landmarks and all the individuals you have, you move on to give each individual a colour, so that in the graph you will obtain with PCA[11] each element will be visible and recognisable. Before doing this, you have to select "Row attribute" and three more columns of a different colour will appear. In the column entitled "Name", the name of each individual is entered in each row, so that in addition to the colour and/or symbol, it is also recognisable by that. In the column entitled "Symbol" a different symbol is to be assigned to each individual, a similar operation is to be carried out for the column entitled "Colour". It is not essential that everything be done at this time, but it must be done before doing the PCA, because it is precisely for interpreting the graph that will come out.

Before doing the PCA, another operation must be done. You select all the landmarks in the programme and then go to the menu bar and click on "*Transform*". In the drop-down menu that buys you click on "*Landmark*" and three options appear, you have to click on "*Procrustes*[12] *(2D+3D)*". In the window that appears you must select "3D" on the "Dimensionality" section and then select "*Rotate to the major axis*". Finally click on "*Ok*".

Once this step is done, you move on to do the PCA. In order to do the PCA, first of all, you select all the data at our disposal, then you proceed to click, again on the menu bar, on "Multivariate" and in the drop-down menu that appears, you click on the first item, "Ordination". There will be various options here, but to do the PCA, you have to click on the first option that is given, which is "Principal component (PCA)". You will not have to do anything else, as the programme will directly do all the analysis and present the graphs with the results already done.

In the resulting graph, it will be possible to see whether the hypothesis made that there is a correlation between the shape of the pelvis and the shape of the proximal part of the femur are correlated with each other.

from other hominids (the anthropomorphic African gorillas and chimpanzees); it is also called human palaeontology (Enciclopedia Treccani, 2023b).

[11] Principal component analysis is a technique for simplifying data used in the field of multivariate statistics. The aim of the technique is to reduce the larger or smaller number of variables describing a data set to a smaller number of latent variables, limiting the loss of information as much as possible (Tufféry, 2011).

[12] In statistics, Procrustes analysis is a form of statistical shape analysis used to analyse the distribution of a set of shapes (Dryden and Mardia, 1998).

# 5 Results

After having applied all the procedures explained in Methods (see point 3.2) we move on to analyse the graphs that have been obtained. We will first explain AMH, then *Homo neandethalensis* and finally proceed to explain in Discussion and Conclusion (see points 5 and 6) what the general conclusions of this analysis might be.

## 5.1 AMH

For Anatomically Modern Human, the sample was analysed by dividing it into the following categories:

- Femur;
- Pelvis.

For each of these anatomical parts, further subdivisions were made, resulting in this subdivision:

- Femur:
    - 20 to 30 years old (males and females);
    - 31 to 40 years old (males and females);
    - 41 to 50 years (males and females);
    - 20 to 50 years old (females);
    - 20 to 50 years old (males);
    - 20 to 50 years old (males and females);
- Pelvis:
    - 20 to 30 years old (males and females);
    - 31 to 40 years old (males and females);
    - 41 to 50 years (males and females);
    - 20 to 50 years old (females)
    - 20 to 50 years old (males);
    - 20 to 50 years old (males and females);

### 5.1.1 Femur

**20 to 30 years old (males and females)** This first group consists of individuals AMH_F_01, AMH_F_02, AMH_F_03, AMH_F_04, AMH_M_01, AMH_M_02, AMH_M_03 and AMH_M_04. They are male and female individuals aged between 20 and 30 years (see **Tab.1**).
As can be seen from the graph (**Graph.1**), there are no close values between males and females of the same age. Six individuals (AMH_F_02, AMH_F_03, AMH_F_04, AMH_M_01, AMH_M_02, AMH_M_03) do not have the same values, but are close enough to infer that there are similar values for males and females of the same age, although males have values that place them more

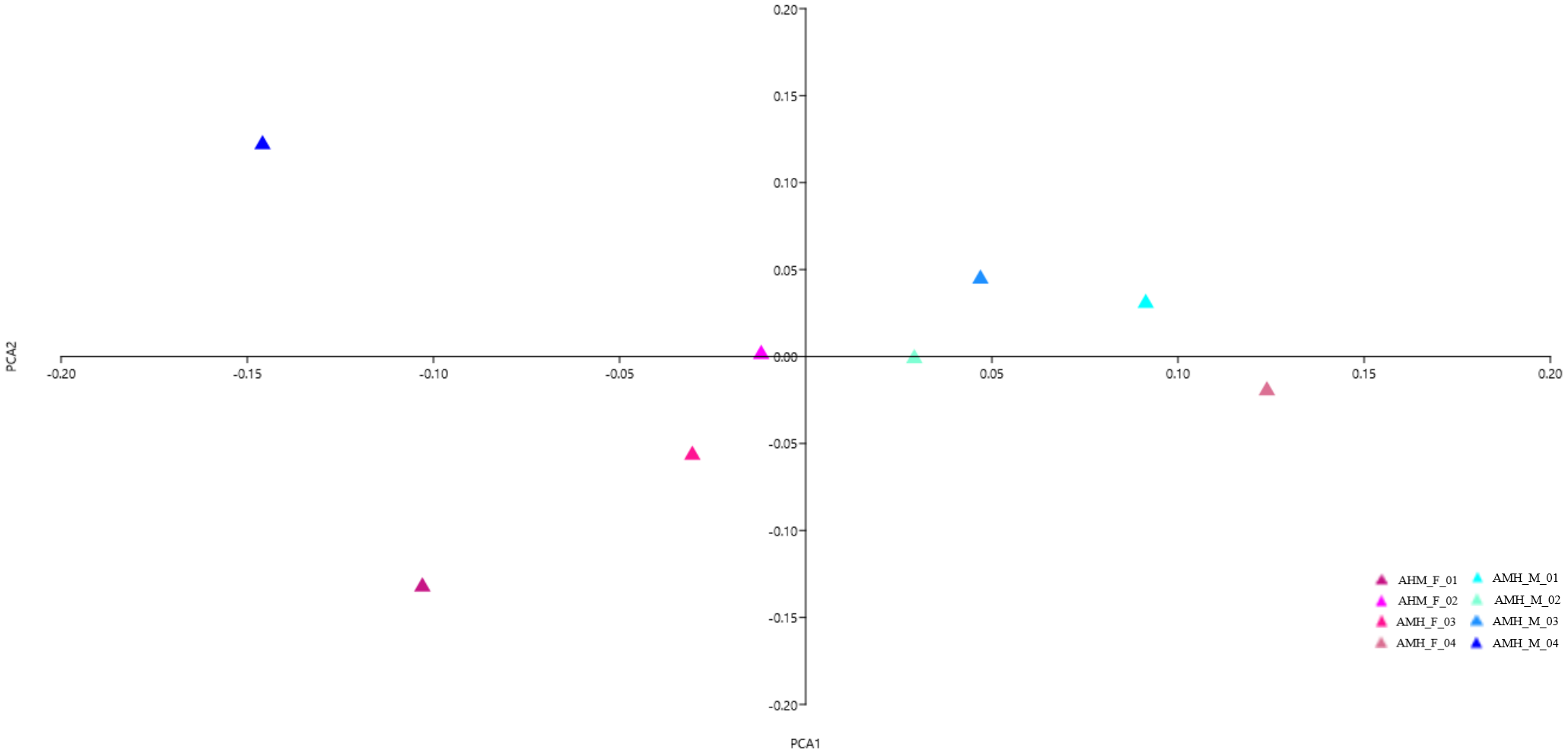


**Graph.1** *PCA graph of males and females aged 20 to 30 years obtained using the PAST software*

towards the right-hand side of the graph, compared to females who are more on the left-hand side. Two individuals (AMH_F_01, AMH_M_04) show almost no affinity with the other individuals in the sample.

Possible causes will be discussed in Discussion (item 5).

**31 to 40 years (males and females)** This second group consists of the individuals AMH_F_05, AMH_ F_06, AMH_ 07, AMH_F_08, AMH_M_05, AMH_M_06 and AMH_M_07. They are male and female individuals aged between 31 and 40 years (see **Tab.1**).

As can be seen from the graph (**Graph.2**), there are not very many equal values between the various individuals in the sample. In this case there is only one individual that does not lie with the others, and that is AMH_M_05. All the others, however, are on the same side of the graph, not very close to each other, so not with very similar values, but still not too far apart. It can be seen that the male individuals lie above the X-axis, while the female individuals lie below the X-axis.

Possible causes will be discussed in Discussion (item 5).

**41 to 50 years old (males and females)** This third group consists of individuals AMH_F_09, AMH_F_10, AMH_F_11, AMH_F_12, AMH_M_08, AMH_M_09, AMH_M_10 and AMH_M_11. They are all male and female individuals aged between 41 and 50 years (see **Tab.1**).

As can be seen from the graph (**Graph.3**), there are not very many equal values, but still seven out of eight individuals but some have fairly similar values to keep them on the same side of the graph. Only one individual (AMH_M_09) is completely detached from the others, the others are all on the left side of the Y-axis, while this individual is on the right side. In this case, males and females are not divided by one of the two axes, but are mixed, i.e. they are indifferently located, whether male or female, above or below the X-axis.

Possible causes will be discussed in Discussion (item 5).

**20 to 50 years (females)** This group consists of all female individuals taken into account for all previous analyses (AMH_F_01, AMH_F_02, AMH_F_03, AMH_F_04, AMH_F_05, AMH_F_06, AMH_F_07, AMH_F_08, AMH_F_09, AMH_F_10, AMH_F_11 and AMH_F_12) and compared with each other; thus, the sample ranges from 20 to 50 years (see **Tab.1**).

In this case, we can see in the graph (**Graph.4**) that the female individuals are almost all grouped together, there are two individuals that stand out from the others, but are not too far apart from the others (AMH_F_03 and AMH_F_04). There are not many differences between them, i.e. the individuals, although with different ages, all have more or less the same same value, except for the two individuals mentioned above and another one that is a little further away from the others (AMH_F_02), which are part of the first group and are therefore younger individuals than the others.

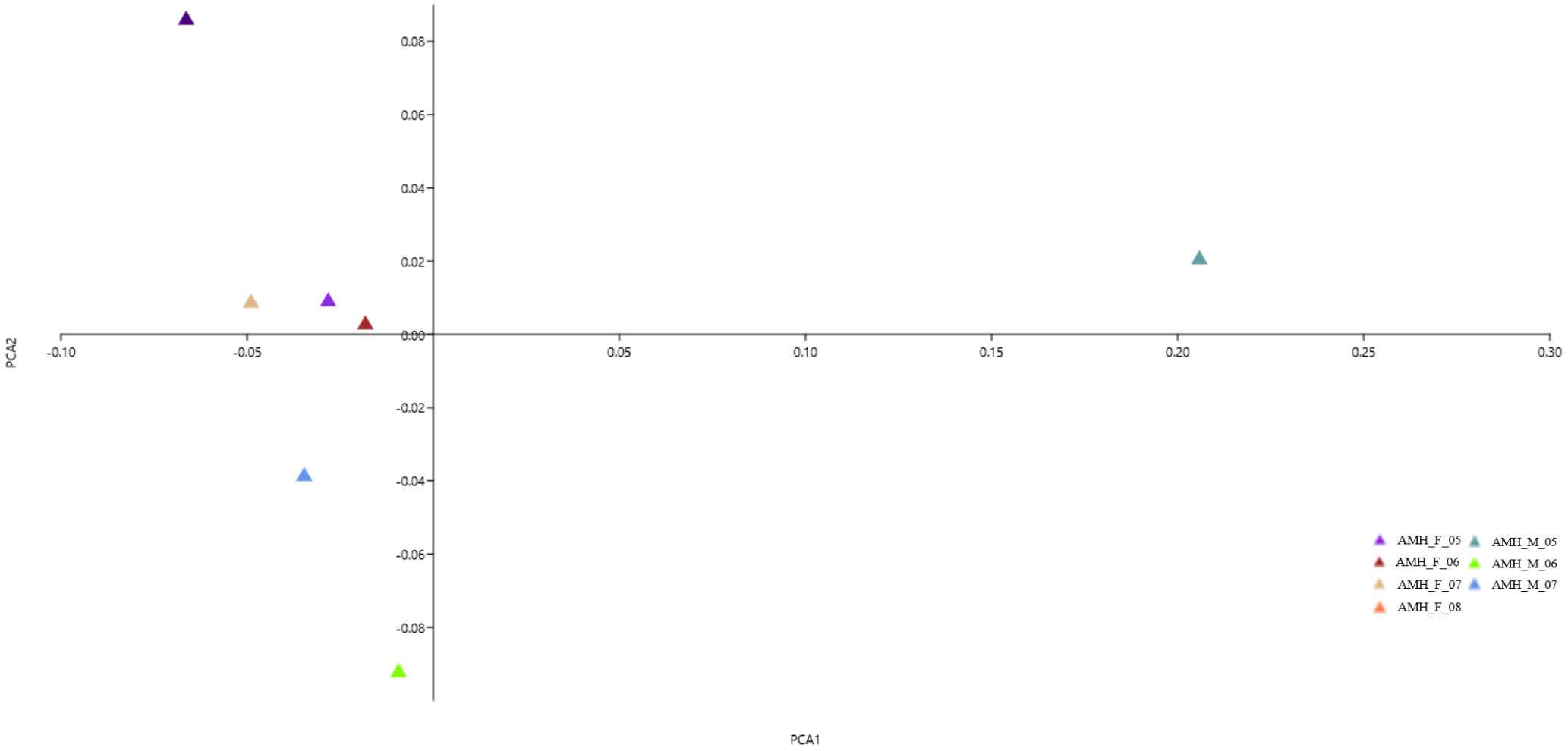


**Graph.2** *PCA graph of males and females aged 31 to 40 years obtained using the PAST software*

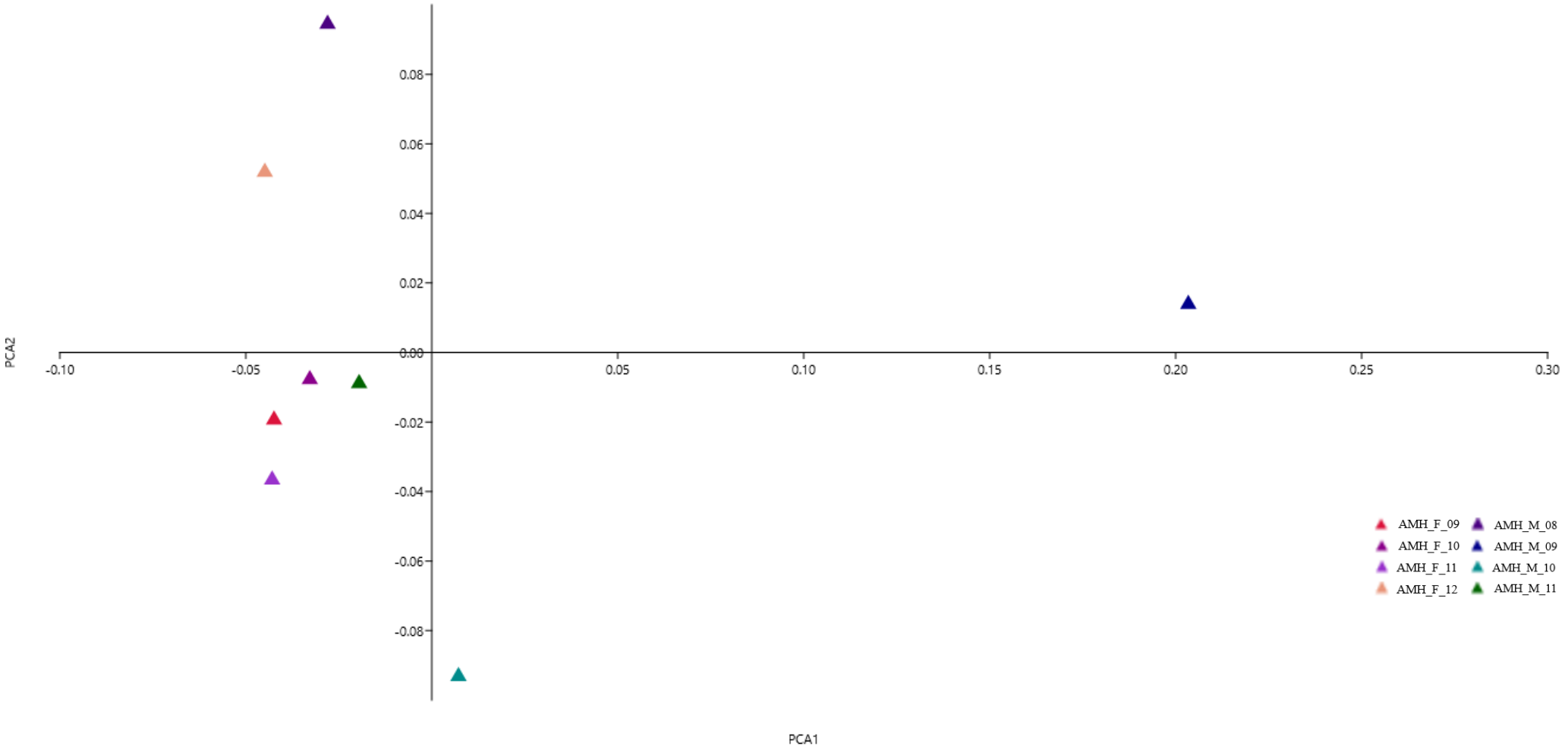


**Graph.3** *PCA graph of males and females aged 41 to 50 years obtained using the PAST software*

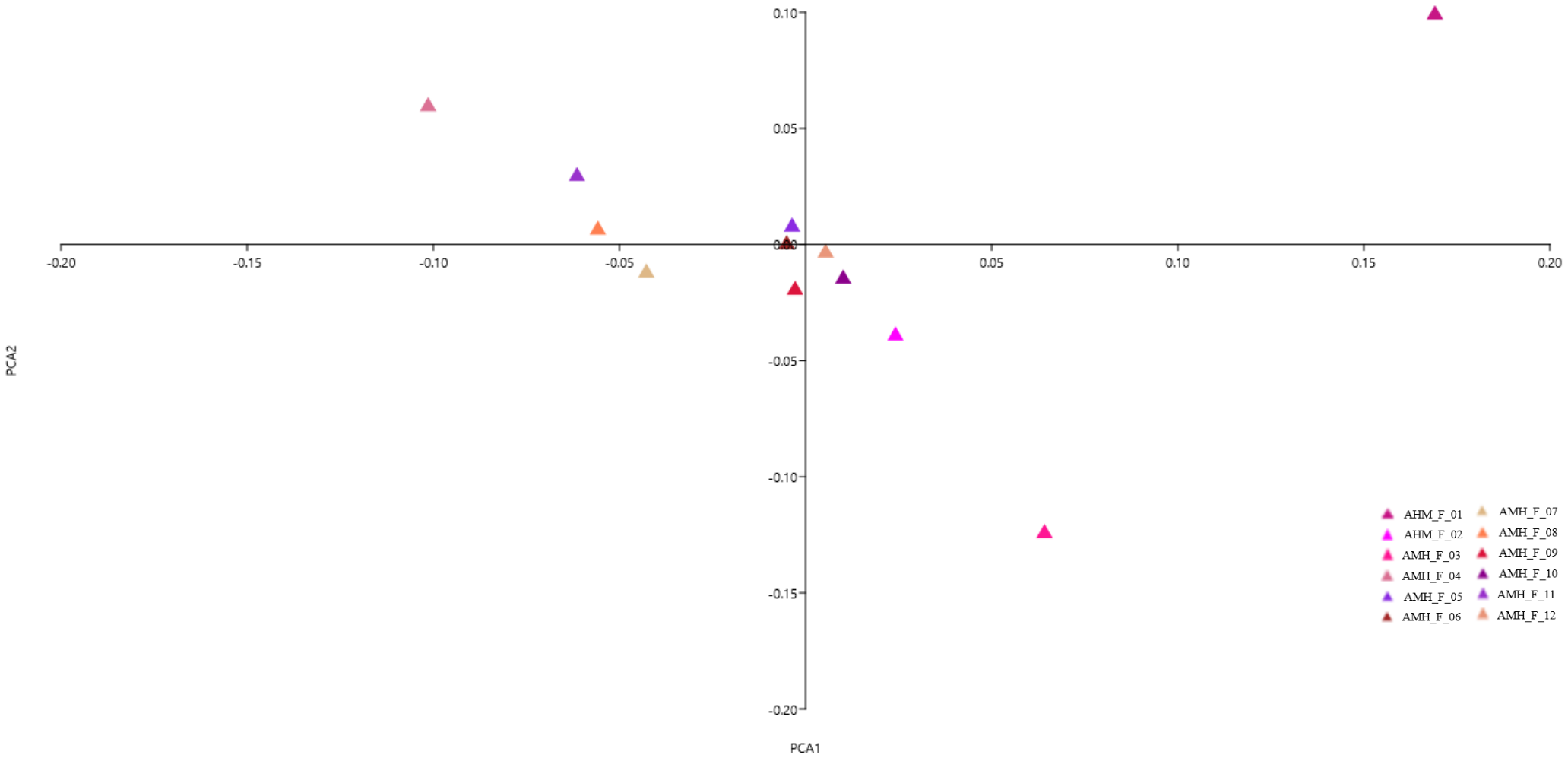


**Graph.4** *PCA graph of females aged 20 to 50 years obtained using the PAST software*

Although individuals aged 31 to 40 and those aged 41 to 50 all have more or less the same value, it can be seen that those aged 31 to 40 (almost all) lie to the right of the Y-axis, while those aged 41 to 50 (almost all) lie to the left of the Y-axis.

Possible causes will be discussed in Discussion (item 5).

**20 to 50 years old (males)** This group consists of all female individuals taken into account for all previous analyses (AMH_M_01, AMH_M_02, AMH_M_03, AMH_M_04, AMH_M_05, AMH_M_06, AMH_M_07, AMH_M_08, AMH_M_09, AMH_M_10 and AMH_M_11) and compared with each other; thus, the sample ranges from 20 to 50 years (see **Tab.1**).

In the case of men (**Graph.5**), there is no distinction by age; almost all individuals are located at the same point on the graph, regardless of their age. The exception is three individuals, one (AMH_M_04) is on the left side of the Y-axis like all the other individuals; the other two are on the right side of the Y-axis, one above (AMH_M_09) and one below (AMH_M_05) the X-axis. These are individuals that were also distant from the others in the previous graphs. The landmarks were checked, but the results did not change.

Possible causes will be discussed in Discussion (item 5).

**20 to 50 years (males and females)** This group consists of all individuals wh o were examined (see **Tab.1**).

In this case (**Graph.6**) where they are all compared, all the specimens are more or less in the same place, they all have more or less similar values. The only one that is not at the same point is AMH_M_09, which is well away from the others. All the others are to the left of the X-axis or in its proximity near the others. The values are more or less the same and very similar. There is no breakdown by age or gender, because the individuals are very heterogeneous, one can only note that, predominantly, the individuals in the 41 to 50 year old group are very close to the X-axis than the other groups of individuals.

Possible causes will be discussed in Discussion (item 5).

### 5.1.2 Pelvis

**20 to 30 years old (males and females)** This first group consists of individuals AMH_F_01, AMH_F_02, AMH_F_03, AMH_F_04, AMH_M_01, AMH_M_02, AMH_M_03 and AMH_M_04. They are male and female individuals aged between 20 and 30 years (see **Tab.1**).

In this first graph (**Graph.7**), it can be seen that the female individuals present the same values, including the male individual AMH_M_04, which overlaps with the female individual AMH_F_04. The other male individuals (AMH_M_01, AMH_M_02, AMH_M_03) present very different values. Individual AMH_M_02 has values that are much closer to the other female individuals and AMH_M_04, whereas AMH_M_01 and AMH_M_03 have different values from

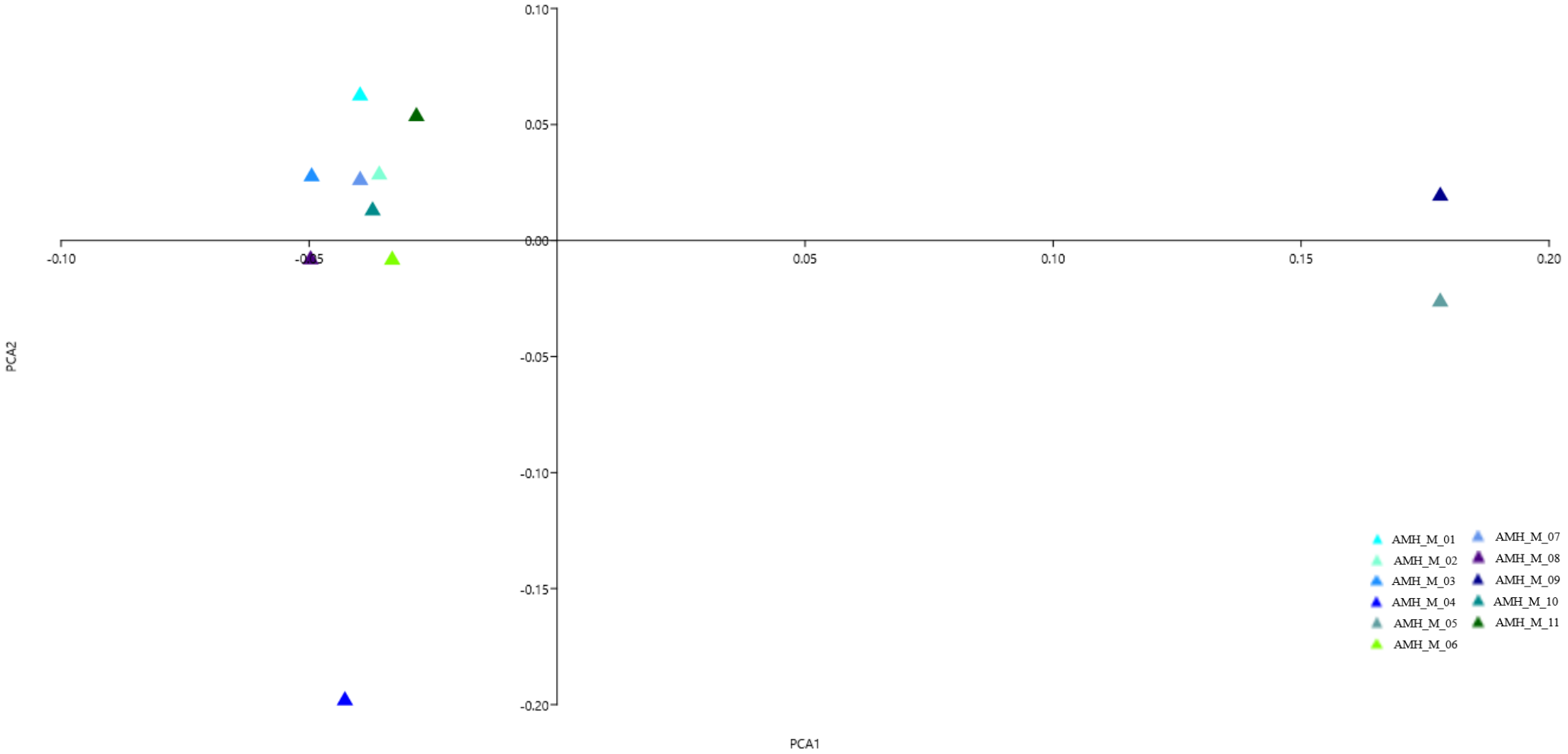


**Graph.5** *PCA graph of males aged 20 to 50 years obtained using the PAST software*

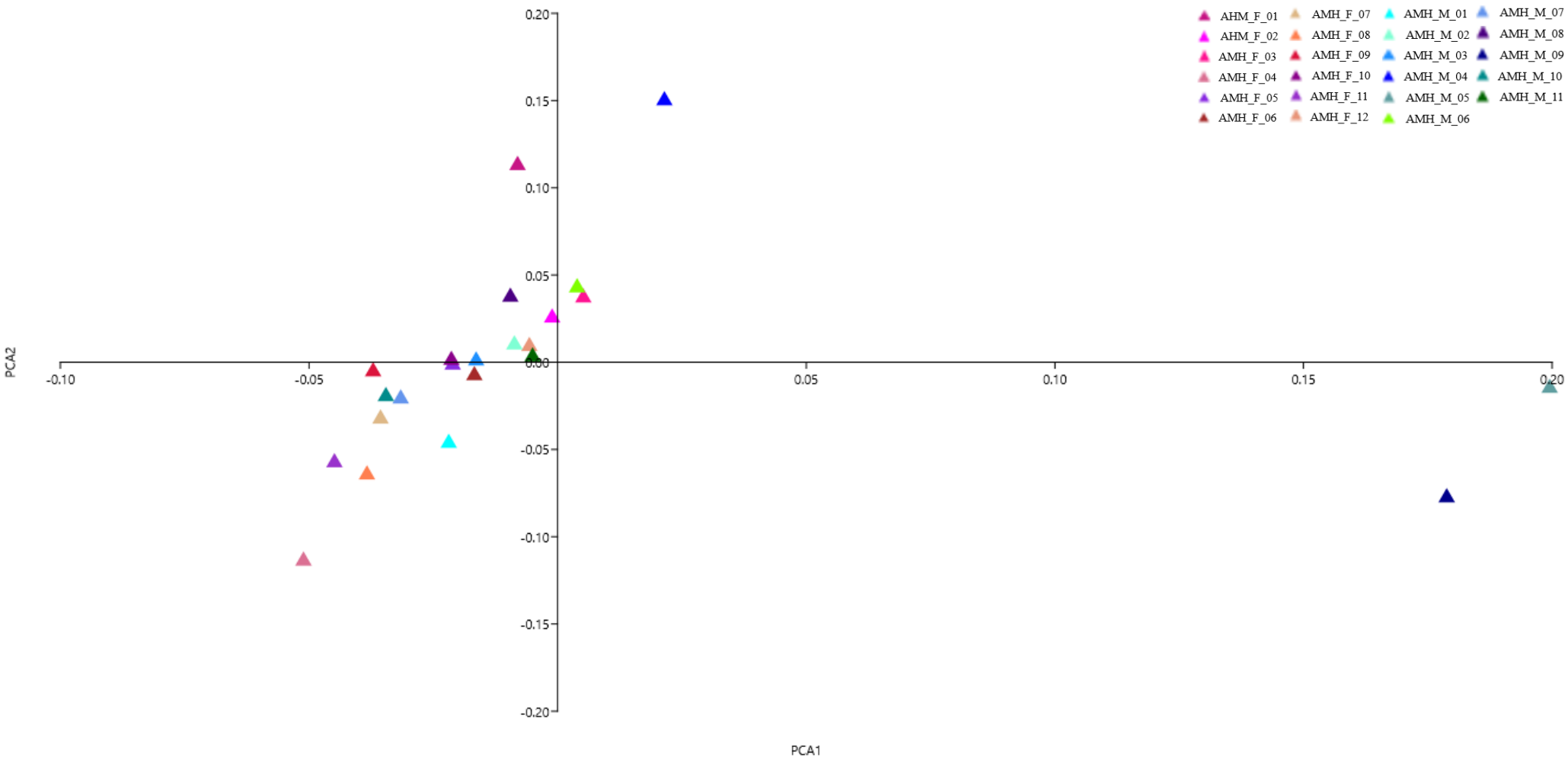


**Graph.6** *PCA graph of males and females aged 20 to 50 years obtained using the PAST software*

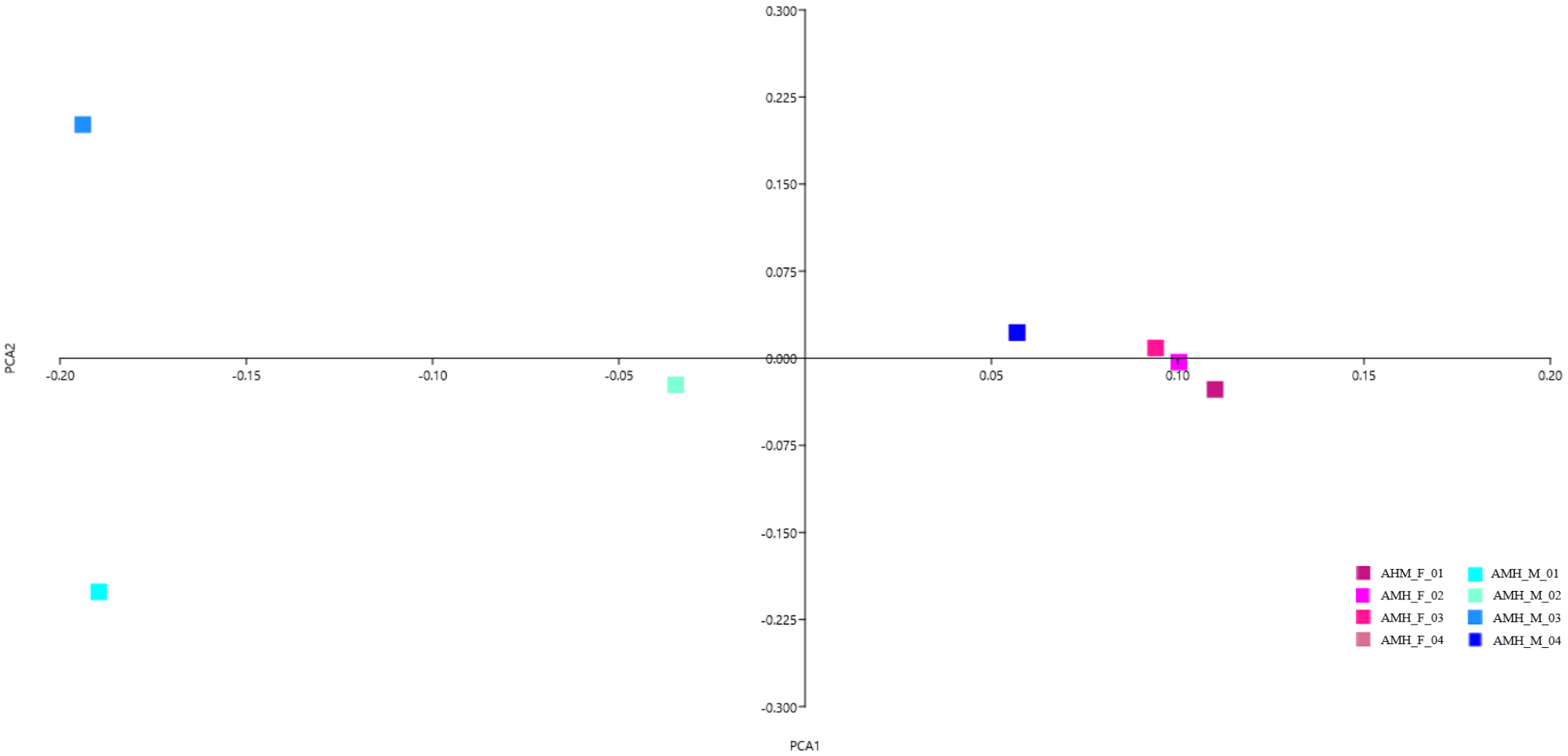


**Graph.7** *PCA graph of males and females aged 20 to 30 years obtained using the PAST software*

the other individuals - they are to the left of the Y-axis - and from each other - AMH_M_01 is below the X-axis and AMH_M_03 is above the X-axis.

Possible causes will be discussed in Discussion (item 5).

**31 to 40 years (males and females)** This second group consists of the individuals AMH_F_05, AMH_ F_06 , AMH_ 07 , AMH_F_08, AMH_M_05, AMH_M_06 and AMH_M_07.

They are male and female individuals aged between 31 and 40 years (see **Tab.1**). In graph (**Graph.8**), the values are far apart, but the individuals are grouped together in three different groups. In fact, it can be seen that AMH_F_05, AMH_M_05 and AMH_M_07 are located above the X-axis and to the left of the Y-axis; AMH_F_06 and AMH_F_07 are also to the left of the Y-axis, but are below the X-axis; AMH_F_08 and AMH_M_06 are both to the right of the Y-axis, but the former is below the X-axis and the latter is above the X-axis.

Possible causes will be discussed in Discussion (item 5).

**41 to 50 years old (males and females)** This third group consists of individuals AMH_F_09, AMH_F_10, AMH_F_11, AMH_F_12, AMH_M_08, AMH_M_09, AMH_M_10 and AMH_M_11. They are all male and female individuals aged between 41 and 50 years (see **Tab.1**).

Also in this graph (**Graph.9**), the values are scattered around the graph and grouped together in different groups. What is most noticeable is how AMH_F_09 and AMH_M_09 lie on opposite sides of the Y-axis (AMH_F_09 on the left and AMH_M_09 on the right) but are more or less at the same on the X-axis. The individuals that are above the X-axis and to the left of the Y-axis are both female individuals (AMH_F_10 and AMH_F_12), while those that are below the X-axis and to the right of the Y-axis are both male individuals (AMH_M_08 and AMH_M_11); the remaining three individuals are to the right of the Y-axis, two are above the X-axis (AMH_F_11 and AMH_M_09) and one is below the Y-axis (AMH_M_10).

Possible causes will be discussed in Discussion (item 5).

**20 to 50 years (females)** This group consists of all female individuals taken into account for all previous analyses (AMH_F_01, AMH_F_02, AMH_F_03, AMH_F_04, AMH_F_05, AMH_F_06, AMH_F_07, AMH_F_08, AMH_F_09, AMH_F_10, AMH_F_11 and AMH_F_12) and compared with each other; thus, the sample ranges from 20 to 50 years (see **Tab.1**).

In the graph (**Graph.10**) it can be seen that all individuals are grouped to the right of the Y-axis and are all located around the X-axis and belong to the first group of individuals (females aged 20 to 30 - AMH_F_01, AMH_F_02, AMH_F_03, AMH_F_04) and the third group of individuals (females aged 41 to 50 - AMH_F_09, AMH_F_10, AMH_F_11, AMH_F_12). The individuals belonging to the second group (females aged 31 to 40) are located to the left of the Y-axis, but two are above the X-axis (AMH_F_05 and AMH_F_06) and two below the X-axis (AMH_F_07 and

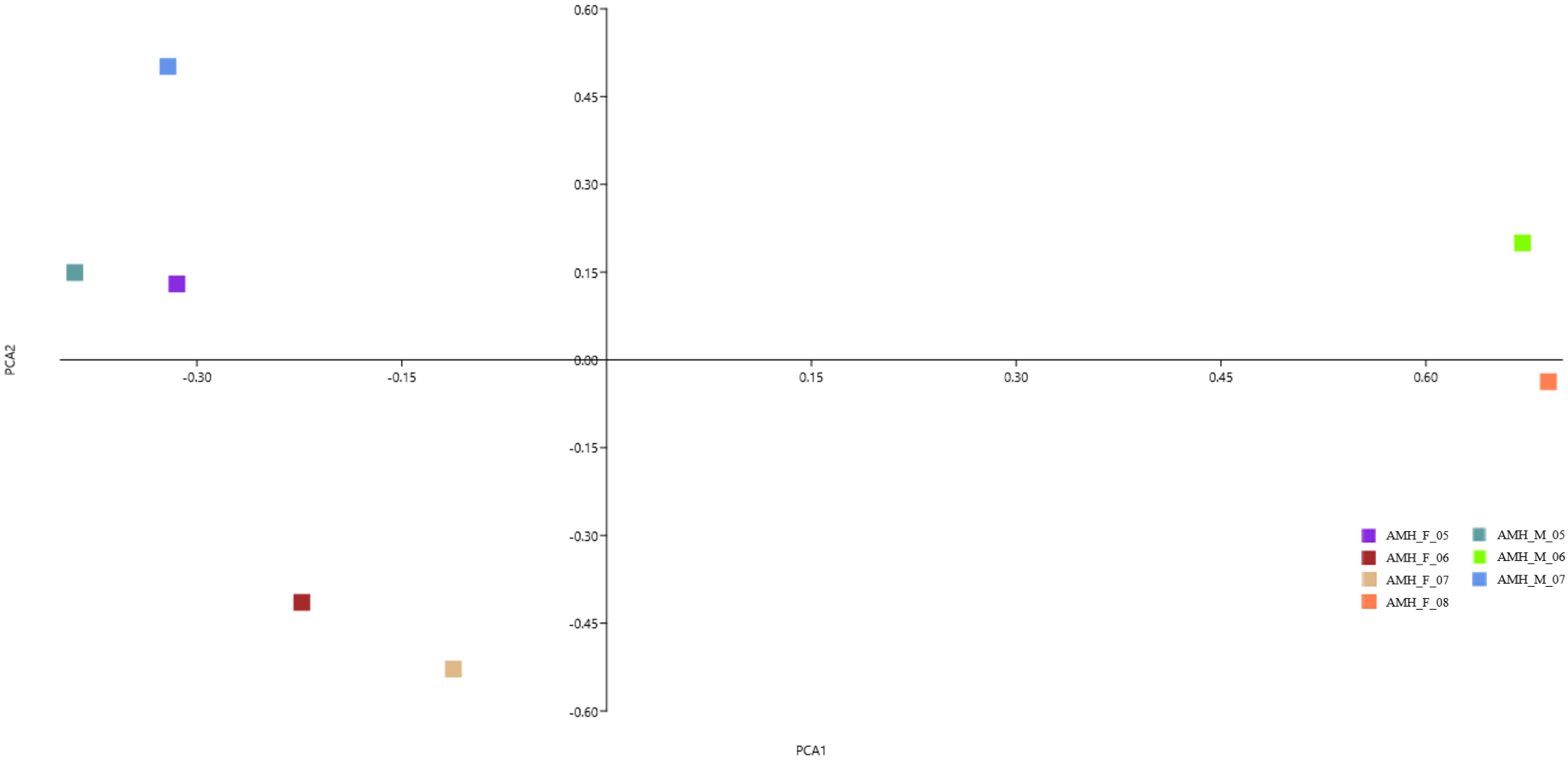


**Graph.8** *PCA graph of males and females aged 31 to 40 years obtained using the PAST software*

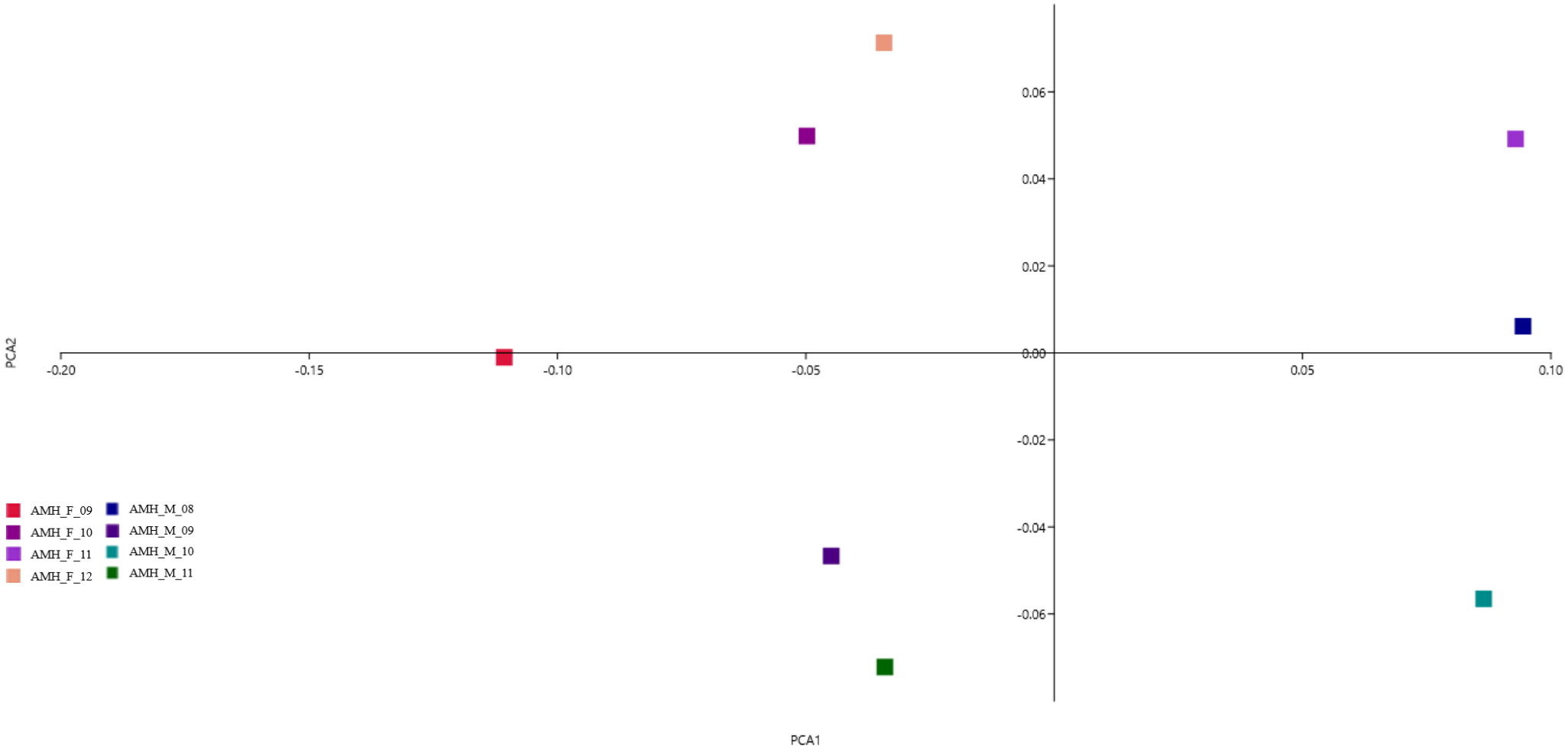


**Graph.9** *PCA graph of males and females aged 41 to 50 years obtained using the PAST software*

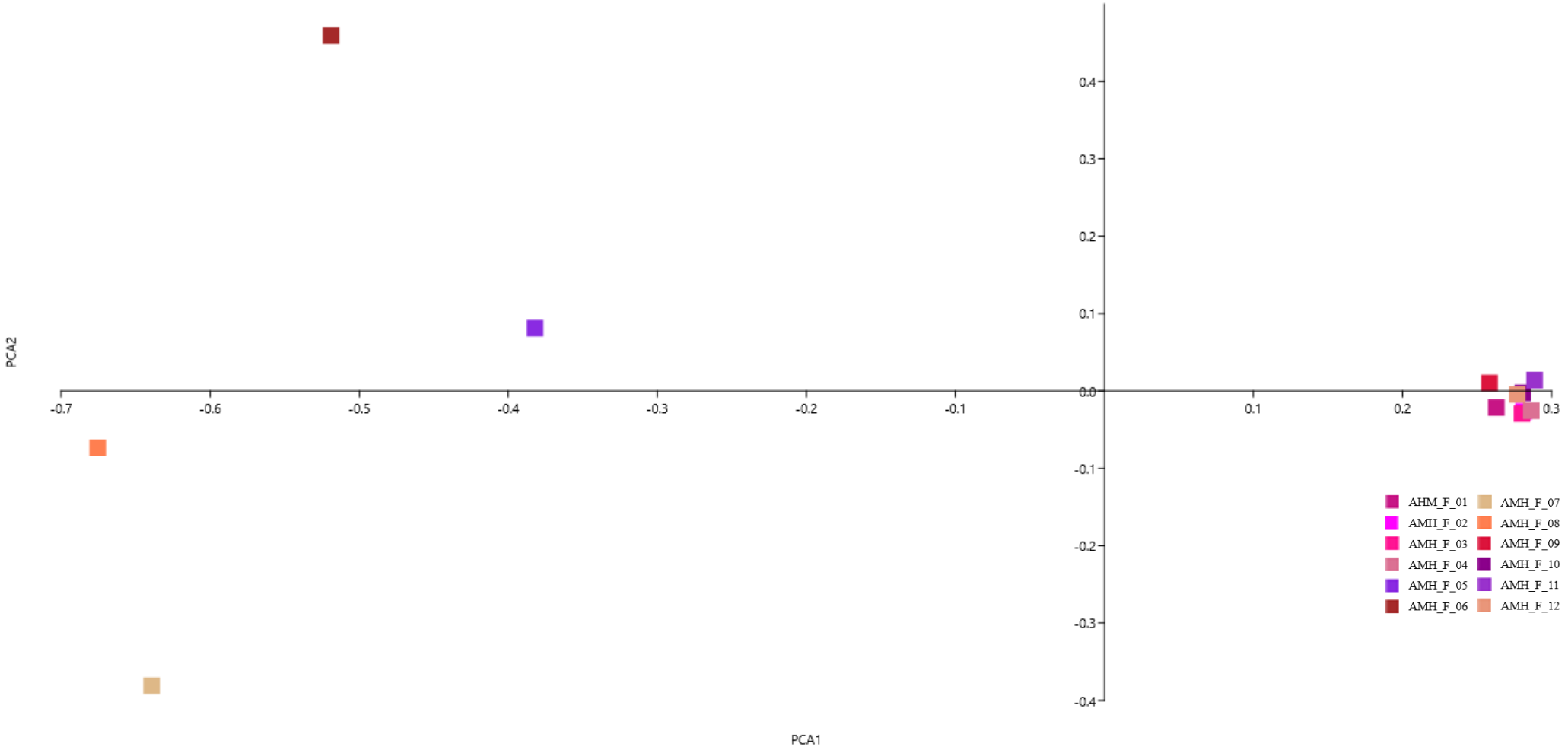


**Graph.10** *PCA graph of females aged 20 to 50 years obtained using the PAST software*

AMH_F_08). However, it can be seen that AMH_F_05 and AMH_F_08 are both located very close to the X-axis, compared to the other two individuals (AMH_F_06 and AMH_F_07).

Possible causes will be discussed in Discussion (item 5).

**20 to 50 years old (males)** This group consists of all female individuals taken into account for all previous analyses (AMH_M_01, AMH_M_02, AMH_M_03, AMH_M_04, AMH_M_05, AMH_M_06, AMH_M_07, AMH_M_08, AMH_M_09, AMH_M_10 and AMH_M_11) and compared with each other; thus, the sample ranges from 20 to 50 years (see **Tab.1**).

In contrast to the graph explained above (**Graph.10**), this graph (**Graph.11**) shows how the male individuals are all clustered in one place, regardless of the group they belong to, except for individuals AMH_M_05 and AMH_M_06. These two individuals both lie to the right of the Y-axis, but AMH_M_05 lies above the X-axis and AMH_M_06 lies below the X-axis, but both have more or less the same value for the Y-axis. The other individuals lie more or less around the X-axis and to the left of the Y-axis. The only individual that deviates a little from the others is AMH_M_03, which lies a little more below the X-axis than the others, but still to the left of the Y-axis, but in line with some individuals for the Y-axis.

Possible causes will be discussed in Discussion (item 5).

**20 to 50 years (males and females)** This group consists of all individuals who were examined (see **Tab.1**).

In the last graph (**Graph.12**) we can see that all the individuals lie to the right of the Y-axis and are all around the X-axis, except for a few individuals (AMH_M_05, AMH_M_06, AMH_F_05, AMH_F_06, AMH_F_07, AMH_F_08) are on the left side of the Y-axis, but AMH_M_05, AMH_F_05, AMH_F_06 and AMH_F_08 are above the X-axis and AMH_M_06 and AMH_F_07 are below the X-axis. All of these individuals belong to the group of individuals aged 31 to 41, while the others, of the two groups – individuals 20 to 31 years and individuals aged 41 to 50 - present more or less similar values. Only two individuals in this group present somewhat contrasting values for the Y-axis, AMH_M_01 and AMH_M_03, which lie below the Y-axis compared to the others.

Possible causes will be discussed in Discussion (item 5).

## 5.2 Comparison of AMH and *Homo neanderthalensis*

After analysing the correlation between sex and age of the AMH individuals, those data were compared with those obtained for *Homo neanderthalensis*. As mentioned above (see section 3.1.2), 3Ds for the pelvis and femur fossils of *Homo neanderthalensis* were obtained by cast photogrammetry from the MNHN in Paris.

The sample was divided as for AMH:

- Female:

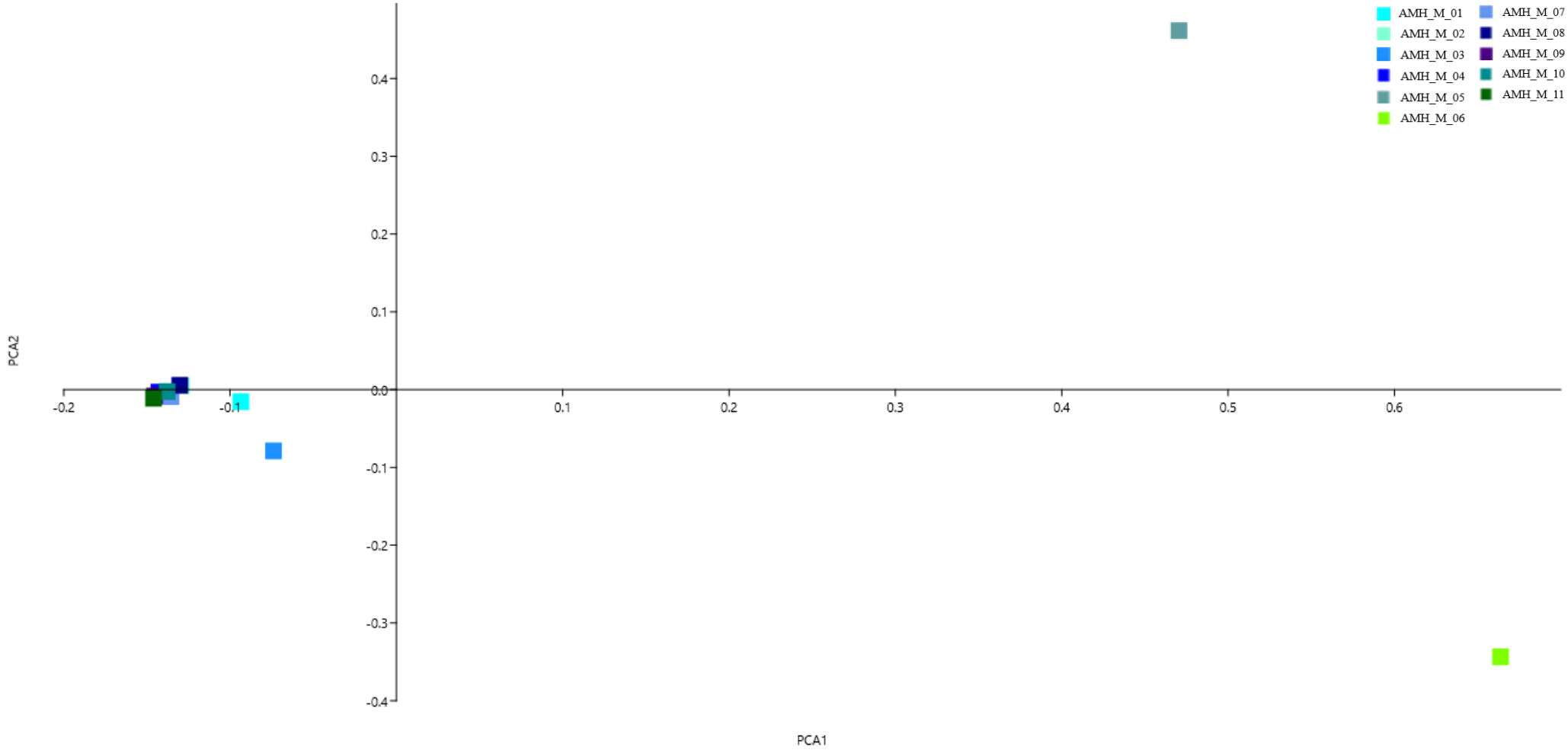


**Graph.11** *PCA graph of males aged 20 to 50 years obtained using the PAST software*

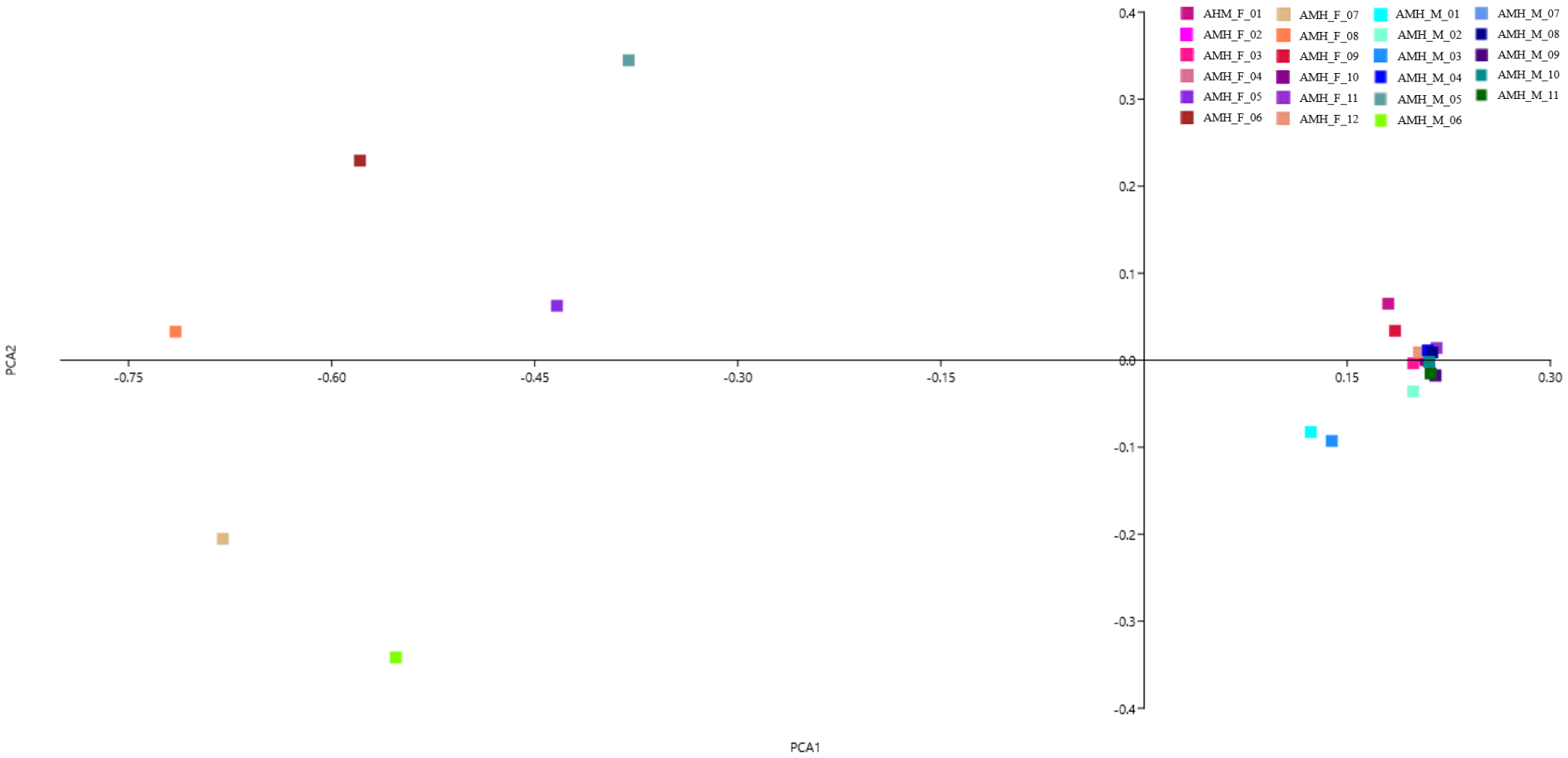


**Graph.12** *PCA graph of males and females aged 20 to 50 years obtained using the PAST software*

- 20 to 30 years old (male and female);
- 31 to 40 years old (males and females);
- 41 to 50 years (males and females);
- 20 to 50 years old (females)
- 20 to 50 years old (males);
- 20 to 50 years old (males and females);

- Pelvis:
  - 20 to 30 years (males and females);
  - 31 to 40 years old (males and females);
  - 41 to 50 years (males and females);
  - 20 to 50 years old (females)
  - 20 to 50 years old (males);
  - 20 to 50 years old (males and females).

### 5.2.1 Femur

**20 to 30 years old (males, females and *Homo neanderthalensis*)** In this group, individuals AMH_F_01, AMH_F_02, AMH_F_03, AMH_F_04, AMH_M_01, AMH_M_02, AMH_M_03 and AMH_M_04 for AMH and 213-2, 27825-FR, 28120-FR and 17648 for *Homo neanderthalensis* (see **Tab.1** for AMH and **Tab.2** for *Homo neanderthalensis*).

As can be seen from the graph (**Graph.13**) the values for AMH femurs (AMH_F_01, AMH_F_02, AMH_F_03, AMH_F_04, AMH_M_01, AMH_M_02, AMH_M_03, AMH_M_04) are all more or less the same and lie to the right of the Y-axis, whereas the values for the femurs of *H. neanderthalensis* (213-2, 27825-FR, 28120-FR, 17648) lie to the left of the Y-axis. Whereas for the X-axis values, one can see that AMH values are more or less the same, for *H. neanderthalensis* values are very different, in fact 28120-FR and 17648 are above the X-axis, whereas 213-3 and 27825-FR are below the X-axis. Furthermore, it can be seen that the values for 28120-FR and 17648 have more or less similar values, whereas 213-2 and 27825-FR have different values.

Possible causes will be discussed in Discussion (item 5).

**31 to 40 years (males, females and *Homo neanderthalensis*)** In the second group, individuals AMH_F_05, AMH_F_06, AMH_07, AMH_F_08, AMH_M_05 were analysed, AMH_M_06 and AMH_M_07 for AMH and 213-2, 27825-FR, 28120-FR and 17648 for *Homo neanderthalensis* (see **Tab.1** for AMH and **Tab.2** for *Homo neanderthalensis*).

As can be seen from the graph (**Graph.14**), the values for the femurs of AMH (AMH_F_05, AMH_F_06, AMH_07, AMH_F_08, AMH_M_05, AMH_M_06, AMH_M_07) are all more or less the same and lie to the right of the Y-axis, while the values for the femurs of *H. neanderthalensis* (213-2, 27825-FR, 28120-FR, 17648) lie to the left of the Y-axis. While for the

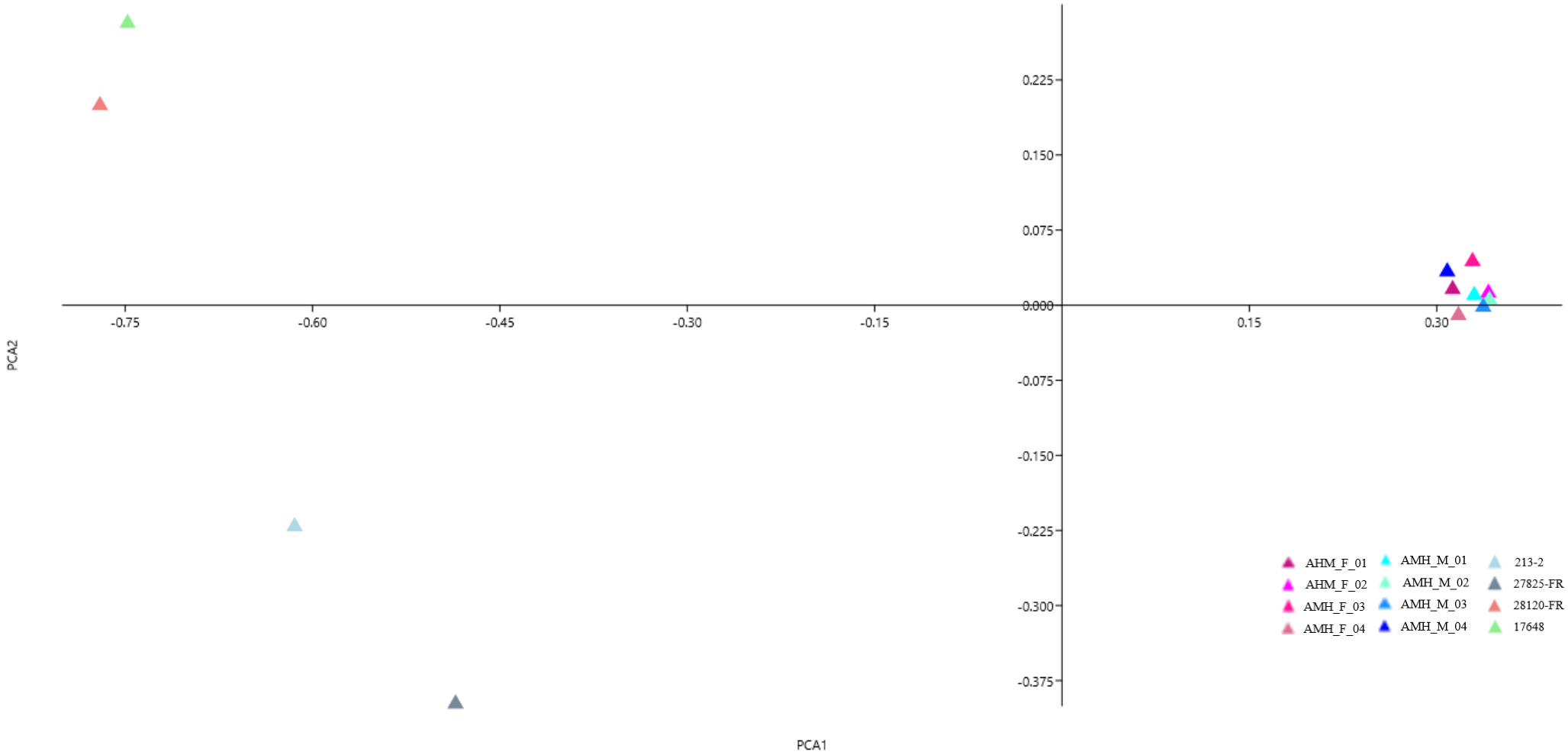


**Graph.13** *PCA graph of males and females aged 20 to 30 years and Homo neanderthalensis obtained using the PAST software*

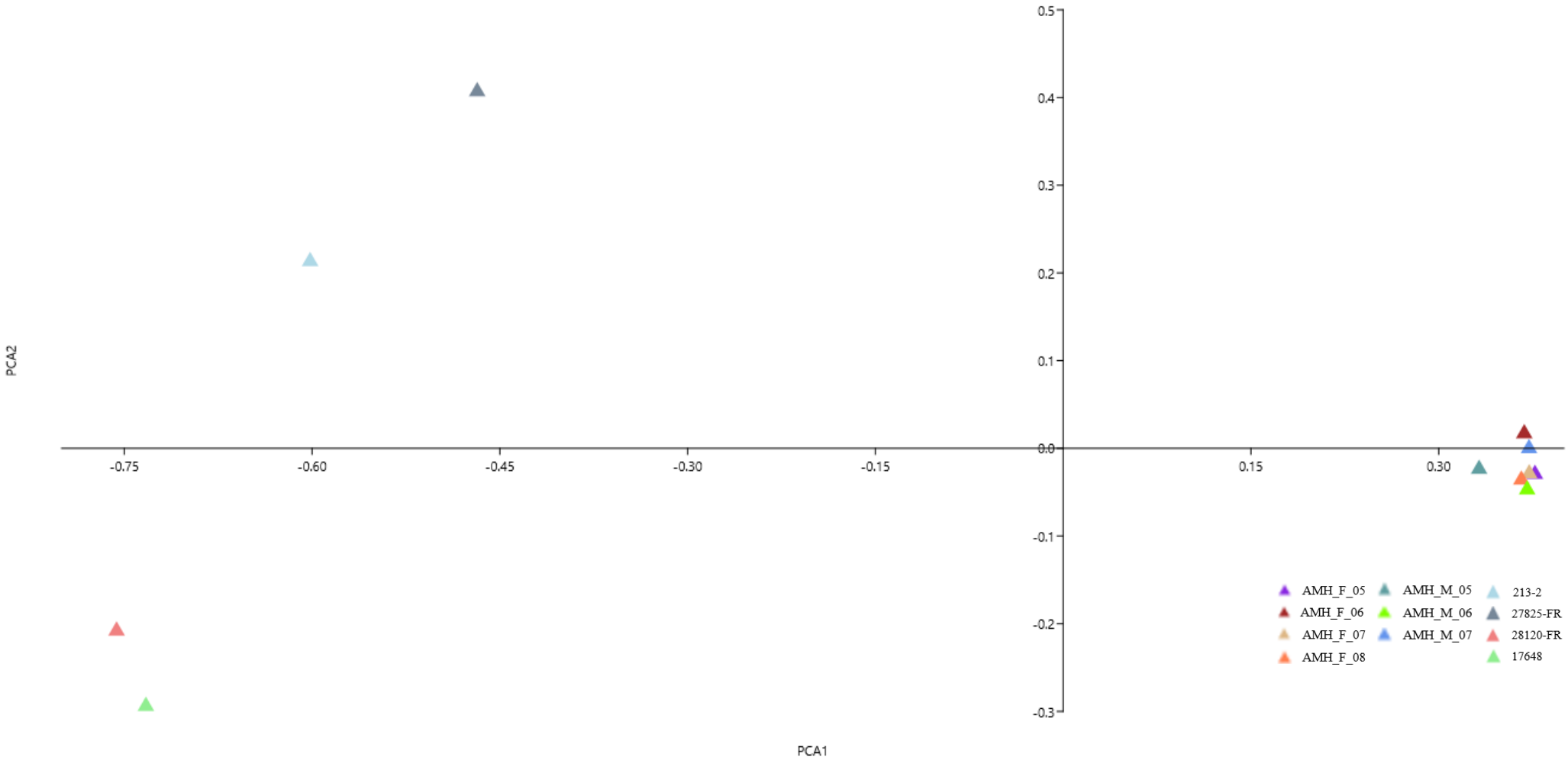


**Graph.14** *PCA graph of males and females aged 31 to 40 years and Homo neanderthalensis obtained using the PAST software*

X-axis values, one can see how AMH values are more or less the same, the values for *H. neanderthalensis are* very different, in fact 28120-FR and 17648 lie below the X-axis, while 213-3 and 27825-FR lie above the X-axis.

It can be seen that the values for 28120-FR and 17648 have more or less similar values, whereas 213-2 and 27825-FR have different values. Furthermore, for AMH it can be seen that the values are almost all below the X-axis, unlike in the previous graph where the values for femur were much more varied.

Possible causes will be discussed in Discussion (item 5).

**41 to 50 years (males, females and *Homo neanderthalensis*)** This third group consists of individuals AMH_F_09, AMH_F_10, AMH_F_11, AMH_F_12, AMH_M_08, AMH_M_09, AMH_M_10 and AMH_M_11 for AMH and 213-2, 27825-FR, 28120-FR and 17648 for *Homo neanderthalensis* (see **Tab.1** for AMH and **Tab.2** for *Homo neanderthalensis*).

As can be seen from the graph (**Graph.15**) the values for AMH femurs (AMH_F_09, AMH_F_10, AMH_F_11, AMH_F_12, AMH_M_08, AMH_M_09, AMH_M_10, AMH_M_11) are all more or less the same and lie to the right of the Y-axis, whereas the values for the femurs of *H. neanderthalensis* (213-2, 27825-FR, 28120-FR, 17648) lie to the left of the Y-axis. While for the X-axis values, one can see how AMH values are more or less the same, the values for *H. neanderthalensis are* very different, in fact 28120-FR and 17648 lie below the X-axis, while 213-3 and 27825-FR lie above the X-axis.

It can be seen that the values for 28120-FR and 17648 have more or less similar values, whereas 213-2 and 27825-FR have different values. Furthermore, for AMH, it can be seen that the values for female individuals are above the X-axis, whereas the values for male individuals are below the X-axis.

Possible causes will be discussed in Discussion (item 5).

**20 to 50 years (females and *Homo neanderthalensis*)** This group consists of all female individuals taken into account for AMH (AMH_F_01, AMH_F_02, AMH_F_03, AMH_F_04, AMH_F_05, AMH_F_06, AMH_F_07, AMH_F_08, AMH_F_09, AMH_F_10, AMH_F_11 and AMH_F_12) and 213-2, 27825-FR, 28120-FR and 17648 for *Homo neanderthalensis* (see **Tab.1** for AMH and **Tab.2** for *Homo neanderthalensis*).

In this case, as can be seen from the graph (**Graph.16**), the values are reversed; in fact, all female AMH individuals are found (AMH_F_01, AMH_F_02, AMH_F_03, AMH_F_04, AMH_F_05, AMH_F_06, AMH_F_07, AMH_F_08, AMH_F_09, AMH_F_10, AMH_F_11, AMH_F_12) to the left of the X-axis, while the individuals of *H. neanderthalensis* (213-2, 27825-FR, 28120-FR, 17648) are to the right, unlike the previously seen graphs.

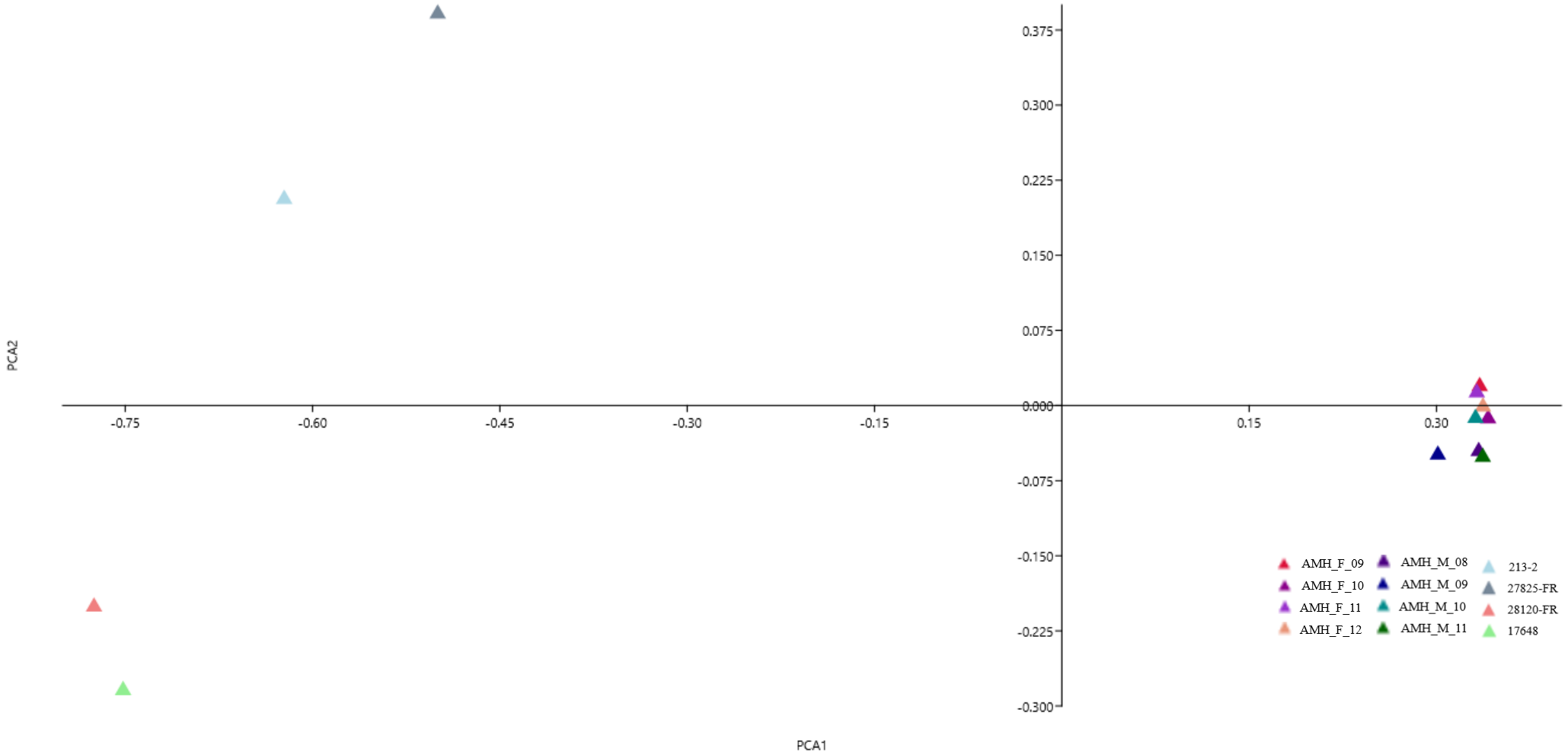


**Graph.15** *PCA graph of males and females aged 41 to 50 years and Homo neanderthalensis obtained using the PAST software*

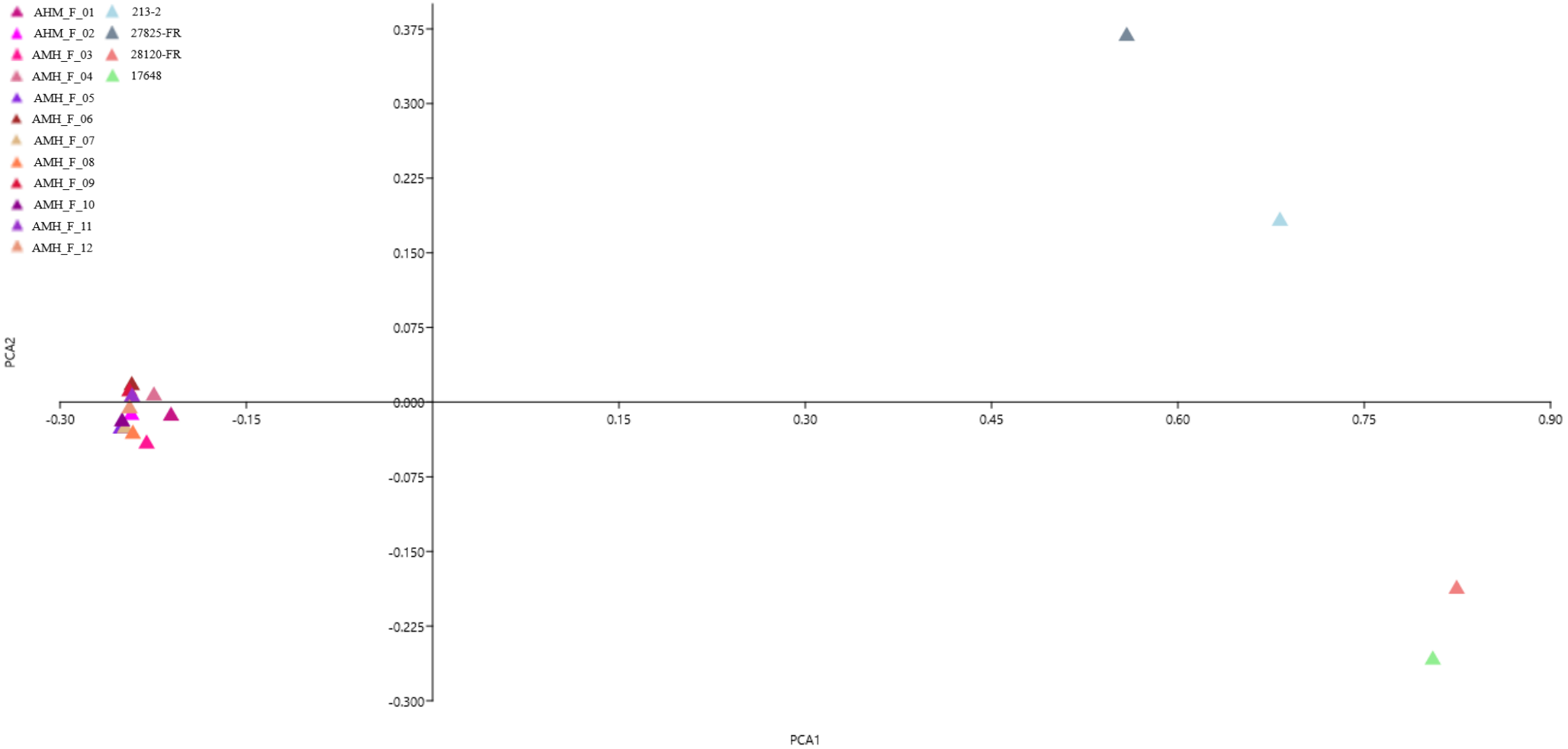


***Graph.16*** *PCA graph of females aged 20 to 50 years and Homo neanderthalensis obtained using the PAST software*

As seen in the two previous graphs, 28120-FR and 17648 lie below the X-axis, while 213- 3 and 27825-FR lie above the X-axis.

Possible causes will be discussed in Discussion (item 5).

**20 to 50 years old (males and *Homo neanderthalensis*)** This group consists of all male individuals taken into account for AMH (AMH_M_01, AMH_M_02, AMH_M_03, AMH_M_04, AMH_M_05, AMH_M_06, AMH_M_07, AMH_M_08, AMH_M_09, AMH_M_10 and AMH_M_11) and 213-2, 27825-FR, 28120-FR and 17648 for *Homo neanderthalensis* (see **Tab.1** for AMH and **Tab.2** for *Homo neanderthalensis*).

This graph (**Graph.17**) closely resembles the first graph brought in for this analysis group (20 to 30 years (males, females and *Homo neanderthalensis*); in fact, the values for the Y-axis of AMH (AMH_M_01, AMH_M_02, AMH_M_03, AMH_M_04, AMH_M_05, AMH_M_06, AMH_M_07, AMH_M_08, AMH_M_09, AMH_M_10, AMH_M_11) are to the right of the graph, while those of *H. neanderthalensis* (213-2, 27825-FR, 28120-FR, 17648) are to the left. In addition, the values for *H. neadnerthalensis* have reversed again: as in Graph. 13, 28120- FR and 17648 are above the X-axis, while 213-2 and 27825-FR are below the X-axis.

Possible causes will be discussed in Discussion (item 5).

**20 to 50 years (males, females and *Homo neanderthalensis*)** This group consists of all AMH individuals who were examined and 213-2, 27825-FR, 28120-FR and 17648 for *Homo neanderthalensis* (see **Tab.1** for AMH and **Tab.2** for *Homo neanderthalensis*).

The results of these analyses, as can be seen from Graph (**Graph.18**), are very similar to those seen in Graph.13 and Graph.17, i.e. the values for AMH are all to the right of the Y-axis, while those for *H. neanderthalensis are* to the left. Furthermore, the values for *H. neanderthalensis are* different from each other and 213-2 and 27825-FR are below the X-axis, while 28120-FR and 17648 are above the X-axis. Furthermore, 28120-FR and 17648 have similar values to each other, whereas 213-2 and 27825-FR have different values to each other.

Possible causes will be discussed in Discussion (item 5).

### 5.2.2 Pelvis

**20 to 30 years old (males, females and *Homo neanderthalensis*)** Individual AMH_F_01, AMH_F_02, AMH_F_03, AMH_F_04, AMH_M_01 were analysed in this group, AMH_M_02, AMH_M_03 and AMH_M_04 for AMH and 28120-CR, 27806-CL, 28120-CL, 28123- CR for *Homo neanderthalensis* (see **Tab.1** for AMH and **Tab.2** for *Homo neanderthalensis*).

In this graph (**Graph.19**) the pelvis values are different between AMH and *Homo neanderthalensis*. In fact, AMH individuals lie to the right of the Y- axi s and H . *neaderthalensis* individuals lie to the left of the Y-axis. Furthermore, individuals 27806-CL and 28120-CL do not

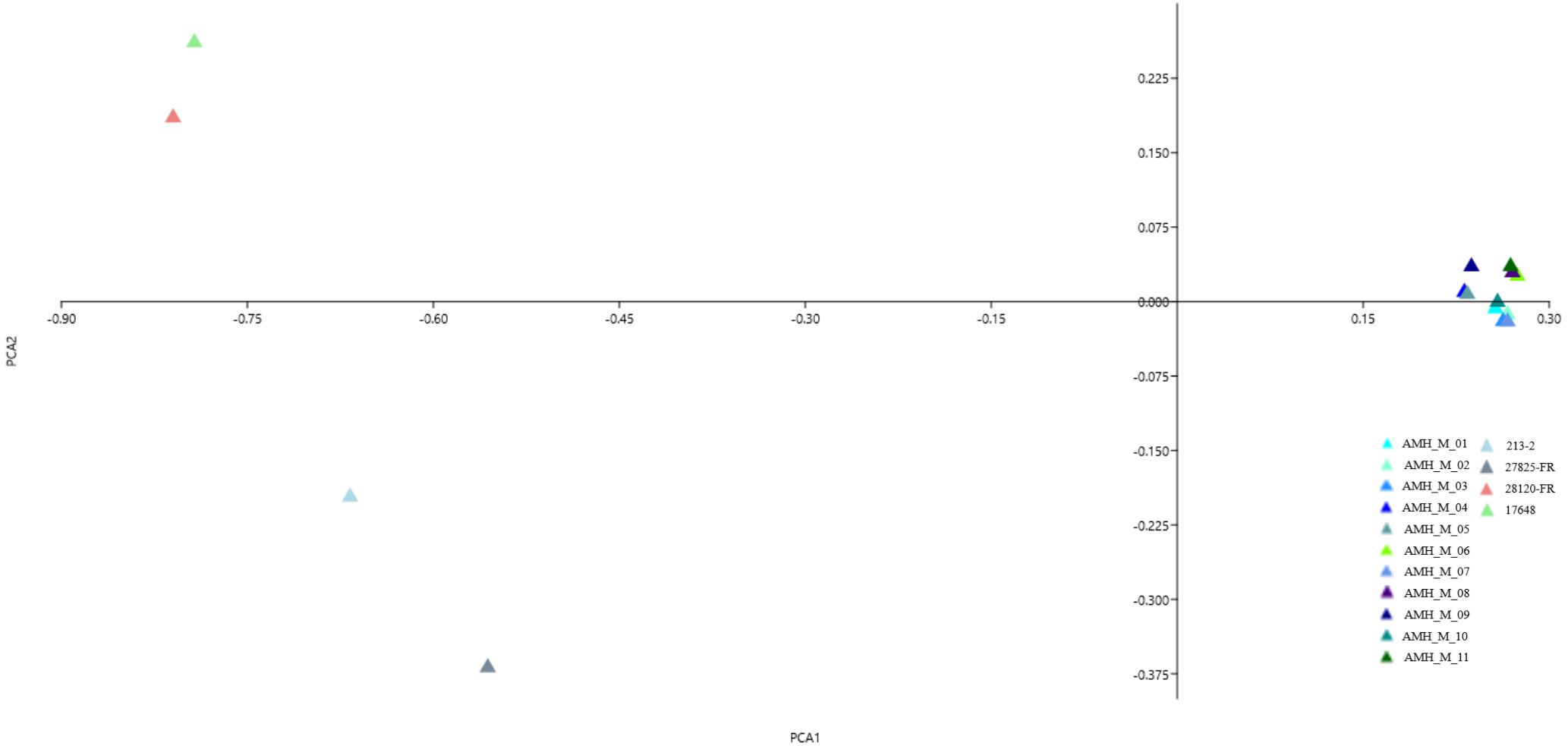


**Graph.17** *PCA graph of males aged 20 to 50 years and* Homo neanderthalensis *obtained using the PAST software*

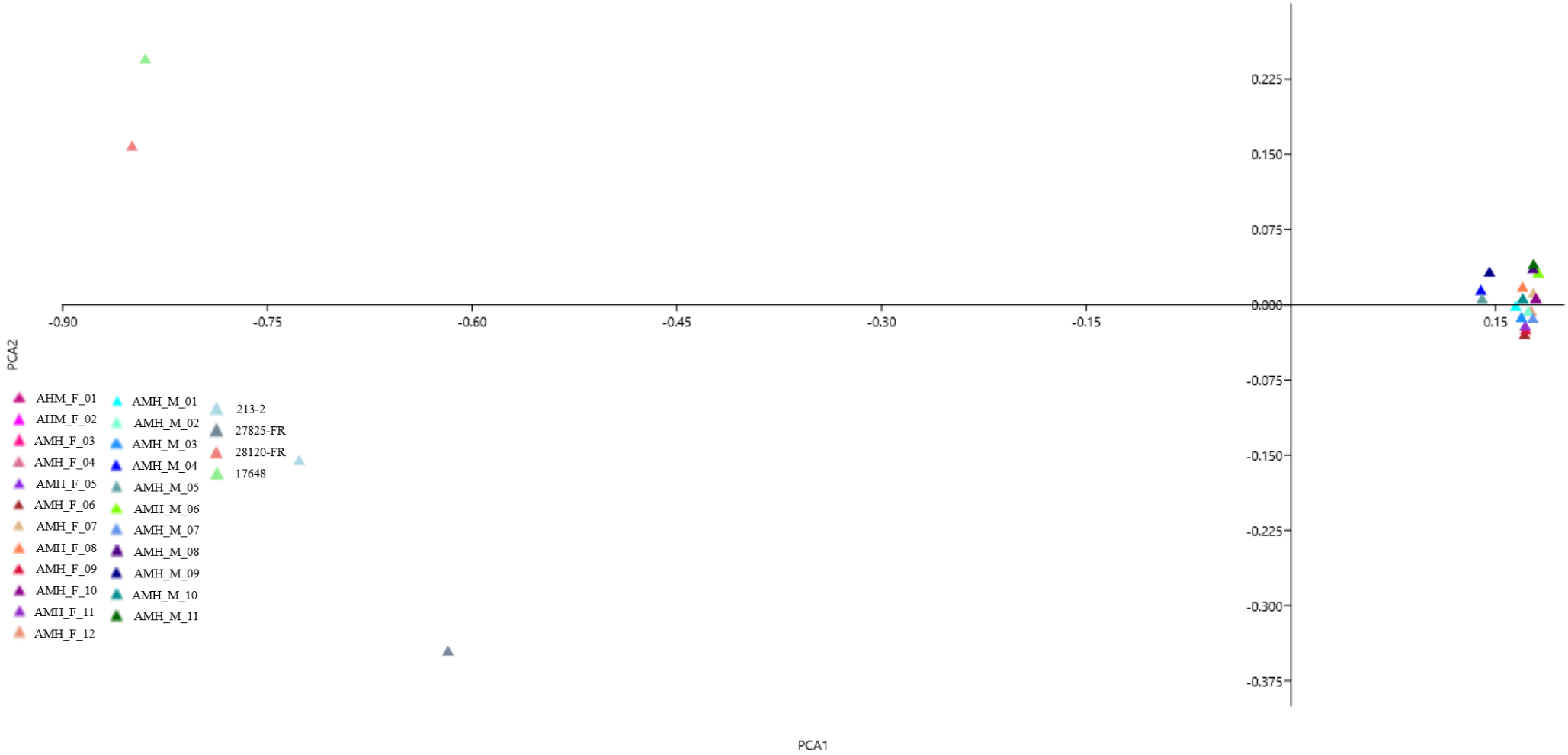


**Graph.18** *PCA graph of males and females aged 20 to 50 years and* Homo neanderthalensis *obtained using the PAST software*

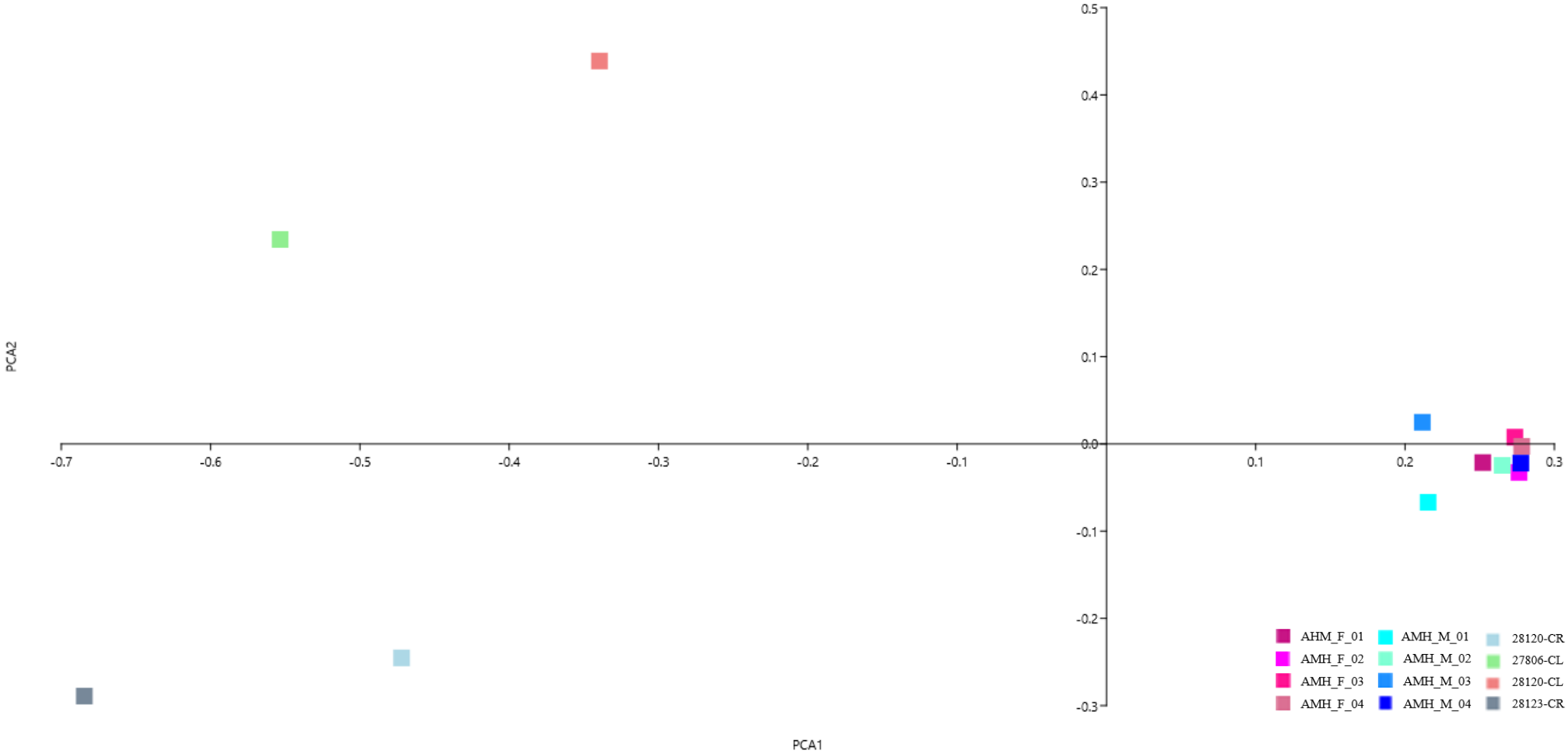


**Graph.19** *PCA graph of males and females aged 20 to 30 years and* Homo neanderthalensis *obtained using the PAST software*

show similar values with any *Homo neanderthalensis* individuals are AMH_F_08 and AMH_M_06, which are below the X-axis and to the left of the Y-axis.

Possible causes will be discussed in Discussion (item 5).

**41 to 50 years old (males, females and *Homo neanderthalensis*)** In the second group, individuals AMH_F_09, AMH_F_10, AMH_F_11, AMH_F_12, AMH_M_08, AMH_M_09, AMH_M_10 and AMH_M_11 were analysed for AMH and 28120-CR, 27806-CL, 28120-CL, 28123-CR for *Homo neanderthalensis* (see **Tab.1** for AMH and **Tab.2** for *Homo neanderthalensis*).

This graph (**Graph.21**) closely resembles **Graph.19**, i.e. the AMH individuals lie to the right of the Y-axis and those of *H. neaderthalensis lie to the* left of the Y-axis. The values for *Homo neanderthalensis*, however, are different, as 28120-CR and 28123-CR are above the X-axis, while 27806-CL and 28120-CL are below the X-axis.

Possible causes will be discussed in Discussion (item 5).

**20 to 50 years (females and *Homo neanderthalensis*)** This group consists of all female individuals taken into account for AMH (AMH_F_01, AMH_F_02, AMH_F_03, AMH_F_04, AMH_F_05, AMH_F_06, AMH_F_07, AMH_F_08, AMH_F_09, AMH_F_10, AMH_F_11 and AMH_F_12) and 28120-CR, 27806-CL, 28120-CL and 28123-CR for *Homo neanderthalensis* (see **Tab.1** for AMH and **Tab.2** for *Homo neanderthalensis*).

In this graph (**Graph.22**), the individuals of *Homo neanderthalensis* (28120-CR, 27806-CL, 28120-CL, 28123-CR) present similar values with some individuals of AMH (AMH_F_05, AMH_F_06, AMH_F_07, AMH_F_08). As can be seen, in fact, 28123-CR lies above the X-axis and to the left of the Y-axis as AMH_F_06, AMH_F_07 and AMH_F_08; whereas 28120-CR, 27806- CL and 28120-CL lie below the X-axis and to the left of the Y-axis lie with AMH_F_05.

All other AMH individuals are located to the right of the Y-axis and almost all above the X-axis.

Possible causes will be discussed in Discussion (item 5).

**20 to 50 years old (males and *Homo neanderthalensis*)** This group consists of all male individuals taken into account for AMH (AMH_M_01, AMH_M_02, AMH_M_03, AMH_M_04, AMH_M_05, AMH_M_06, AMH_M_07, AMH_M_08, AMH_M_09, AMH_M_10 and AMH_M_11) and 28120-CR, 27806-CL, 28120-CL and 28123-CR for *Homo neanderthalensis* (see **Tab.1** for AMH and **Tab.2** for *Homo neanderthalensis*).

Also in this graph (**Graph.23**) we can see that some AMH individuals have values similar to *Homo neanderthalensis*. In fact 28120-CR and 28123-CR are found with AMH_M_05 and AMH_M_06 above the X-axis and to the right of the Y-axis. 27806-CL and 28120-CL do not have similar values for any AMH individuals, in fact they are below the X-axis, but still to the right of the Y-axis.

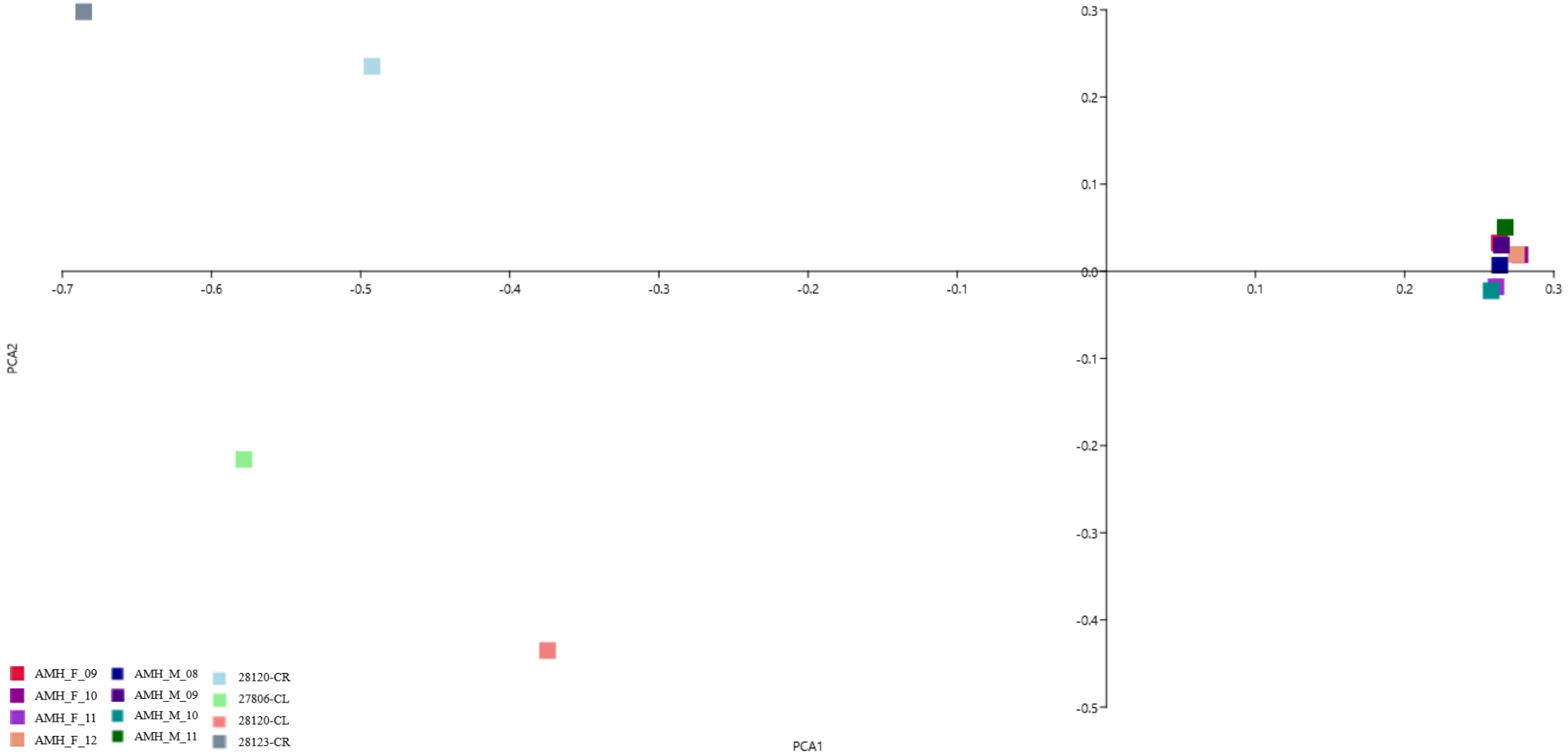


**Graph.21** *PCA graph of males and females aged 41 to 50 years and* Homo neanderthalensis *obtained using the PAST software*

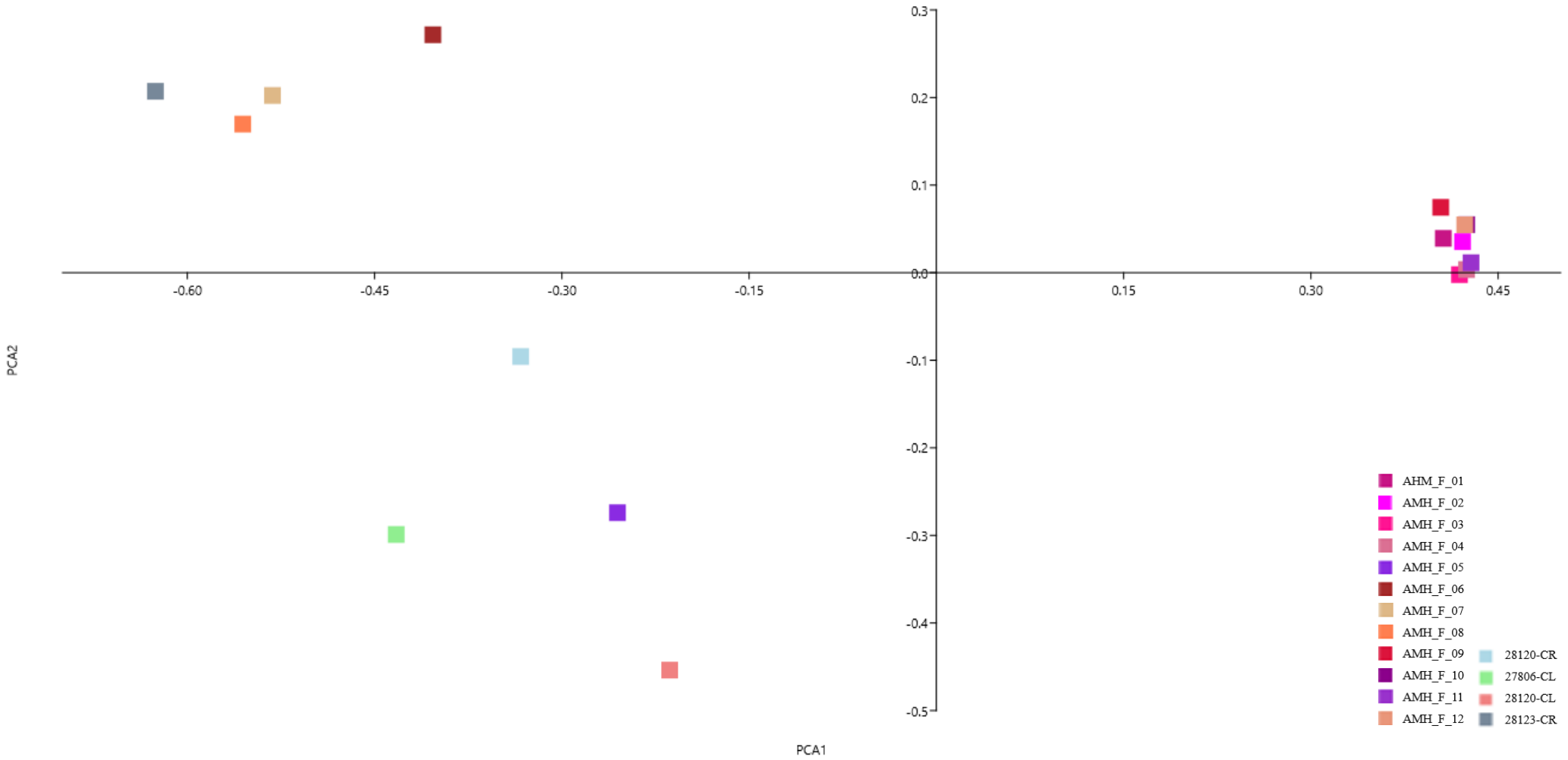


**Graph.22** *PCA graph of females aged 20 to 50 years and* Homo neanderthalensis *obtained using the PAST software*

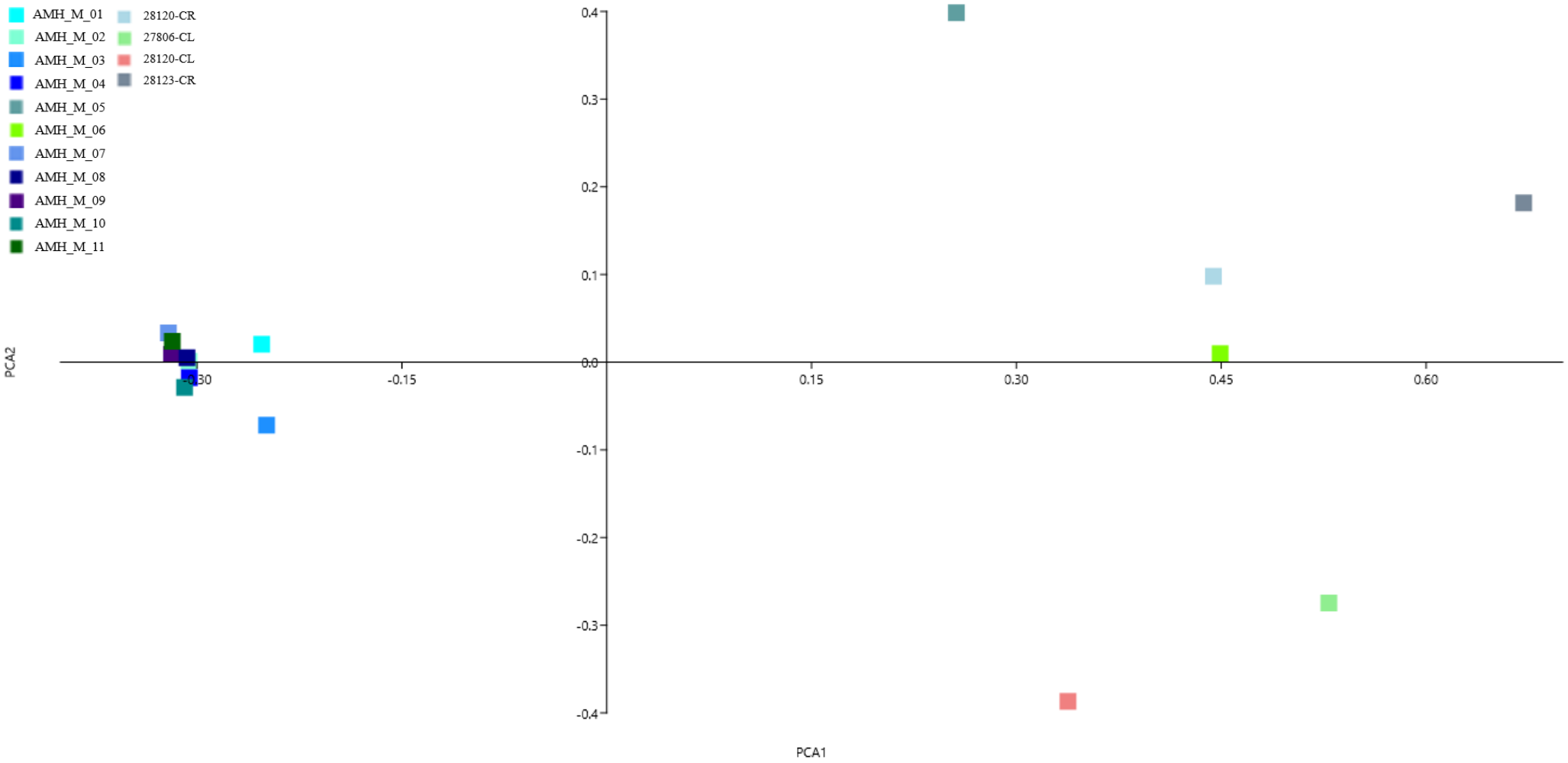


**Graph.23** *PCA graph of males aged 20 to 50 years and* Homo neanderthalensis *obtained using the PAST software*

All AMH's individuidual anterograms (AMH_M_01, AMH_M_02, AMH_M_03, AMH_M_04, AMH_M_07, AMH_M_08, AMH_M_09, AMH_M_10 and AMH_M_11) are located to the left of the Y-axis, some are below the X-axis, and the remainder are above the Y-axis.

Possible causes will be discussed in Discussion (item 5).

**20 to 50 years (males, females and *Homo neanderthalensis*)** This group consists of all AMH individuals who were examined and 28120-CR, 27806-CL, 28120-CL and 28123-CR for *Homo neanderthalensis* (see **Tab.1** for AMH and **Tab.2** for *Homo neanderthalensis*)

As with the previous graph (**Graph.23**), all individuals of *Homo neanderthalensis* lie to the right of the X-axis. But as with **Graph.20**, **Graph.22** and **Graph.23** the values for *Homo neanderthalensis* and some individuals of AMH are very similar. In fact 28123-CL, 27806- CL and 27806-CR lie above the X-axis with AMH_F_05; whereas 28123-CR lies below the X-axis with AMH_F_06, AMH_F_07, AMH_F_08, AMH_M_05 and AMH_M_06.

Possible causes will be discussed in Discussion (item 5).

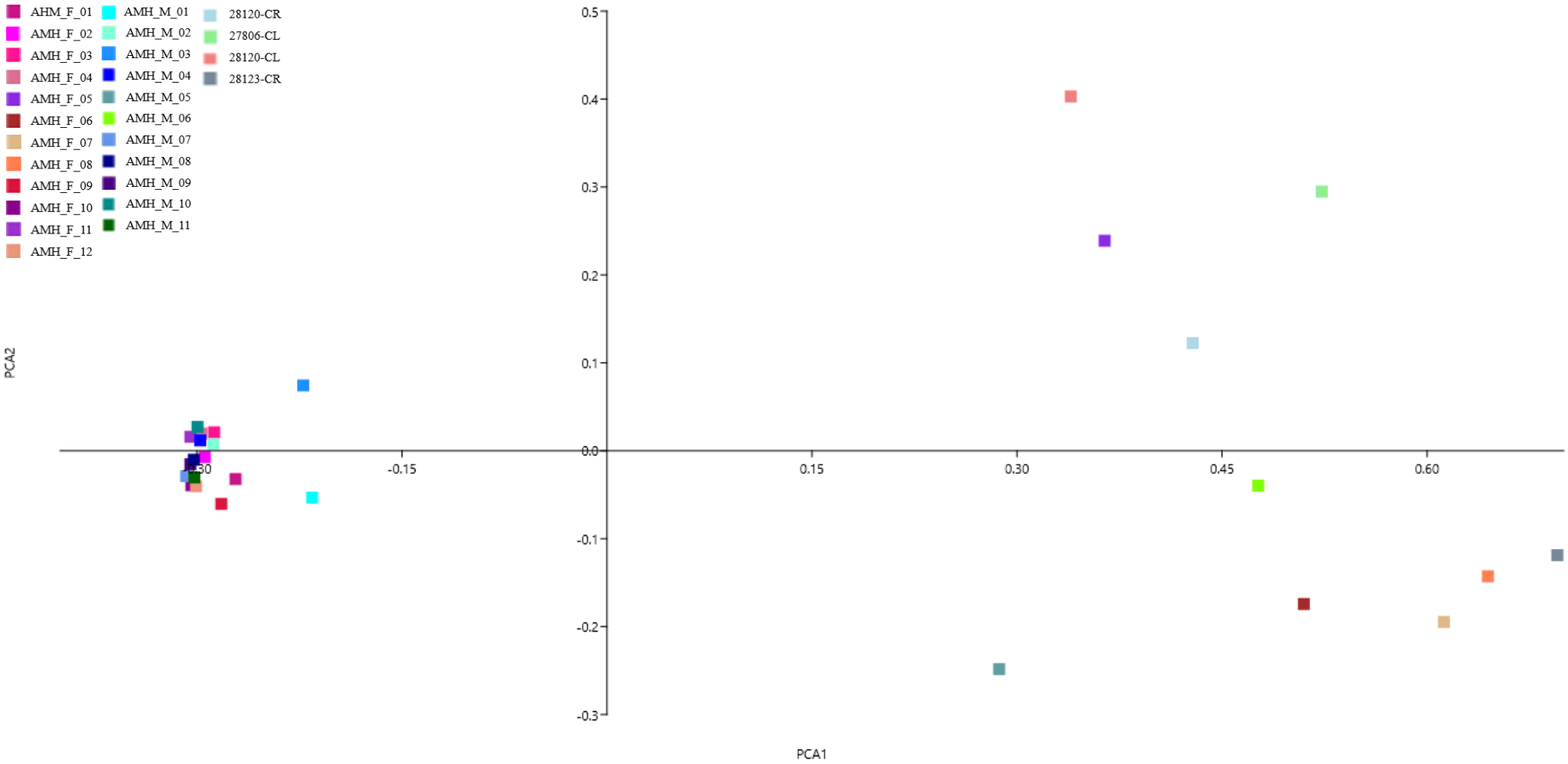


**Graph.24** *PCA graph of males and females aged 20 to 50 years and* Homo neanderthalensis *obtained using the PAST software*

# 6 Discussion

In this part of the paper, the results of the analyses made and explained in Results (point 4) will be discussed. Before going on to explain each anatomical part examined specifically and its comparison with the findings of Homo neanderthalensis, we would like to make a brief general remark.

What was seen in the Results is that for AMH (point 4.1) there are values for sex distinction (male or female), but less important for age. If only age is considered, it can be seen that some values (which are only for one of the two axes) are equal to each other and not very different. More contrasting values, especially from the point of view of sex, are found in pelvic analyses, as they are clearly different between males and females; for females, on the other hand, this distinction in values is much less clear-cut.On the other hand, with regard to what was seen in Results in the comparison between AMH and the fossil remains of Homo neanderthalensis (Section 4.2), it was seen that for the femurs there is no value that is equal between the two species of Homo, whereas for the pelvis it was noted that some of them are very close.

## 6.1 AMH

Now we only consider the graphs (**Graph.1** to **Graph.12**) and the analyses conducted on Anatomically Modern Human (AMN).

### 6.1.1 Femur

As can be seen from the graphs for females, there is not much distinction according to sex, but the distinction is greater according to age. In fact, if one looks at the graphs taking into account the groups of males and/or females from 20 to 50 - thus the complete sample - one can see that male and female individuals, irrespective of sex, show more similar values according to age.

The individuals who stand out most from the others are the individuals in the second group, those aged 31 to 40. In this group, it is noticeable that individuals present very different values and that they are scattered over the graph, compared to the other two age groups (20 to 30 years and 41 to 50 years). Most probably this wide range of values is due to the fact that it is a transitional age group for the sample taken for these analyses.

If one considers the age variable in general, one must take into account the fact that the femur is a very important part for the support of the human body; in fact, the weight of the upper part of the human body, especially when standing in an upright posture, is completely supported by the lower limbs. The pelvis transmits all the weight to the femur, which it then discharges to the ground via the lower limbs (Aiello and Dean, 1996; White and Folkes, 2005; White, Black and Folkes, 2011). So if one considers the important action that the femur has for bipedal individuals, it is normal that the values of the landmarks taken into account vary more with age than with sex.

Obviously, sex is a variable that should not be underestimated, since some of the female individuals - although it is a characteristic that was not taken into account when the sample was selected, since it was not certain that the data provided were true - may have given birth before death or may have been in one of the early stages of pregnancy - thus not very visible or not taken into account in the anamnestic record of the database. This variable could also be very important for future analyses as it changes the morphology of bipedal walking and how weight is transmitted from the upper part of the body to the lower limbs in a fairly consistent manner, giving considerable weight to the neck of the femur (the anatomical part taken into account in this paper) (Aiello and Dean, 1996; White and Folkes, 2005; White, Black and Folkes, 2011).

There is also a fundamental thing to remember that each individual may present characteristics that differ from the standard characteristics attributed to him or her, since the femur is a part of the human and hominid skeleton that is greatly influenced by strain, the way one walks and the place one lives, even the type of life one has led. It should be borne in mind that the individuals taken into consideration are individuals of whom we only have a medical history and do not have a complete picture of where and how they have lived throughout their lives, variables that are also crucial to a well-conducted study (Aiello and Dean, 1996; White and Folkes, 2005; White, Black and Folkes, 2011).

Another fundamental thing that cannot be taken into account because it is not due to the researcher if he or she uses another research organisation to get the CT scans, as in this case, is the location, the machinery and the quality of them. In fact, some values that are different from others for some individuals may be due to different locations, different machines and the quality of the CT scans for each individual, as well as other anatomical reasons that may be found and that were not provided in the NMDID history.

Having said this, it can be deduced that the intermediate age group for the individuals analysed (31 to 40 years) is a transitional age group for AMH and therefore exhibits different characteristics both between individuals in the same group and from individuals in the other age groups. For individuals in the other age groups, although they had similar values and were in the same place on the graph, it was seen that they were still grouped by age group and not mixed together.

### 6.1.2 Pelvis

For the pelvis, the most important feature is the distinction between the sexes. As explained in Anatomy (point 2), one of the main functions of the pelvis is to support and protect the foetus during pregnancy and to enable its delivery (Aiello and Dean, 1996; White and Folkes, 2005; White, Black and Folkes, 2011). In fact, what is noticeable in the analyses carried out for the pelvis is that individuals present different values especially for the sex variable and not age (NB: the age variable is still to be taken into account as it is also important.

One notices, in the various graphs comparing male and female individuals, how female individuals tend to have all the same values, whereas, male individuals have quite different values. Some male individuals have very similar values to female individuals and vice versa. One reason for this may be that the pelvis, both male and female, does not have only and exclusively male or female traits. In fact, when one has to assign a sex to a pelvis one has a series of features and a value is given to them: from the most masculine to the most feminine. However, there are androgynous intermediate forms[13] that do not allow a clear and distinct distinction between male and female. These intermediate cases can distort the results of the analyses, in fact, one can see in some cases how male individuals are closer to the values of female individuals and vice versa.

Moreover, one must consider, as with the femur, the changes that are brought about by pregnancy in the female case. The pelvis undergoes a greater change in response to that of the femur, as it has to adapt its size to that of the foetus (as far as the human skeleton and physique allow). The pelvis during childbirth must widen to allow the birth of the foetus (the foetus also has adaptations to the skull that allow it to help the mother in childbirth), which then change the morphology of a woman's pelvis almost permanently (Aiello and Dean, 1996; White and Folkes, 2005; White, Black and Folkes, 2011).

Having said this, one can consider the fact that in this case the values that have been presented for the pelvises are significant for the sex characteristic, but it is not a characteristic that presents clear-cut and specific characters for one of the two sexes. Thus, it must be taken into account that some male individuals present a set of traits that brings them closer to female and vice versa. These individuals should not be discarded because they distort the analysis, but rather are crucial if one wants to know how many there are and whether it is an important feature in the change of sexual dimorphism[14] in AMH. Furthermore, they are important if we are to understand, especially in the next section (section 4.2), whether this characteristic was also common in *Homo neanderthalensis* or whether this tendency invalidates the analyses.

In addition to the considerations just made, there is a variable that has also been explained for the femur, namely that the middle age group (31 to 40 years) presents different values between individuals. It is noticeable in the graph only examining this range (**Graph.8**) that male and female individuals (with the exception of a few) are always grouped by gender, but between them they all present different values, which places them in different parts of the graph. This may depend on the age of the individual and also on the previously explained characteristics of the pelvis and its changes.

[13] "Having physical appearance and behaviour with characteristics peculiar to both sexes" (Vocabolario Treccani, 2023a).
[14] "The systematic difference existing between individuals belonging to the same species but of different sexes" (Enciclopedia Treccani, 2023a).

This also applies to the next age group (41 to 50 years), i.e. age plays a fairly important role in the values attributed to each individual, but less so than in the middle age group. The age factor, however, is not very relevant for the first age group (20 to 30 years), as the individuals all present very similar values, especially for women, whereas for men they are quite contrasting.

For the age group of 20 to 30 years, the lack of a significant difference between female individuals could be due to the fact that they have never had children and/or have never been pregnant (this also includes pregnancies with a miscarriage in the first trimester of gestation). Thus, pregnancy could be an important factor affecting individuals' values.

## 6.2 Comparison of AMH and Homo neanderthalensis

In this second part of the Discussion we consider the graphs (**Graph.13** to **Graph.24**) and analyses conducted on Anatomically Modern Human (AMN) and *Homo neanderthalensis* fossils.

### 6.1.2 Femur

As mentioned in the general explanation, it was noted that the femurs of *Homo neanderthalensis* do not show any conflicting values with those of AMH. There is no error in the positioning of the landmarks, because it was checked several times that they were positioned correctly.

This difference in values between *Homo sapiens* (*Homo* species of AMH) and *Homo neanderthalensis* could be due to multiple factors:

- the fossils show a strong distortion, which does not allow the landmarks to be positioned correctly, causing the results of the analyses to be skewed and incorrect: even if the femur, due to its osteological conformation, presents a greater resistance to fossilisation (if one can call it that), it can still show deformations due to taphonomic processes[15] (Aiello and Dean, 1996);
- the shape of the femur in *Homo neanderthalensis* is different from that of AMH: the morphology is different between the two species of *Homo* because the skeletal morphology is different, so the attachment of muscles, tendons and ligaments is different. This different skeletal morphology also leads to a different weight load on the femurs and lower limbs, leading to different values for the femurs and thus not being congruent with those of AMH (Aiello and Dean, 1996).

It should be noted that these femurs, albeit with different values and comparing **Graph.2** with **Graph.14** belonging to a different species of *Homo*, their values behave like those of the middle age group (31 to 40 years) for AMH. By this is meant that they also present contrasting values to each other and cluster two by two above and below the Y-axis. This could mean that they are also part of a transitional age group or they could simply be two female and two male individuals, or both.

[15] "Processes of transformation of organic matter following the death of organisms, including those leading to the formation of fossils" (Vocabolario Treccani, 2023e).

### 6.2.2 Pelvis

In contrast to the contrasting data between AMH and *Homo neanderthalensis* with regard to the analysis of the femur, if one looks at the analyses conducted on the pelvis of these two *Homo* species, one can see that here the values are very similar and in some cases in common.

The values for *Homo neanderthalensis* and AMH, however, are not the same for the 20-30 year age group. Here, in fact, it can be seen that *H. neanderthalensis* has opposite values to those of AMH. In the graph (**Graph.19**), it can be seen that Neanderthal is on the opposite side of the graph from AMH. The same is true for the graph of the third age group (41 to 50 years), the two *Homo* species have opposite values, but they too are different from those in the first age group. In fact, the two individuals that are above the X-axis in Graph.19 are below it in **Graph.21**.

The fossils examined of *Homo neanderthalensis* have similar values only in the case of the second age group (31 to 40 years). In this case, it can be seen that the four specimens are very close in values to some individuals:

- 28123-CL is very close in values to the two individuals AMH_F_06 and AMH_F_07: this suggests that this individual, having similar values to AMH, is a female specimen in the age range of 31 to 40 years (Tague, 1992);
- 28120-CL, 28120-CR and 27806-CL have very similar values to AMH_M_05 and AMH_M_07: 28120-CL and 27806-CL are both close to AMH_M_05, while 28120-CR is very close to AMH_M_07:
    - 28120-CL and 28120-CR both belong to the same individual of *H. neanderthalensis* they do not have values that unite them this may mean that there is no symmetry between the two parts of the pelvis, but both are close to a male individual (even though they are two different ones) ranging from 31 to 40 years old, so it can be assumed that this Neanderthal may also be a male individual between 31 and 40 years old (Tague, 1992);
    - these similar values to individuals in the 31-40 male age group could mean that thes two individuals also belong to this group.

The data obtained from this analysis suggest that this sample, albeit small, of *Homo neanderthalensis* is part of the intermediate age group (31 to 40 years) examined in this paper. Another hypothesis might be that *Homo neanderthalensis* had very different values from individual to individual as is the case for the middle age group for AMH. If the second hypothesis just stated is taken into account, however, it can be deduced that 28123-CL may belong to a female individual, whereas 28120-CL/28120-CR and 27806- CL may belong to a male individual, as both do not interact with individuals of the opposite sex to that of the most similar value (Tague, 1992; Weaver and Hublin, 2009).

# 7 Conclusion

The pelvis and femur, as mentioned earlier, were the subject of this paper. The study of these anatomical parts is intended to be the beginning of a new approach to the study of the Obstetrical dilemma and to try to provide an explanation for this anatomical dilemma, which has still not been resolved to this day, as fossils are lacking and conclusions are very different and sometimes conflicting. It is also meant to be a start, because only two features are examined here, which are important in some respects - as explained above - in order to be able to identify an individual; these features are the sex and age of an individual.

In these analyses, it was seen that age and gender for these two different anatomical parts (the two characters examined) are not equally relevant:

- femur is more influenced by age character: femurs show distinctions more influenced by age than by sex;
- the pelvis is more influenced by sex than by age.

These two traits were then also applied to *Homo neanderthalensis*, which showed that the femurs do not follow the same characteristics as AMH, i.e. they did not have similar values for PCA either by sex or by age; whereas the pelvises have similar values for PCA as AMH, allowing sex to be estimated as well (this is only an assumption as we do not have enough data).

What has just been said leads one to believe that this type of analysis could only be applied to the pelvis and not to the femurs, but being only at an early stage and expanding the AMH sample, it may perhaps also be applicable to the femurs.

These similarities with AMH, may suggest that through this new approach it is possible to estimate the sex and perhaps even the age of the fossilised individual being examined. It must also be said that the sample analysed is very small; therefore, the statement made may not be true, but if the analyses were to be carried out, it may reveal that what has just been said is true and thus prove to be a valid new approach to studying the pelvis and femurs.

The problem with carrying out these analyses is the lack of sufficient fossils to be able to make a sufficiently valid statistical analysis to be able to state with certainty what has been said. As with all issues concerning palaeoanthropology, it would be necessary to have many more fossils and also in a good state to be able to have analyses that give real certainty, but unfortunately the fossilisation process, in many cases, does not allow for a good state of preservation of the fossil.

This problem of fossilisation could also distort the results obtained, as in this case, as some of the fossils examined were very distorted, fragmented and then reconstructed, or missing parts. These common features in the fossils mean that the position of the landmarks is not true, and therefore the result obtained is not true, but only partly close to the truth. In these analyses, an

attempt was made, as mentioned above, to give an objectivity to the analyses, but this was very difficult, because the missing data made it difficult to make a clear and truthful analysis.

In conclusion, it can be said that this project certainly needs to be expanded, both from the point of view of AMH and fossil individuals. The problem with the fossil record is that we should have well-preserved fossils or 3D reconstructions that do not rely too much on what AMH looks like, but take more into account what other species of *Homo* might have looked like, not relying on what *Homo sapiens* looks like.

The problem with studying fossils, however, is that we have to start from what we, AMH, look like in order to apply our parameters to fossil species and then study their differences and similarities. It is precisely the differences and similarities that we want to see with these analyses. It is reiterated that this is only meant to be the antechamber to a broader study of pelvises and femurs, so that we can get a new perspective on this anatomical dilemma.

It is hoped that in the future, more fossils will be found in good condition, technologies and software will be available that allow for a more truthful reconstruction of fossils and other innovations that will allow for a more objective and less *Homo*-centric advancement of prehistoric and even *Obstetrical dilemma* research.

# Bibliography


Adegboyega, M. T. *et al.* (2021) 'Virtual reconstruction of the Kebara 2 Neanderthal pelvis', *Journal of Human Evolution*, 151, p. 102922. doi: 10.1016/j.jhevol.2020.102922.

Agisfot LLC (2006) *Agisoft*.

Aiello, L. and Dean, C. (1996) *An Introduction to Human Anatomy*. San Diego, CA, USA: Academic Press, Inc. doi: 10.1093/ptj/16.4.170a.

Audenaert, E. A. *et al.* (2021) 'Ischiofemoral impingement: the evolutionary cost of pelvic obstetric adaptation', *Journal of Hip Preservation Surgery*, 7(4), pp. 677–687. doi: 10.1093/jhps/hnab004.

Bonneau, N. *et al.* (2012) 'A three-dimensional axis for the study of femoral neck orientation', *Journal of Anatomy*, 221(5), pp. 465–476. doi: 10.1111/j.1469-7580.2012.01565.x.

Bourke, P. (2020) *PLY - Polygon File Format*. Available at: https://paulbourke.net/dataformats/ply/.

Candelas González, N. *et al.* (2017) 'Geometric morphometrics reveals restrictions on the shape of the female os coxae', *Journal of Anatomy*, 230(1), pp. 66–74. doi: 10.1111/joa.12528.

DICOM (2019) *Does DICOM work with other standards-development organizations?*, *The Medical Imaging Technology Association (MITA)*. Available at: http://dicom.nema.org.

Dryden, I. L. and Mardia, K. V. (1998) *Statistical Shape Analysis*. doi: https://doi.org/10.1002/1097-0258(20001015)19:19<2716::AID-SIM590>3.0.CO;2-O.

Edgar, H. *et al.* (2020) *New Mexico Decedent Image Database*, *Office of the medical Investigator, University of New Mexico*. doi: doi.org/10.25827/5s8c-n515.

Enciclopedia Treccani (2023a) *Dimorfismo sessuale*. Available at: https://www.treccani.it/enciclopedia/dimorfismo-sessuale_%28Dizionario-di-Medicina%29/.

Enciclopedia Treccani (2023b) *Paleoantropologia*. Available at: https://www.treccani.it/enciclopedia/paleoantropologia.

Enciclopedia Treccani (2023c) *Paleontologia*. Available at: https://www.treccani.it/enciclopedia/paleontologia#:~:text=Disciplina che studia gli animali,attraverso i loro resti fossili.

Fedorov, A. *et al.* (2012) '3D Slicer as an Image Computing Platform for the Quantitative Imaging Network', *Magn Reson Imaging.*, 30(9), pp. 1323–1341. doi: 10.1016/j.mri.2012.05.001.

Ficarra, S. and Lauria, G. (2022) 'Gli Archivi Digitali e l ' Antropologia Virtuale . Ricostruzione 3D di un cranio umano mediante la moderna tecnica della Fotogrammetria', *Archivio per l'Antropologia e la Etnologia*, CLII.

Friess, M. (2012) 'Scratching the Surface ? The use of surface scanning in physical and

paleoanthropology', 90, pp. 1–26. doi: 10.4436/jass.90004.
Ghesu, F. C. *et al.* (2017) 'Multi-Scale Deep Reinforcement Learning for Real-Time 3D-Landmark Detection in CT Scans', 8828(c), pp. 1–14. doi: 10.1109/TPAMI.2017.2782687.
Harmon, E. H. (2007) 'The shape of the hominoid proximal femur: A geometric morphometric analysis', *Journal of Anatomy*, 210(2), pp. 170–185. doi: 10.1111/j.1469-7580.2006.00688.x.
Harmon, E. H. (2009) 'The shape of the early hominin proximal femur', *American Journal of Physical Anthropology*, 139(2), pp. 154–171. doi: 10.1002/ajpa.20966.
Holliday, T. W. *et al.* (2010) 'Geometric morphometric analyses of hominid proximal femora: Taxonomic and phylogenetic considerations', *HOMO- Journal of Comparative Human Biology*, 61(1), pp. 3–15. doi: 10.1016/j.jchb.2010.01.001.
Lycett, S. J. and von Cramon-Taubadel, N. (2013) 'Understanding the comparative catarrhine context of human pelvic form: A 3D geometric morphometric analysis', *Journal of Human Evolution*, 64(4), pp. 300–310. doi: 10.1016/j.jhevol.2013.01.011.
Martin, R. D. *et al.* (no date) 'Computer-Assisted Paleoanthropology', pp. 41–54.
Netter, F. H. (2022) *Netter Atlas of Human Anatomy*. Eighth Edi, *Elsevier*. Eighth Edi. Philadelphia, PA: O'Grady, Elyse.
Pujol, A. *et al.* (2014) 'Ontogeny of the female femur: Geometric morphometric analysis applied on current living individuals of a Spanish population', *Journal of Anatomy*, 225(3), pp. 346–357. doi: 10.1111/joa.12209.
Richtsmeier, J. T., Lele, S. R. and Cole, T. M. I. (2018) 'Landmark Morphometrics and the Analysis of Variation', in. Public Health Service, pp. 49–69.
Rohlf, F. J. (2000) 'On the use of shape spaces to compare morphometric methods', *Hystrix*, 11(1), pp. 9–25. doi: 10.4404/hystrix-11.1-4134.
Tague, R. G. (1992) 'Sexual dimorphism in the human bony pelvis, with a consideration of the Neandertal pelvis from Kebara cave, Israel', *American Journal of Physical Anthropology*, 88(1), pp. 1–21. doi: 10.1002/ajpa.1330880102.
Tufféry, S. (2011) *Data mining and statistics for decision marking*. Wiley. Available at: https://www.wiley.com/en-us/Data+Mining+and+Statistics+for+Decision+Making-p-9780470688298.
Velazquez, E. R. *et al.* (2013) 'Volumetric CT-based segmentation of NSCLC using 3D-Slicer', pp. 1–7. doi: 10.1038/srep03529.
Vocabolario Treccani (2023a) *Androgino*. Available at: https://www.treccani.it/vocabolario/androgino/.
Vocabolario Treccani (2023b) *Artrite*. Available at: https://www.treccani.it/vocabolario/artrite.
Vocabolario Treccani (2023c) *Osteoporosi*. Available at:

https://www.treccani.it/vocabolario/osteoporosi/.
Vocabolario Treccani (2023d) *Reumatismo*. Available at: https://www.treccani.it/vocabolario/reumatismo/.
Vocabolario Treccani (2023e) *Tafonomia*. Available at: https://www.treccani.it/vocabolario/tafonomia/#:~:text=– In biologia%2C lo studio dei,fossilizzazione).
Ward, C. V., Maddux, S. D. and Middleton, E. R. (2018) 'Three-dimensional anatomy of the anthropoid bony pelvis', *American Journal of Physical Anthropology*, 166(1), pp. 3–25. doi: 10.1002/ajpa.23425.
Weaver, T. D. and Hublin, J. J. (2009) 'Neandertal birth canal shape and the evolution of human childbirth', *Proceedings of the National Academy of Sciences of the United States of America*, 106(20), pp. 8151–8156. doi: 10.1073/pnas.0812554106.
Wells, J. C. K., DeSilva, J. M. and Stock, J. T. (2012) 'The obstetric dilemma: An ancient game of russian roulette, or a variable dilemma sensitive to ecology?', *Yearbook of Physical Anthropology*, 149(SUPPL.55), pp. 40–71. doi: 10.1002/ajpa.22160.
White, T. D., Black, M. T. and Folkes, P. A. (2011) *Human Osteology*. Third Edit, *Acatemic Press*. Third Edit. Edited by K. Anderson. Ox. doi: https://doi.org/10.1016/C2009-0-03221-8.
White, T. D. and Folkes, P. A. (2005) *The Human Bone Manual*. California: Academic Press. doi: https://doi.org/10.1016/C2009-0-00102-0.
Witham, D. (1987) 'The relationship of neck orientation to the shape of the proximal femur', *Journal of Arthroplasty*, 2(2), pp. 99–109. doi: 10.1016/S0883-5403(87)80016-5.